JPRS L/10338

19 February 1982

USSR Report

ELECTRONICS AND ELECTRICAL ENGINEERING

(FOUO 2/82)

FBIS FOREIGN BROADCAST INFORMATION SERVICE

NOTE

JPRS publications contain information primarily from foreign
newspapers, periodicals and books, but also from news agency
transmissions and broadcasts. Materials from foreign-language
sources are translated; those from English-language sources
are transcribed or reprinted, with the original phrasing and
other characteristics retained.

Headlines, editorial reports, and material enclosed in brackets
[] are supplied by JPRS. Processing indicators such as [Text]
or [Excerpt] in the first line of each item, or following the
last line of a brief, indicate how the original information was
processed. Where no processing indicator is given, the infor-
mation was summarized or extracted.

Unfamiliar names rendered phonetically or transliterated are
enclosed in parentheses. Words or names preceded by a ques-
tion mark and enclosed in parentheses were not clear in the
original but have been supplied as appropriate in context.
Other unattributed parenthetical notes within the body of an
item originate with the source. Times within items are as
given by source.

The contents of this publication in no way represent the poli-
cies, views or attitudes of the U.S. Government.

FOR OFFICIAL USE ONLY

JPRS L/10338

19 February 1982

USSR REPORT

Electronics and Electrical Engineering

(FOUO 2/82)

Contents

FOR OFFICIAL USE ONLY

- c -

FOR OFFICIAL USE ONLY

AEROSPACE & ELECTRONIC SYSTEMS

UDC 621.396.96

RADIO RELAY AND SATELLITE TRANSMISSION LINE RELIABILITY

Moscow NADEZHNOST' RADIORELEYNYKH I SPUTNIKOVYKH LINIY PEREDACHI in Russian
1981 (signed to press 2 Jul 81) pp 2-3, 160

[Annotation, foreword and table of contents from book "Radio Relay and Satellite
Transmission Line Reliability", by Ariy Izrailevich Rakov, Izdatel'stvo
"Radio i svyaz'", 5800 copies, 160 pages]

[Text] The reliability of radio relay and satellite transmission lines (RR and
STL) is investigated: mathematical and physical models are analyzed, as are the
interdependence among reliability indicators and the laws for distribution of
failures and down-time duration. Ways to improve RR and STL reliability are
examined and recommendations are made for the sequence in which they should be
realized, taking technical efficiency into consideration. Methods are proposed
for optimization of RR and STL structure based on reliability and cost criteria.
Examples of calculations are given.

For engineering and technical workers specializing in radio relay and satellite
communications.

Reviewer: G. V. Vodop'yanov

Foreword

The high reliability which is created in our country by the United Automated
Communications Network (YeASS) can be provided if the necessary level of reli-
ability is achieved in each of its individual links. The role of radio relay
and satellite transmission lines as the most important components of YeASS in-
creases annually. However, not all of the questions associated with providing
radio relay and satellite transmission line reliability have been adequately
covered in the literature. In the book offered to the reader, the theoretical
bases for studying radio relay and satellite transmission line reliability are
systematized, the experience of operating these lines is analyzed and recommenda-
tions for improving reliability are made. Methods have been developed for the
optimal synthesis of radio relay and satellite transmission lines and their
components which insure that the prescribed level of reliability is achieved at
minimal cost.

1

CONTENTS

2

COPYRIGHT: Izdatel'stvo "Radio i svyaz'", 1981

9194
CSO: 1860/117

UDC 629.3.002.72.002.54(075.8)

ELECTRIC NAVIGATION INSTRUMENTS

Moscow ELEKTRONAVIGATSIONNYYE PRIBORY in Russian 1980 (signed to press 9 Dec 80) pp 2-4, 444-447

[Annotation, foreword, introduction (excerpt) and table of contents from book "Electric Navigation Instruments", by Igor' Aleksandrovich Blinov, Aleksandr Vasil'yevich Zherlakov, Vladimir Konstantinovich Perfil'yev, Yevgeniy Leonidovich Smirnov and Andrey Andreyevich Yakushenkov, reviewed by Ye. F. Ludchenko, 4th edition, revised and supplemented, Izdatel'stvo "Transport", 12,000 copies, 448 pages]

[Text]   The fourth edition of this textbook is written in accordance with the new program of the course "Technical Maritime Navigation Aids" for students of higher marine engineering schools specializing in maritime navigation. It presents the theory of modern gyroscopic and hydroacoustic instruments, logs and autopilots, and examines the prospects of the development and practical uses of these instruments on vessels of the marine fleet.

In preparing the new edition of this textbook, the material of the preceding edition (1973) was revised considerably and supplemented with new data reflecting the improvement of electric navigation instruments in recent years, as well as suggestions of instructors of maritime vuzes, shipping lines land and seagoing personnels.

This book can be used by students of higher maritime educational institutions specializing in radio engineering and hydrography as a textbook for the appropriate section of their program. It will certainly be useful for navigators of the maritime fleet, particularly in the part of the descriptions of new electric navigation instruments which are being introduced on seagoing vessels.

Figures -- 241, tables -- 6, bibliography -- 28 items.

Introduction

Resolutions of CPSU Congresses and five-year plans for the development of the national economy of the USSR envisaged further development of sea transportation and replenishing of the fleet with faster large-capacity vessels of new types.

The most important role in achieving the highest economic effect in the operation of each vessel and the fleet as a whole, as well as navigation safety, is played by electric navigation instruments (ENP) which are used to determine the course and speed of the vessel, the depth of the sea, and to control the vessel automatically.

4

For the convenience of studying, all electric navigation instruments are divided by the principle of operation and by the value they measure.

By the principle of operation, electric navigation instruments are subdivided into gyroscopic, hydroacoustic, hydrodynamic and electrodynamic (induction).

The following division is accepted with respect to measured values: meridian plane indicators; azimuth indicators; horizon plane indicators; meters of angular velocities and acceleration of vessel movement; vessel steering angle meters; meters of position coordinates; meters of linear speed and acceleration of the vessel; sea depth meters.

Depending on their purposes, ENP have the following names:

hydroscopic compasses -- meridian plane indicators;
directional gyroscopes (azimuth gyroscopes) -- azimuth indicators;
gyro-magnetic compasses -- magnetic meridian plane indicators;
vertical gyroscopes (gyro horizons) -- horizon plane indicators;
gyrostabilizers -- commanded position indicators;
gyrotachometers (differentiating gyroscopes) -- meters of angular speed of moving objects;
gyrotachoaccelerometers -- meters of angular speed and angular acceleration of the vessel;
accelerometers -- meters of linear accelerations of the vessels;
integrating gyroscopes -- steering angle meters;
inertial navigation systems -- meters of distance traveled;
hydrodynamic logs -- meters of relative speed of the vessel;
electrodynamic (induction logs -- meters of relative speed of the vessel;
hydroacoustic logs -- meters of absolute (in relation to ground) speed of the vessel;
echo depth sounders -- sea depth meters.

Electric nagivation instruments can work in the indicator mode, when the information obtained from them is used only for navigational orientation, and in the control mode, when information is delivered to the automatic movement control systems of the vessel.

Such automatic control systems using information of ENP are control systems of the vessel's movement at a fixed course and along a prescribed trajectory and vessel stabilization systems used in rough seas.

This book consists of two parts. The first part presents the theory of electric navigation instruments, and the second part describes their designs. The sequence of chapters is determined by the interrelation among various instruments.

Much attention in the book is given to the theory and the design principles of modern electric navigation instruments. Errors of instruments, causes of their appearance, and methods of their compensation are discussed in detail.

Considering the tendency in the development of electric navigation instruments of the maritime fleet, considerable attention is given to new promising instruments and systems.

5

FUR OFFICIAL USE ONLY

Contents	Page

6

FOR OFFICIAL USE ONLY

8

FOR OFFICIAL USE ONLY

FOR OFFICIAL USE ONLY

COPYRIGHT: Izdatel'stvo "Transport", 1980.

10,233
CSO: 1860/103

ANTENNAS & PROPAGATION

ABSTRACTS FROM COLLECTION 'NONCOHERENT SCATTERING OF RADIO WAVES'

[Annotation and abstracts of articles in collection "Noncoherent Scattering of Radio Waves", edited by B. Ye. Bryunelli, doctor of physical and mathematical sciences, et al., Kol'skiy filial AN SSSR, 400 copies, 167 pages]

[Text] Various aspects of the method of noncoherent scattering of radio waves are discussed in the collection, a new highly informative method of studying the ionosphere. Theory of the method, questions of the effect of collisions on the spectrum, the effect of continuous magnetic and electrical fields, and possible occurrence of nonlinear effects during measurements using the method of noncoherent scattering are discussed.

Methods and techniques of conducting experiments are examined, as are questions of enhancing their informativeness. A brief description of the Noncoherent Scattering Research Complex of Kharkov Polytechnical Institute and the type of results obtained there are given. Information resources of the method are analyzed in terms of literary sources.

UDC 533.951+550.388

THE KINETIC THEORY OF RADIO WAVE SCATTERING IN A HETEROGENEOUS PLASMA

[Abstract of article by V. V. Belyy, Yu. L. Klimontovich, V. A. Puchkov and A. S. Sidorenko]

[Text] The theory of kinetic plasma fluctuations is presented as it pertains to problems of noncoherent scattering of electromagnetic waves. The effect of colliding particles on spectra of noncoherent scattering is studied within model integrals of BGK collision. A discussion is conducted based on parametric instabilities which may be generated by the field of a powerful probe signal.

11

UDC 533.932

FLUCTUATIONS OF CHARGED PARTICLE DENSITY OF COLLISION PLASMA IN CROSSED
ELECTRIC AND MAGNETIC FIELDS

[Abstract of article by V. D. Tereshchenko and Ye. D. Tereshchenko]

[Text] Based on kinetic theory, the spectrum of density fluctuations of
charged particles is calculated for a collision plasma located in an
external crossed electrical and magnetic fields. A model integral of
BGK collisions is used for to describe the collision effects in an kine-
tic equiaton. It is shown that the colliding member of BGK can be used
to evaluate the effect of collision of electrons and ions on the spec-
trum of noncoherently scattered emission.

UDC 550.388.2

ELECTRON PORTION OF SPECTRUM OF NONCOHERENTLY SCATTERED EMISSION

[Abstract of article by V. D. Tereshchenko and Ye. D. Tereshchenko]

[Text] The effect of a small addition of epithermal electrons on total
intensity of electron lines of the spectrum of noncoherently scattered
radio emission is studied. The influence of collision on intensity of
scattering in plasma oscillations is analyzed. General results and
conclusions are applied to calculation of the altitude profile of the
total cross section of plasma line in the polar ionosphere.

UDC 551.510.535

STATISTICAL CHARACTERISTICS OF NONCOHERENTLY SCATTERED SIGNAL

[Abstract of article by E. G. Mizer]

[Text] The statistical characteristics of ionic and electronic com-
ponents of the spectrum of noncoherently scattered signals in iono-
spheric plasma are considered. The process of formation of a scattered
signal is considered; distributive laws, space and time correlation
functions of the signal are derived. Physical processes of shaping of a
signal scattered on longitudinal plasma waves is examined. Methods are
recommended for receiving the signal of a plasma line permitting im-
provement of the signal-to-noise ratio with respect to power.

UDC 550.388.2

EFFECT OF MAGNETIC FIELD IN QUASIEQUILIBRIUM PLASMA ON IONIC PORTION OF
SPECTRUM OF A NONCOHERENTLY SCATTERED SIGNAL

[Abstract of article by A. D. Tereshchenko]

[Text] The effect of a magnetic field on the process of noncoherent
scattering of radio waves in a quasiequilibrium plasma is studied. The
spectrum of radio wave scattering in the meter range is determined by
longitudinal (with respect to magnetic field bearing) temperature com-
ponent and longitudinal component of electron directional velocity.

12

UDC 551.510.535

ROLE OF NONLINEAR EFFECTS IN THE NONCOHERENT SCATTERING METHOD

[Abstract of article by V. A. Misyura, S. I. Martynenko and L. F. Chernogor]

[Text] For the case of the heating mechanism of nonlinear effects, "engineering" formulas are derived which enable us to assess the minimum effective output at which perturbation of the medium due to sensing pulses becomes noticeable. Perturbations are calculated for two typical meter and decimeter range facilities. It is shown that strong radio pulses can increase electron temperature T_e in the D-region by a factor of ten. The change in T_e in the E and F regions is small. Perturbation of electron concentration may also be ignored. The principle of construction of an approximate nonlinear theory of noncoherent scattering (NR) of radio waves is described. It is shown that the use of increased output installations expands the resources of the NR method.

UDC 621.371+550.388

SYNTHESIS OF MULTIPARAMETRIC EVALUATION PROCESSOR STRUCTURE FOR NON-COHERENTLY SCATTERED SIGNALS

[Abstract of article by I. N. Presnyakov, A. N. Blinkov, S. S. Smol'yaninov, M. I. Kochkin, Ye. A. Pis'michenko and V. A. But]

[Text] Questions of synthesis of structures of special digital processors are considered for real-time processing signals of noncoherent scattering (NR) are considered. Basic aspects of computer routines are analyzed; on this basis, requirements for processing system structure are worked out. Basic circuits of a system for processing NR signals are considered, including special processors oriented to compute correlation function or energy spectrum; their basic merits and shortcomings are analyzed. A programmable matrix-structured multiprocessor is proposed as an all-purpose special processor. Principles of operation of such processors are considered; it is shown to be highly efficient in processing NR signals.

UDC 621.3.088

QUESTIONS OF PROCESSING NONCOHERENTLY SCATTERED SIGNALS WHILE SENSING DOUBLE RADIO PULSES

[Abstract of article by O. I. Tsilyurik]

[Text] Effect of distortion of signal shape in experiments on non-coherent scattering with various receiving and processing equipment parameters are considered. Methods of correcting the results are discussed.

13

UDC 551.501.8

POSSIBLE USE OF OPTIMUM PROCESSORS FOR A SIGNAL REFLECTED ON A DISCRETE
OBJECT, TO MEASURE THE POWER OF "IONIC" COMPONENT OF NONCOHERENTLY SCAT-
TERED SIGNAL

[Abstract of article by G. N. Tkachev]

[Text] It is shown that current devices for processing echo-signal from
a point target, synthesized on basis of distribution of a signal by
modulation noise, may be used to measure the output of the "ionic" com-
ponent of a noncoherently scattered (NR) signal. Correlation function
of the modulating coefficient is defined by autocorrelation function of
thermal fluctuations of electronic concentration of the ionosphere, the
law of intrapulse modulation of sensing pulses and the law of distribu-
tion of electrons with respect to range. Parameters of the device are
specified; the effectiveess of their use to measure power of NR signals
is evaluated.

UDC 551.501.8

POSSIBLE MEASURING OF THE "ELECTRONIC" COMOPNENT OF A NONCOHERENTLY
SCATTERED SIGNAL TO SENSE THE IONOSPHERE WITH BROAD-BAND PULSES

[Abstract of article by G. N. Tkachev and A. A. Martynov]

[Text] Expressions are derived and analyzed for signal-to-noise ratio
(in power) at the output of the linear part of a receiver matched with a
sensing pulse. It is revealed that while sensing the ionosphere with
pulses having linear frequency modulation (LFM), the signal-to-noise
ratio can be higher than in the case of sensing with a "smooth" pulse of
the same length by a factor of $\triangle FT$, where F is deviation of the LFM
pulse; T is pulse length. Resolution of LFM pulse in terms of range
deteriorates by a factor of $\triangle FT$ and is determined only by length of the
LFM pulse.

UDC 551.510

PHASE-MANIPULATED SIGNAL FOR NONCOHERENT SENSING OF THE IONOSPHERE

[Abstract of article by V. T. Sarychev]

[Text] The possible use of phase manipulated signals for noncoherent
sensing of the ionosphere is considered. Expressions are derived which
establish a link between signal parameters at the output of the re-
ceiving/processing installation for complex signals and the concentra-
tion and spectrum of fluctuations in electron concentration. Results of
calculation are cited in graphic form, illustrating expressions for
Barker, Longer codes and M-sequences. Analysis of results of calcula-
tion produces negative conclusions: enhancement of altitude resolution
for measurement of electron concentration is achieved at the cost of
loss of information about layer temperatures.

14

UDC 621.371+550.388

MULTIPARAMETRIC EVALUATION OF SIGNALS OF NONCOHERENT SCATTERING

[Abstract of article by I. N. Presnyakov, S. S. Smol'yaninov,
A. N. Blinkov and M. I. Kochkin]

[Text] Algorithms of multiparametric evaluation of the state of the
ionosphere obtained via maximization of the probability function of
noncoherently scattered (NR) signals are investigated. It is shown that for
a small signal-to-noise ratio, the procedure of seeking evaluations of
ionosphere parameters reduces to measurement of the correlation function
(energy spectrum) of NR signals and subsequent minimization of the quad-
ratic form of measured function and its model. An algorithm of matrix
filtration is derived which permits enhancement of the informativeness
of measurements of parameters of a nonhomogeneous ionosphere. Results
of mathematical simulation are cited.

UDC 551.510:621.396

METER RANGE NONCOHERENT SCATTERING RESEARCH COMPLEX

[Abstract of article by V. I. Golovin]

[Text] Basic parameters and structural diagram of a special noncoherent
scattering complex are cited. A description of its operation and quoted
research are explained as report summaries; in this connection refe-
rences are given to the literature which contains more questions on this
report in terms of equipment and methods of measurement.

UDC 550.388.2

RESULTS OF STUDY OF THE F2 REGION BY NONCOHERENT SCATTERING

[Abstract of article by D. A. Dzyubanov]

[Text] Results of measurements of electron concentration, electronic
and ionic temperatures obtained in Kharkov Polytechnical Institute's
measurement complex for individual days in the winter and summer of 1975
are cited.

15

UDC 621.371.165

SCATTERING OF ELECTROMAGNETIC WAVES ON RANDOM HETEROGENEITIES IN THE
IONOSPHERE

[Abstract of article by A. G. Tyzhnenko, N. A. Khizhnyak and
G. K. Solodovnikov]

[Text] Assuming that heterogeneities of electron concentration in iono-
spheric plasma have a sharp ellipsoidal boundary, an exprsssion is ob-
tained for mean effective dielectric permeability of plasma with fluc-
tuating heterogeneities. By given formula is calculated the total cross
section of scattering of electron waves on random heterogeneities. It is
necessary to consider scattering on turbulent heterogeneities to in-
terpret vertical distributions of electron concentration obtained by the
method of noncoherent scattering of radio waves in the auroral zone.

UDC 621.371

EFFECT OF IONOSPHERIC HETEROGENIETIES ON OPERATION OF THE ANTENNA OF
NONCOHERENT RADIO WAVE SCATTERING STATION

[Abstract of article by A. S. Shchennikov]

[Text] The function of three-dimensional coherence is found for spheri-
cal waves passing through a layer of anisotropic ionospheric hetero-
geneities. Change in mean beam pattern is analyzed with respect to the
output of the antenna of a noncoherent scattering station in the azi-
muthal plane as a function of the characteristics of ionospheric hetero-
genities.

16

FOR OFFICIAL USE ONLY

UDC 550.388

STUDY OF IONOSPHERE BY NONCOHERENT SCATTERING OF RADIO WAVES (REVIEW)

[Abstract of article by B. Ye. Bryunelli]

[Text] A review of foreign publications. Basic attention is paid to
results obtained in recent years: construction of models of thermosphere
and thermospheric circulation. MS-NR model, constructed on basis of
mass spectrometric measurements from satellites and data of noncoherent
scattering seems to be best method proposed. Subsequent research re-
fined nature of dependence of model parameters as a function of ac-
tivity. Observation of motion of air masses over NR stations esta-
blished the dominating harmonics of the wind system; its correspondance
to daily geomagnetic variation is shown. The wave nature of the vertical
distribution of winds determines wind shifts creating not only sporadic
layers, but also the intermediate layers in nighttime middle-latitude
ionosphere detected by the NR method. General tendency of development
of research by NR method is an even greater departure from traditional
ionospheric research of electron density distribution.

8617
CSO: 1860/37

FOR OFFICIAL USE ONLY

FOR OFFICIAL USE ONLY

UDC 550.388.2+621.396.24

HIGH LATITUDE PROPAGATION OF DECAMETER RADIO WAVES

Moscow RASPROSTRANENIYE DEKAMETROVYKH RADIOVOLN V VYSOKIKH SHIROTAKH in
Russian 1981 (signed to press 27 Mar 81) pp 2-5, 179-180

[Annotation, introduction and table of contents from book "Propagation
of Decameter Radio Waves in High Latitudes" by Donat Vladimirovich Bla-
goveshchenskiy, Izdatel'stvo "Nauka", 750 copies, 180 pages]

[Text] Based on signal representation, the features of propagation of
decameter radio waves in high latitudes are considered in the book. The
results of comprehensive experiments on radio routes having various
orientations toward the aurora borealis zone are presented. Research is
based on all geophysical and radiophysical methods. In the first case,
the study object is the polar ionosphere, its fine structure; in the
second case, properties of signals after ionospheric reflection, as a
randomly nonhomogeneous medium. Patterns between the statistical char-
acteistics of signals in radio channels and parameters of the high lati-
tude ionosphere as a function of time of day, season, solar activity,
degree of ionospheric perturbation, etc. are cited. Considerable at-
tention is given to methods of rapid prognosis of abnormal states of the
ionosphere and radio channels according to signal transmittance monitor-
ing, radio noise levels, angular sensing data and ionospheric condi-
tions. Questions of simulation of radio wave propagation using com-
puterized trajectory parameter plotting are discussed. Problems of
enhancing the reliability of radio communications in the higher lati-
tudes are discussed.

The book may prove useful to science workers and specialists in iono-
spheric studies, radio wave propagation and radio communications.

Fifteen tables; 56 figures; 377 references.

Introduction

The pattern of human activities in the Far North (and South) has given
impetus to new studies in the propagation of decameter radio waves in
these regions. Experimentally obtained data on the transmittance of
radio signals in high latitude ionospheric radio channels in response to
various geophysical influences is a major scientific interest: theo-
retical models of such channels are not always valid. On the other
hand, the problem of guaranteeing stable radio communications in the
high latitudes is very important. This also involves observing processs

18

FOR OFFICIAL USE ONLY

identified as solar-terrestrial communications which occur in the atmosphere and magnetosphere of the earth under the influence of the sun. These processes have a direct effect on propagating radio waves in various ranges. On the other hand, the problem of guaranteeing stable radio communications in the high latitudes is extremely important. As we know, for the decameter range the transmission of signals largely depends on the state of the medium of propagation. The latter, in turn, is subject to various high latitude effects and phenomena. Thus to take advantage of decameter waves in comparison to waves of other ranges, their propagation should be thoroughly studied in high latitudes and only then should radio communications be developed.

The complexity of the problem is that the space and time distribution of basic parameters of the polar and subpolar ionosphere indicate a lack of isotoropic conditions affecting propagation. Anisotropy is due to the presence of zones of maximum auroral activity, subauroral red arcs, the nonhomogeneous ionospheric structural band, the primary ionization gap, etc. All of these phenomena are governed by the state of the geomagnetic field. Estimating changes in the ionosphere due to geomagnetic activity is difficult because we lack knowledge of the mechanics of interaction between various geophysical phenomena. Consequently, a study of the propagation of decameter radio waves in high latitudes requires a comprehensive examination of the behavior of key parameters of radio signals along various radio routes and their comparison with geophysical concepts. Similar problems have been solved in both the USSR and abroad. Research findings have been published in scientific periodicals, as a rule as separate articles, reports, summaries, and accounts. We should note that in most cases these studies have one main direction, either considering the actual conditions of propagation without the physics of the effect, or ionospheric processes which only have an indirect effect on propagation. The comprehensive description is comparatively small and few studies can be found which summarize scientific advancements in this field.

In this respect, the present monograph attempts to partially fill in this gap. It tries to explain the extent to which statistical characteristics of radio signals depend on the range and bearing of the propagation route, operating frequencies, time of day, season, degree of magnetic activity, etc. It is important to understand the essence and meaning of mechanisms which affect signal propagation, considering external geophysical factors, so that these general patterns can be extended to similar radiolines in high latitudes. A comprehnsive study of the problems (using radiophysical and geophysical methods) not only clarifies the physical situation of conditions of radiowave propagation, but may also serve as a starting point for predicting transmission of frequencies and planning of radio communications. Material presented in the book is mainly based on experiments conducted in northern Siberia (Taymyr Peninsula).

19

In the first chapter, primary attention is given to the structure of the ionosphere and space-time variations: the main electron gap, sporadic ionization in E and F regions of the ionosphere, perturbation in the D region, altitude dependencies of the electron concentration. The characteristics of the fine structure of the ionosphere are analyzed in terms of test data in high latitude routes under various geophysical conditions, specifically during subgales.

The second chapter is devoted to the properties of high latitude radio channels. Indiators characterizing the non-steady state of channels are first discussed (as illustrated by auroral routes during subgales). The distributive functions of signal amplitudes for rapid and slow signal fluctuations are considered from general positions. Statistics are cited for parameters of this function in the routes. Experimental research on the characteristics of the selective properties of channels with respect to time, frequency and space are evaluated; at the same time, several parameters for high latitudes, their comparison with theoretical values and their difference from middle-latitude values are examined. In conclusion transmission functions of radio channels (as linear systems) are analyzed for four groups of test energy spectra of signal fluctuations.

In the third chapter are presented materials of experimental research on the statistical characteristic of signals and radio noises in six high latitude radio routes in Siberia. Primary attention is focused on diurnal and seasonal variations in parameters, the effect of subgales and geomagnetic activity at the signal and noise level is analyzed in detail. Trajectory characteristics of radio beams on a route situated in a zone of auroral ionization to the north of the primary electron gap are considered.

The fourth and last chapter is related to questions of radio communications. Methods of research of precursors of ionospheric perturbation are discussed for prediction of communication conditions. The current role of angular sensing of the ionosphere for arranging radio communications is shown. Advantages of automated communications systems in high latitudes are analyzed based on the specifications of the propagation medium. Notions about using antenna systems, method of separate reception and conditions of transmission of radio frequencies in high latitude radio routes.

In conclusion, the author expresses his indebtedness to N. M. Yerofeyev, corresponding member of the Tadzhik SSR Academy of Sciences for his continuous attention to the work, V. M. Driatskiy, editor of the book and doctor of physico-mathematical sciences for his valuable comments during preparation of the material and to G. A. Zherebtsov, candidate of physico-mathematical sciences for collaboration in conducting the experiments.

20

FOR OFFICIAL USE ONLY

Table of Contents

21

FOR OFFICIAL USE ONLY

FOR OFFICIAL USE ONLY

COPYRIGHT: Izdatel'stvo "Nauka", 1981

8617
CSO: 1860/49

22

FOR OFFICIAL USE ONLY

UDC 621.371

SHORT- AND ULTRASHORT-WAVE PROPAGATION

Moscow RASPROSTRANENIYE KOROTKIKH I UL'TRAKOROTKIKH RADIOVOLN (MASSOVAYA
RADIOBIBLIOTEKA, VYPUSK 1034) in Russian 1981 (signed to press 5 Jun 81)
pp 2-3, 80

[Annotation, foreword and table of contents from book "Short- and Ultrashort-
Wave Propagation", by Galina Petrovna Grudinskaya, Izdatel'stvo "Radio i
svyaz'", 50,000 copies, 80 pages]

[Text]   Annotation

This book presents basic information on shortwave and ultrashort wave
propagation. Problems involving long-distance reception of television
and amateur radio are examined. The second edition was published in 1960.
The present edition has been supplemented with information on radio wave
propagation in space and using satellites to relay radio waves.

The book is intended for trained radio amateurs. [The book was reviewed by
A.N. Shcherbitskiy].

                              Foreword

Questions of the propagation of short and ultrashort waves have been
developed further since the publication of the last edition of this book.
Completely new areas have appeared in the science and practice of radio
wave propagation: propagation in space; utilization of earth satellites to
relay radio transmissions; and investigating the surface and atmosphere of
the earth and other planets using radio technical methods. Conceptions of the
propagation of radio waves in the shortwave band have been extended and
developed further.

These and other achievements in the area of radio wave propagation are of
major interest for a broad group of radio amateurs. Therefore, the third
revised and supplemented edition of the book devotes a significant amount of
space to new data on radio wave propagation, describes methods for experimental
ionospheric research in more detail, provides expanded material on super-long
range ultrashort wave propagation, and contains a chapter on radio wave pro-
pagation in space.

23

A great deal of theoretical and experimental research has been devoted to the study of ultrashort wave propagation. The soviet scientists B.A. Vvedenskiy, V.A. Fok and M.A. Kolosov have made a major contribution to this matter; work in this area continues today. New types of ultrashort wave applications are being sought out continually. Long-range ultrashort wave radio communication utilizing scattering of radio waves on heterogeneities in the troposphere and ionosphere, and using radio wave reflection from meteor trails, has been developed. Satellite relay of radio communications and television transmission has been accomplished. Soviet scientists have been able, for the first time in the history of mankind, to transmit images from the backside of the Moon to the Earth. Significant successes have been achieved in studying the surface and atmosphere of Venus and Mars. This evidences the urgency of the problems of radio wave propagation, especially ultrashort wave.

The book uses mainly the name for the radio wave bands which has been established in the radio amateur literature -- short, ultrashort -- and indicates their name according to the new standard.

Radio amateurs were the pioneers in shortwave communications. Through their efforts they promoted expansion of information on ultrashort wave propagation, and their experiments in long-distance television reception are providing valuable material for new scientific generalizations.

The present book, expanding the field of view of radio amateurs in the area of radio wave propagation, will facilitate their further active work in mastering new bands and conducting experiments in long and super-long range television reception.

Table of Contents

24

FOR OFFICIAL USE ONLY

FOR OFFICIAL USE ONLY

COPYRIGHT: Izdatel'stvo "Radio i svyaz'", 1981.

6900
CSO: 1860/130

ANTENNA ARRAYS: TRIAL CLASSIFICATION

[Article by A.R. Vol'pert]

[Text]   A classification is given for antenna arrays which is based
         on the most characteristic features: geometrical, electrical
         and functional. Further development of the classification
         is possible as array theory and technology develops. The
         classification is useful for drafting monographs on arrays
         and in developing scientific programs; it is especially needed
         in compiling terminological glossaries.

General considerations. Antenna arrays differ from all other antenna devices
in their relatively greater flexibility and multifaceted nature. Antenna
arrays can be defined as a combination of radiating (receiving) elements which
are arranged in some manner and excited by one source or a group of coherent
sources[1].

As we know, the operating flexibility of antenna arrays results from the
capability of configuring them in different ways, as a result of which they
can be deployed on bodies with complex shapes. The required directivity pattern
can be achieved by appropriate phasing of the currents (or fields) in the
elements. Adjustable phasing makes it possible to change the patterns of arrays
rapidly, and in a special case makes electrical scanning possible.

Multi-element construction of arrays and element-by-element processing makes
possible more effective use of the information from the waves incident on the
array; the same sort of processing is possible during transmission, and various
adaptation and self-guidance methods result in multifunctional array utilization.
It is also possible to increment the radiated power by adding amplifiers to the
element circuits; this use of amplifiers is also possible during reception. The
efficiency of the entire antenna can be increased in both cases. Methods are
also being developed for using arrays during reception to convert the incident
wave energy to dc.

The numerous varieties of arrays and their broad capabilities have long required
the establishment of an appropriate classification. However, the primary

attention in available publications is devoted to geometric features [1], or to features which poorly reflect the characteristic singularities of the arrays [2].

The present article proposes a classification (cf. diagram) which is based on three groups of features: geometrical, electrical and functional with no loss of systematicity, no clear boundaries between them (especially between the last two). However, these groups are arranged sequentially in the diagram (and are set off there by circles).

The features within corresponding groups can be further developed (and refined) through parallel development of the classification; this makes it possible to introduce new features when necessary, thus expanding it (indicated in the diagram by broken lines).

Geometric features. The simplest features are those which characterize the general shape of the arrays and the arrangement of the elements. Therefore, we sometimes see excessive efforts to enumerate the largest possible number of different shapes.

Although array geometry affects their electrical properties to some extent, it is still advisable to limit ourselves to typical configurations, since various modifications of known shapes produce no qualitative changes in the electrical picture. Therefore, the diagram uses as a basis arrays in which the elements are arranged in a line or on the surface.

Volumetric arrays are presented only to complete the picture. In principle, the third dimension in these arrays can be used to form a "reflecting screen effect", making it possible to orient one-way radiation in any direction [3, volume II, page 67, 4]. However, the difficulties in making up the corresponding excitation circuits makes the construction of these arrays extremely laborious (cf. Lüneberg lens below).

Geometric features also include the positioning of the elements. The classification gives the best-known cases, and others can be added as necessary.

Electrical features. The basic division of arrays here is into passive and active (the latter means arrays which contain amplifying, oscillating or converting devices). These devices may be contained in each radiating (receiving) element, or in individual groups of elements[2].

The further features define the methods of exciting (feeding) the array elements. There are two main excitation methods: feeder, in which the array elements are excited by multi-port networks formed of coaxial feeder segments, waveguides or other lines, and spatial, in which the elements are excited by an omnidirectional source such as a horn, reflector, etc.[3]. Both of these methods can be combined.

(1) Антенные решетки

(2) Линейные (3) Поверхностные (4) Объемные

(5) Прямолинейные Дуговые Кольцевые (6) (7) Плоские (8) Цилиндрические (9) Сферические (10)

(11) Эквидистантные Неэквидистантные (12) Разреженные (13) Со случайным распределен. (14)

(15) Пассивные Активные (16)

(17) Фидерное возбуждение (18) Пространств. возбуждение (19) Комбинированное возбуждение

Параллельное (20) Последовательна (21) Проходное (22) Отражательное (23)

Вибраторные (24) Щелевые (25) Волноводные (26) Рупорные (27) Диэлектрические (28) Директорные (29)

(30) Передающие Приемопередающие (31) Приемные (32)

(33) Формирующие фиксированные диаграммы (34) Управляющие положением диаграмм

Одно-диаграммные (35) Много-диаграммные (36) Электромеханическим сканированием (37) Электрическим сканированием (38)

Механическое управление фазой (39) Электрическое управление фазой (40)

Матрица Бласса (41) Матрица Батлера (42) Изменением дисперсии (43) Фазовращателями (44)

(45) Фазовращатели (46) Временная задержка (47) Частотное (48) Лазичное преобразование частоты (49)

(50) Решетки с обработкой сигналов

Адаптивные (51) С поэлементной обработкой (52) С синтезированием апертуры (53) С нелинейной обработкой (54) С изменяющимися во времени параметрами (55) Ректенны (56)

Самофокусирующи (57) Переизлучающи (58) Оптическая (59) Цифровая (60) Перемножением (61) Корреляция (62) Логическ синтез (63) Проблема дифф (64) Переключение элементов (65) Изменение ДН (66)

[Key on following page]

Key:
1. antenna arrays
2 linear
3. surface
4. volumetric
5. rectangular
6. curved
7. round
8. planar
9. cylindrical
10. spherical
11. equidistant
12. non-equidistant
13. sectioned
14. randomly distributed
15. passive
16. active
17. feeder excitation
18. spatial excitation
19. combined excitation
20. parallel
21. serial
22. straight-through
23. reflecting
24. dipole
25. slot
26. waveguide
27. horn
28. dielectric
29. director
30. transmitting
31. transceiving
32. receiving
33. producing fixed patterns

34. controlling pattern position
35. single-pattern
36. multi-pattern
37. electromechanical scanning
38. electrical scanning
39. mechanical phase control
40. electrical phase control
41. Blass matrix
42. Butler matrix
43. by varying dispersion
44. by phase inverters
45. by phase inverters
46. time delay
47. frequency
48. dual frequency conversion
49. at i-f
50. single-processing arrays
51. adaptive
52. element-by-element processing
53. synthetic aperture
54. nonlinear processing
55. time-varying parameters
56. rectennas
57. self-focusing
58. re-radiating
59. optical
60. digital
61. multiplication
62. correlation
63. logical synthesis
64. length modulation
65. element switching
66. directivity pattern variation

Of the several varieties of feeder excitation, we make note here of parallel and serial. Spatial excitation is divided into straight-through and reflected. In straight-through excitation, the radiation source excites the receiving elements of the array which transmit power through transfer devices to the radiating elements; in reflected excitation the array elements re-reflect the radiation field in some direction, depending upon the phasing of the elements, i.e., they act as transceivers.

The general electrical features culminate in the type of actual elements (radiators). The classification gives only some of the most widely used reflectors (dipole, slot, waveguide (open-ended), horn, dielectric, director).

Functional features. The capabilities of antenna arrays result in a more
complicated picture when classifying them in terms of functional features.
Arrays are first divided in terms of transceiving functions. They are then
divided into arrays which:

-- form patterns with fixed position relative to the array aperture;

-- control the position of the patterns, i.e., scan;

-- process the signals.

Arrays which produce fixed patterns include both single-pattern arrays which
were in use in the 1920's ("Telefunken"-type antennas [5, page 289]), as well
as modern multi-pattern structures for direction-finding tasks and for
parallel or switched spatial scanning in radar. Single-pattern arrays may
differ in the configuration of the patterns and their positioning with
respect to the aperture. Multi-pattern arrays differ mainly in the
arrangement of the pattern-formation circuits (the term "circuits" is under-
stood in the broadest sense, e.g., in the form of a Lüneberg lens with an
array of independent radiators [6, Figure 13-15])[4]. Of the pattern-forming
circuits, we have shown serial ones (Blass matrix [6, Figure 14-13]) and
parallel ones (Butler matrix [6, Figure 14-14]). No division is given for
arrays which form patterns in the same plane or in space.

Arrays with controllable pattern position are divided into electromechanically-
scanning arrays and electrically-scanning arrays. The classification does not
include so-called mechanical scanning done by turning or rotating the entire
array, since this is not associated with the arrangement of the array, but of
the facility within which it is used.

A variety of features resulting from different methods of controlling the
current (or field) phases in the array elements is characteristic for
electrically-scanning arrays[5].

The classification includes the following:

-- electrically controlled phase inverters;

-- time delays for wideband scanning, when the phase shift occurs in real
time without "phase reset" [8, page 38];

-- frequency method, by changing the phase velocity of propagation in the
feed circuit;

-- dual frequency conversion using an auxiliary local oscillator [3, volume III,
page 306; 9, page 382];

-- intermediate-frequency phase control [10, page 343]. The number of methods
can be increased, and detailed further. Some of the electrical control methods

given in the classification can also be implemented with mechanical devices.

So-called signal-processing arrays hold an important place in terms of functional features. We have in mind various special types of preliminary processing which the signals undergo, mainly during reception, before they are combined in a common channel, in contrast to simple direct addition of the signals from all of the elements[6]. The broken line which connects with the transmitting arrays indicate that some types of processing can also be done during transmission.

In terms of processing methods, arrays can be subdivided into:

-- adaptive;

-- arrays with element-by-element processing;

-- with synthetic aperture;

-- with nonlinear processing;

-- with time-varying parameters;

-- with element-by-element rectification of incident wave in receiving arrays.

Adaptive arrays are defined as antennas whose parameters are automatically adjusted to meet assigned requirements when the transmission or reception conditions change. In self-focusing arrays, automatic adjustment is provided by phased addition of the signals from all of the elements with a complex incident-wave phase front and different phase errors occurring within the arrays themselves [3, volume III, page 383]. In transceiving-radiating arrays (or Van Ett arrays), the received signals are re-radiated back in the direction of the signal source [3, volume III, page 411].

The use of arrays with element-by-element processing makes it possible to make fuller use of the information contained in the incident wave. This is a relatively new area in antenna enginnering; therefore, it will be refined and expanded in the classification. The classification now contains coherent optical and digital processing. In optical processing, like in the aforementioned multi-pattern construction using matrix circuits, a group of patterns can be formed simultaneously [14; 12, page 60; 13, page 124]. The optical processing of the signals coming from the array elements is analog, and allows large amounts of information to be processed without scanning at extremely high speeds. In digital processing, the signals coming from the array elements first undergo analog-digital conversion, followed by processing according to some algorithm. [14, 15].

Synthetic-aperture arrays [16], in contrast to those which simultaneously use the information coming from all elements, include arrays which sample the elements sequentially, then add the signals together through corresponding

time-delay devices[7]. In this case, the processing can be done by various methods, especially optical [18]. The classification of these arrays may be detailed further in terms of the methods used to form the synthetic aperture.

The use of strictly linear combinations of signals from the array elements limits the shape of the patterns obtained. Array capabilities are expanded with nonlinear signal processing, for which the following are typical: multiplication of signals from individual elements, division of signals, raising signals to a power, multiplication followed by averaging, i.e., correlation, etc. [19, page 306]. The Mills cross is a simple example [17, page 125]. Nonlinear processing also includes so-called logical synthesis, in which the main controlling factor is usually the received signal, depending upon the level of which the individual sections comprising the array are activated or deactivated [19, page 301; 20, page 327].

Further expansion of array capabilities involves introducing time as an additional controllable parameter. Arrays with time-variable parameters belong to an area which is relatively undeveloped. At present, it is difficult to provide a detailed classification of the varieties of such arrays; however, we can point out modulation of the effective array length in order to reduce the side lobe level [3, volume III, page 355; 10, page 349], as well as sequential activation of elements [21] located along some length[8] (so-called "Doppler arrays" [22, page 85]). In general, the overall pattern of an array, and its phase pattern in particular, change over time due to variation over time of the parameters which influence the field. If the phase pattern depends upon the angular coordinates of the observation point, the instantaneous frequency of the radiation field changes, thus becoming a function of the angular coordinates. As a result of this, the radiation field undergoes "frequency painting". Because of the mutuality principle, the instantaneous frequency of the emf at the output of the receiving antenna during reception, in turn, depends upon the position of the source of the wave with respect to the antenna[9]. These circumstances can be used to solve direction-finding problems.

Signal-processing arrays also include receiving arrays in which each receiving element is loaded to a rectifier, so that "processing" consists of both rectification and later addition of the dc energy caused by the incident wave. These arrays have come to be called rectennas.[26-28].

FOOTNOTES

1. "Element" here is understood in the broad sense, in which it may be implemented in a complex manner and, in particular, can itself be an array.

33

2. In the latter case, it is incorrect to characterize the array as "semi-active".

3. Spatial excitation is sometimes called "optical". We do not feel that this definition is correct.

4. A Lüneberg lens excited by a group of radiators can be considered as an example of a volumetric array.

5. In contrast to the expression "electronic scanning" which is sometimes used, the term "electrical scanning" [7] encompasses all cases in which the phase state caused by scanning is changed by means of electrical devices.

6. Although, of course, this addition is also a type of processing.

7. In radio astronomy, this type of synthesis is called "aperture synthesis" [17].

8. The picture of the phenomena here is different from that occurring during length synthesis (cf. above). However, the possible degree of angular resolution during direction finding remains the same for different array lengths [23; 24, page 117].

9. The mutuality principle is known for systems which have time-constant parameters. However, [25] shows that this principle is retained when time dispersion is present in the media.

BIBLIOGRAPHY

1. Reznikov, G.B. RADIOTEKHNIKA, Vol 31, No 3, 1976.

2. Kyun, R. "Mikrovolnovye antenny." [Microwave antennas]. Moscow, Izdatel'stvo Sudostroyeniye, 1967.

3. "Skaniruyushchiye antennye sistemy SVCh." [Scanning microwave antennas]. Vol II-III. Translated from English, G.T. Markov and A.F. Chaplin, editors. Moscow, Izdatel'stvo Sovetskoye Radio, 1969-1971.

4. Merkulov, V.V., Shishlov, A.V. RADIOTEKHNIKA I ELEKTRONIKA, 1980, Vol 25, No 6.

5. Dombrovskiy, I.A. "Evolyutsiya antennykh sistem. Ocherki istorii radiotekhniki." [Evolution of antenna systems. Outline of history of radio engineering]. Moscow, Izdatel'stvo AN SSSR, 1960.

6. Markov, G.T., Sazonov, D.M. "Antenny." [Antennas]. Moscow, Izdatel'stvo Energiya, 1975.

7. "Electrically-scanning antenna arrays." TIIER, Thematic edition. Vol 56, No 11, 1968.

8. Vol'pert, A.R. In "Antenny" [Antennas], No 17, A.A. Pistol'kors, editor. Moscow, Izdatel'stvo Svyaz', 1973.

9. Skol'nik, M. "Vvedeniye v tekhniku radiolokatsionnykh sistem" [Introduction to radar system technology]. Moscow, Izdatel'stvo, Mir, 1965.

10. Fradin, A.Z. "Antenno-fidernye ustroystva" [Antenna feeder devices]. Moscow, Izdatel'stvo Svyaz', 1977.

11. Lambert, Arm, Aymet. ZARUBEZHNAYA RADIOELEKTRONIKA, No 8, 1968.

12. Svet, V.D. "Opticheskiye metody obrabotki signalov" [Optical signal processing method]. Moscow, Izdatel'stvo Energiya, 1971.

13. "Antenny (sovremennoye sostoyaniye i problemy)" [Antennas (current status and problems)]. L.D. Bakhrakh and D.I. Boskresenskiy, editors. BIBLIOTEKA RADIOINZHENERA, No 16. Moscow, Izdatel'stvo, Sovetskoye Radio, 1979.

14. Dadzhon. TIIER, Vol 65, No 6, 1977.

15. Bogachev, A.S. RADIOTEKHNIKA, Vol 33, No 6, 1978.

16. Karavayev, V.V., Sazonov, V.V. "Osnovy teorii sintezirovannykh antenn" [Fundamentals of theory of synthetic antennas]. Moscow, Izdatel'stvo Sovetskoye Radio, 1974.

17. Yesepkina, N.A., Korol'kov, D.V., Pariyskiy, Yu.N. "Radioteleskopy i radiometry" [Radio telescopes and radiometers]. Moscow, Izdatel'stvo Nauka, 1973.

18. Katron, Leyt, Porchello, Vivian. TIIER, Vol 54, No 8, 1966.

19. "Antennye reshetki" [Antenna arrays]. L.S. Benenson, editor. Moscow, Izdatel'stvo Sovetskoye Radio, 1966.

20. Kocherzhevskiy, G.N. "Antenno-fidernye ustroystva" [Antenna feeder devices]. Moscow, Izdatel'stvo Svyaz', 1972.

21. Prokynin, L.M. RADIOTEKHNIKA I ELEKTRONIKA, Vol 10, No 2, 1965.

22. Boldin, V.A. "Radiotechnical devices for air traffic control."
    ITOGI NAUKI I TEKHNIKI, SER. RADIOTEKHNIKA, Vol 10, Book 1. Moscow,
    Izdatel'stvo VINITI, 1976.

23. Urkovits, Khatser. Koval'. TIRI, Vol 50, No 10, 1962.

24. Vakman, D.Ye. "Slozhnye signaly i printsip neopredelennosti v radio-
    lokatsii" [Complex signals and principle of ambiguity in radar]. Moscow,
    Izdatel'stvo Sovetskoye Radio, 1965.

25. Kazyulin, A.F. RADIOTEKHNIKA I ELEKTRONIKA, Vol 10, No 1, 1965.

26. Braun. ZARUBEZHNAYA RADIOELEKTRONIKA, No 8, 1970.

27. Gutmann, R.J., Borrego, J.M. Trans. IEEE, 1979, v. MTT-27, No 12.

28. Remizov, V.A., Klassen, V.I., Shishlov, A.V. ZARUBEZHNAYA RADIOELEKTRONIKA,
    No 5, 1980.

6900
CSO: 8144/0486

BROADCASTING, CONSUMER ELECTRONICS

UDC 621.314.632:621.374

SEMICONDUCTOR CONVERTERS IN THE CHARGE SYSTEMS OF RESERVOIR CAPACITORS

Leningrad POLUPROVODNIKOVYYE PREOBRAZOVATELI V SISTEMAKH ZARYADA NAKOPITEL'NYKH KONDENSATOROV in Russian 1981 (signed to press 17 Feb 81) pp 2-5, 156

[Annotation, foreword and table of contents from book "Semiconductor Converters in the Charge Systems of Reservoir Capacitors", by Vladimir Aristarkhovich Knysh, reviewed by V. A. Galanov, Energoizdat, 6500 copies, 160 pages]

[Text] This book deals with the analysis, calculation and description of semiconductor converting devices for charging reservoir capacitors in power supply systems of pulsed electrical installations. It presents the theory of electromagnetic processes in converters, examines circuit designs which are optimal with respect to the minimum weight criterion when supplied from independent sources; examples of computations are given.

This book is intended for use by engineers and technicians specializing in the area of power and semiconductor engineering and can also be useful to senior students studying industrial electronics.

Foreword

Electrical installations and devices using electric energy accumulated in electrical fields of capacitors are being used more and more widely in modern engineering. Such installations and devices serve for pumping pulsed quantum oscillators, and for creating the electrohydraulic effect, pulsed acceleration of plasma, and strong short-term magnetic fields.

The development and improvement of installations and devices using energy accumu-. lated in capacitors make it necessary to develop charge systems for reservoir capacitors and to study the processes in these systems in order to raise the energy indexes and to reduce their weight and dimensions. Of particular interest are the least developed methods of calculating converters ensuring the charge of reservoir capacitors in the interval of time corresponding to a large number of voltage periods of the source.

At the present time there are no books available to broad sections of engineers and technicians engaged in the designing in this area in order to familiarize themselves with basic ideas and methods of constructing and designing converters in systems of energy transmission to reservoir capacitors periodically discharged to pulsed loads.

37

There are published descriptions and studies on very different circuits of semiconductor converters in charge systems of reservoir capacitors. However, in the majority of the works studies are limited to the determination of the time necessary for charging the capacitor to the prescribed voltage. As a rule, energy indexes are not examined or are determined on the basis of experimental data. The known studies on capacitors are very scattered in nature and make it impossible to perform comparative evaluation of various circuits by the energy indexes.

Rational selection of a circuit variant of a converter in the charging system of a reservoir capacitor, as well as the determination of optimal parameters of the elements of the capacitor can be done only on the basis of theoretical studies. The considerable gap between the theoretical principles of designing converters in the above systems and the practice of their development often lead to decisions which are far from optimal. An attempt was made in this book to fill this gap to some extent. Most of the results of studies and methods of calculations based on these results are being published for the first time.

The analysis of the electromagnetic processes in nonlinear circuits of converters was done by computers, which made it possible, unlike the presently known works dealing with converters of this class, to reveal the dependence of energy indexes on the parameters of elements for a number of circuits. The quantitative results of the analysis were obtained in a normalized form as graphs and make it possible to determine optimal values of the parameters of the elements of converters in the processes of designing by simple calculations. In order to facilitate the use of the results of this work, examples are given for calculating the parameters of the basic elements of the examined circuits of converters.

The first chapter of the book is an introductory chapter. It briefly examines the areas of the applications of charging systems of reservoir capacitors, gives the characteristics of individual sections of systems and charging methods, and surveys circuits of converters in these systems and methods analysis of electromagnetic processes.

The second and third chapters examine the processes in semiconductor converters with current-limiting linear chokes and reactive quadripoles. The special characteristics of the processes in these converters predetermine the expediency of their use when they are fed from networks or from high-power sources. Here, the studies are based on the maximum efficiency criterion. Installed capacities of the main elements of converters are also determined.

The fourth chapter deals with studies of semiconductor converters in systems with limited-power independent sources. The studies and calculations are based on the criterion of maximum utilization of the installed capacity of the independent source.

The methods of designing substantiated and presented in this book make it possible to calculate and select elements of converters working in the range of a medium power intake -- to several dozens of kilowatts; the overall results of the analysis of electromagnetic processes in the devices of the class being examined are also applicable for a broader power range.

In order to reduce the size of the book, it does not include the methods of determining and reducing losses in semiconductor power devices operating in the switching mode which are widely known from published literature.

The author is grateful to the reviewer, Candidate of Technical Sciences V. A. Galanov, for many valuable comments which were taken into consideration in the final revision of the manuscript.

<table>
<tr><td>Contents</td><td>Page</td></tr>
</table>

UDC 621.396.62:621.382

SENSITIVITY OF SOLID-STATE RADIO RECEIVING DEVICES

Moscow CHUVSTVITEL'NOST' RADIOPRIYEMNYKH USTROYSTV NA POLUPROVODNIKOVYKH
PRIBORAKH in Russian 1981 (signed to press 5 Mar 81) pp 2-4, 165-166

[Annotation, foreword and table of contents from book "Sensitivity of Solid-
State Radio Receiving Devices", by Zinoviy Nikolayevich Muzyka, Izdatel'stvo
"Radio i svyaz'", 16,000 copies, 167 pages]

[Text]   Annotation

This book contains a systematic exposition of questions associated with estimat-
ing the sensitivity of radio receiving devices and analyzing the noise character-
istics of stages built with semiconductors (transistors and one-port networks
with negative resistance). The basic sources of internal noise in bipolar and
field-effect transistors, solid-state diodes and their equivalent noise circuits
are examined. The noise factor is examined as a function of frequency, feed-
back and operating state of stages, with examples of calculation given.

The book is intended for engineers involved in designing low-noise radio receiv-
ing devices.

Foreword

The sensitivity of modern radio receiving devices is determined primarily by
the inherent noise of the electronic components and passive elements in the
first stages. Therefore, besides the extensive use of high frequency bipolar
and field-effect transistors in the amplifier and converter stages of radio
receivers, low-noise amplifiers using one-port networks with negative resistance
have recently come into use. The implementation of low-noise amplifiers in
input stages has opened up new prospects for constructing high sensitivity
radio receivers and for increasing the operating range of radio links.

The present book contains a systematic exposition of problems involved in estimat-
ing sensitivity and analyzing the noise factor of radio receiver stages using
transistors and one-port networks with negative feedback.

The basic sources of internal noise of semiconducting devices (diodes and transis-
tors) are examined on the basis of the physical concepts of their operation, and
methods of constructing equivalent noise circuits are given. Equivalent noise

40

circuits are constructued which include equivalent circuits of ideal semiconduct-
ing devices with no noise and noise current and voltage generators connected to the
input and output poles of these circuits. Noise generators are expressed anal-
ytically through direct currents in the initial operating state and the parameters
of the devices measured or calculated on the external poles. Basic analytical
relationships are derived on the basis of the proposed equivalent noise circuits
for determining the noise factor of amplifier and converter stages using transis-
tors and one-port networks with negative feedback. The basic relationships
between the noise factor and frequency, feedback and operating mode of the stages
are investigated. Recommendations are given on the choice of circuit elements.
The equivalent noise circuits and the analytical apparatus of the theory of
amplifier stages using one-port networks with negative feedback are as close as
possible to the circuits and apparatus used in modern amplifier theory. This
creates definite advantages in the systematic study and mastery of analysis of
amplifiers using various amplifying devices. A substantial portion of the find-
ings are supported by experimental research.

The Appendix gives the parameters of modern semiconducting diodes, plots of the
Y-parameters of high frequency bipolar and field effect transistors as a function
of frequency and operating mode (determined by current), as well as other data
needed for engineering calculations.

Table of Contents

41

COPYRIGHT: Izdatel'stvo "Radio i svyaz'", 1981

6900
CSO: 1860/114

UNIT FOR ROTATING TV CAMERA RASTER

[Article by V.I. Shamis, I.S. Serbin, V.V. Korneychuk and I.S. Zadorozhnyy]

[Text] A description is given of a sweep voltage former for a television camera employing an electrostatic vidicon, making it possible to rotate the broadcasting standard scanning raster around its geometrical center by an arbitrary angle with an angular velocity of 3 rad/s.

In the automatic recognition of objects, in observing rotating bodies and in television endoscopy it is necessary to rotate the optical image relative to the television scanning raster around its geometrical center (usually coinciding with the optical axis of the camera). The methods of mechanically rotating the television camera or special optical elements (Dove and Pekhan prisms) used in these cases have an entire range of disadvantages. These include the complexity of manufacturing high-precision electromechanical drives, the low reliability of rotating current conductors, and large overall dimensions and heavy weight of the rotating unit.

These disadvantages can be eliminated if electronic rotation of the scanning raster in the transmitting tube's photoconductive layer is used. It is inapplicable in cameras with magnetic deflection of the tube's beam because of the complexity of forming deflection current of the required form, associated with the substantial influence of the inductance of deflection coils at the line scanning frequency. In recent times in designing applied television apparatus preference has been given to simpler miniature television cameras utilizing electrostatic vidicons. In cameras of this type a rotating scanning raster with parameters conforming to the broadcasting standard can be formed by relatively simple means.

Let us discuss the design of the raster rotation unit. Using the well-known relationships between the coordinates of a point in two orthogonal systems of coordinates with combined centers and axes forming a certain angle α, it is possible to write the voltages, U_a and U_b, which must be created in the deflection plates of the vidicon for producing a raster rotated by angle α relative to the geometrical axes of the deflection system:

43

$$U_a(t) = U_{str}(t) \sin \alpha + U_{kadr}(t) \cos \alpha \, , \tag{1}$$

$$U_b(t) = U_{str}(t) \cos \alpha - U_{kadr}(t) \sin \alpha \, , \tag{2}$$

where $U_{str}(t)$ and $U_{kadr}(t)$ are the sawtooth horizontal and vertical scanning voltages, respectively.

These voltages are formed in the following manner. The angle sine and cosine data transmitter generates quasi-constant voltages proportional to these functions of angle α of rotation of the transmitter's shaft relative to a certain zero position. Line and frame integrators of these voltages, controlled by individual synchronizing pulses (SI's) and having individual time constants, form sawtooth voltages with periods of the horizontal and vertical scanning and with amplitudes proportional to the sine and cosine of the angle. These voltages are added according to equations (1) and (2) by adders. Also added to the sum are the values of the input voltage of the integrators, which makes it possible to produce in the adder's output sawtooth voltages without a direct component and eliminates displacement of the raster's geometrical center when it rotates. The signals from the outputs of the adders are amplified by paraphase amplifiers and are supplied to individual pairs of deflecting plates of the vidicon.

The circuit diagram of one possible implementation of the scanning unit is presented in fig 1.
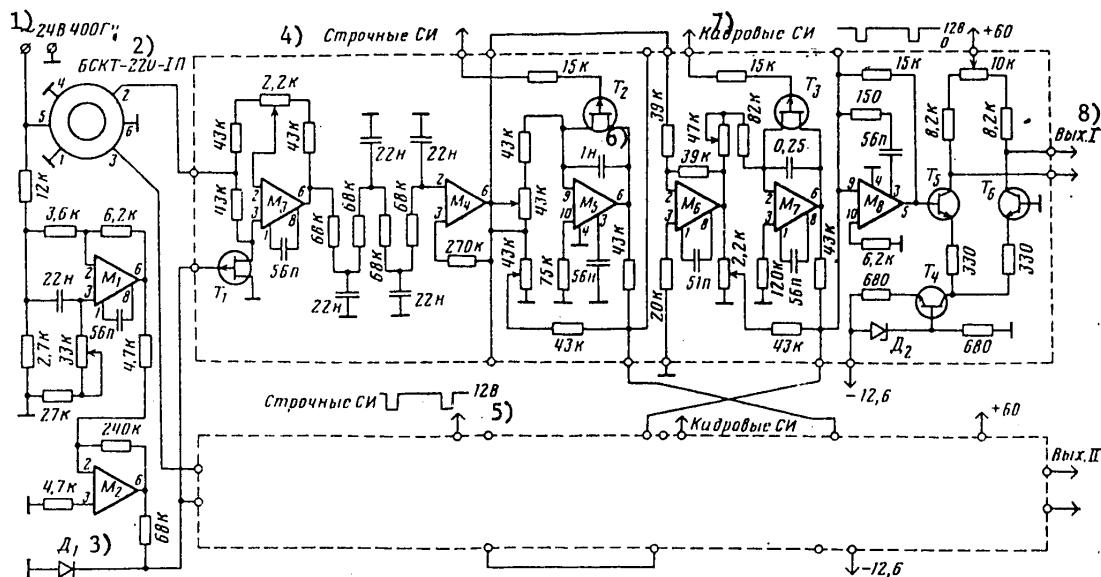
Figure 1. Circuit Diagram of Raster Rotation Unit: M_1 to M_4, M_6--K140UD6, M_5, M_8--K140UD1B; T_1 to T_3--KP103L, T_4--KT312B, T_5, T_6--KT602B; D_1--2D102A, D_2--2S133A

[Key on following page]

44

Key:
1. Approximately 24 V, 400 Hz
2. BSKT-220-IP
3. Diode
4. Line synchronizing pulses

5. 12 V
6. 1 nF
7. Frame synchronizing pulses
8. Output I

As an angle-data transmitter a BSKT-220-IP sine-cosine transformer is used whose excitation coil is supplied from a generator of sinusoidal voltage with an amplitude of 24 V and frequency of 400 Hz. The transformer's sine winding is connected to a phase detector assembled from operational amplifier M_3. The stage in M_3 is in the form of a voltage follower with a $\pm$ 1 alternating-sign transmission factor set by a switch employing field-effect transistor T_1. The switch is controlled by a square reference pulse shaper employing microcircuit M_2. The phase of pulses can be corrected by a phase shifting stage employing M_1. After passing through a multielement RC filter the constant voltage proportional to the sine of the angle of rotation of the transformer's shaft is supplied via follower M_4 to line integrator M_5. Voltage is supplied to frame integrator M_7 via inverter M_6, which makes it possible to change the sign of product $U_{kadr}(t) \sin \alpha$ in keeping with equation (2). The operation of the integrators is controlled via switches employing field-effect transistors T_2 and T_3 by individual line and frame synchronizing pulses whose length determines the length of the forward and reverse scanning strokes.

The addition of voltages is accomplished by an adder assembled from operational amplifier M_8. The output paraphase amplifier is executed according to a balanced circuit employing transistors T_5 and T_6 with a current stabilizer employing transistor T_4.

The second channel, to whose input is supplied a voltage proportional to the cosine of the angle of rotation of the transformer's shaft, is assembled according to a similar circuit. The difference is that on account of external switching of the terminals of operational amplifier M_6 it is converted into a noninverting follower, which makes possible the proper sign of the addends in the sum of (1).

In the phase detectors, followers and frame integrators 140UD6 operational amplifiers are used, which have high input impedance and built-in correction, and 140UD1B wider-band amplifiers are used in the line integrators and adders.

In the circuit presented for the data transmitter for the sine and cosine of the angle of rotation the maximum rate of rotation of the raster which does not cause noticeable geometrical distortion is approximately 3 rad/s without a limitation on the angle. It is limited basically by the time constant of the filters of the phase detectors, the reduction of which results in parasitic modulation of the raster by fluctuations in the supply frequency of the sine-cosine transformer. The rate of rotation can be increased to limits determined by the frame scanning frequency and the vidicon's lag if a function potentiometer is used as the sine and cosine data transmitter. With this the unit's circuit is simplified considerably on account of the elimination of phase detectors, but the frictional torque on the angle-data transmitter's shaft is increased.

45

The scanning unit described was used in a television camera in conjunction with LI-428 and LI-455 electrostatic vidicons.

COPYRIGHT: Izdatel'stvo "Nauka", "Pribory i tekhnika eksperimenta", 1981

8831
CSO: 1860/74

46

FOR OFFICIAL USE ONLY

CIRCUITS & SYSTEMS

LINEAR GATING DEVICE UNIT

[Article by I.B. Mazurov and Yu.G. Sibiryak]

[Text] A description is given of a linear gating device whose distinctive feature is the absence of switched elements in the linear signal transmission section. The unit operates with loads up to $5 \cdot 10^5$ pulses per second. The maximum input signal is 7 V. Control signals are matched in terms of level with TTL [transistor-transistor logic] signals. Temperature instability of the unit's transmission factor is 0.02 percent per degree Celsius. The switch-on delay is 20 ns. The length of the leading edge of the output pulse is 100 ns.

Linear gating devices (LPU's) are used extensively in spectrometric sections for sampling input pulses with reference to a control signal. The familiar LPU's, both those in which stabilizing feedback is not applied to switching elements [1], and LPU's in which a parallel switch switches the direct transmission channel of an operational amplifier (OU) to which 100-percent negative feedback (OOS) is applied [2], have the disadvantage that the switched element is included in the linear signal transmission section. As a result the linearity of the transmission section is worsened and a pedestal appears [3]. In [4] a method is suggested which makes it possible to avoid the use of switched elements in the linear section and to improve considerably the characteristics of the gating circuit.

The LPU described in this article is designed according to this principle and represents an operational amplifier with two differential stages, M_1 and M_2. A structural diagram of the LPU which explains its operation is given in fig 1. The transmission factor of a differential stage equals [5]:

$$K_{\text{д}} = (I_0/2)[R_{\text{к}}/(m\varphi_{\text{т}})].$$

(1)

It is obvious from this equation that with current $I_0 = 0$, $K_d = 0$.

The circuit operates in the following manner. If in the initial stage the switch is in position 2 the LPU is closed. Current I_0 passes through differential stage M_2. The transmission factor in this case from the input to the output is close to zero and the circuit represents an operational amplifier consisting of circuits M_2 and M_3 to which a great amount of negative feedback is applied which stabilizes

47

FOR OFFICIAL USE ONLY

the output zero level. After the arrival of the control signal the control circuit flips the switch to position 1 and current I_0 flows through differential stage M_1. In this case the operational amplifier is formed from circuits M_1 and M_3. As before, a great amount of negative feedback is applied to it, which makes possible transmission of the input signal to the output with a factor of $K \approx 1$, as well as its good stability and linearity.
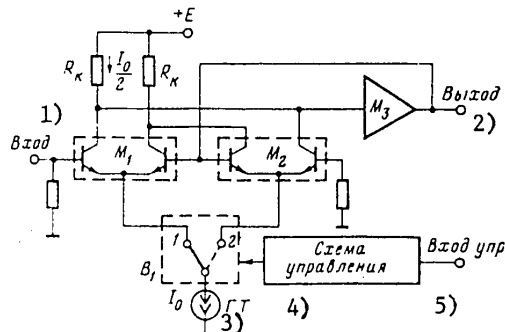
Figure 1. Functional Diagram of Linear Gating Device: GT--current generator

Key:

1. Input
2. Output
3. Current generator

4. Control circuit
5. Control input

The circuit's sampling coefficient is determined by the ratio of the transmission factors of differential stage M_1 in the switched-on and switched-off states, since the transmission factor of circuit M_3 does not change. This ratio in turn is equal to the ratio of currents passing through differential stage M_1 in the switched-on and switched-off states according to equation (1). For example, if in the cut-off state a current of 1 µA flows through the differential stage (1 µA represents current I_{ko} of a KT315 transistor, with which it is possible to construct the current generator), and a current of 2 mA in the switched-on state, then the sampling coefficient equals 2000.

A circuit diagram of the linear gating device is shown in fig 2. It consists of a noninverting follower assembled from microcircuit M_1 and transistor T_1, a direct-current restorer (VPS) assembled from M_2 and M_3 and T_2 to T_4 and the LPU itself, assembled from M_4 to M_6 and T_5 to T_{10}. The direct-current restorer represents an operational amplifier with 100-percent direct-current feedback. Alternating-current feedback is decoupled by means of capacitor C_2. The direct-current restorer's operation is based on discharging of capacitor C_1 in intervals between input pulses by means of current proportional to the steady-level bias. During the time T_1 is recharged, at point A a potential of iR_{vykh} [output] originates (where i is the capacitor recharging current and R_{vykh} is the output impedance of the preceding stage). This results in an increase in the integral nonlinearity of the entire unit [6], since the signal in the output of the LPU equals the difference $U_{vkh}(t_1) - U_C(0)$, where $U_{vkh}(t_1)$ is the amplitude of the pulse and $U_C(0)$ is the voltage across the capacitor at the moment of the arrival of the

48

signal, which voltage is not a constant quantity. In order to lower $U_c(0)$ it is necessary to reduce R_{yykh}; therefore, a follower with low output impedance is installed in the unit's input.
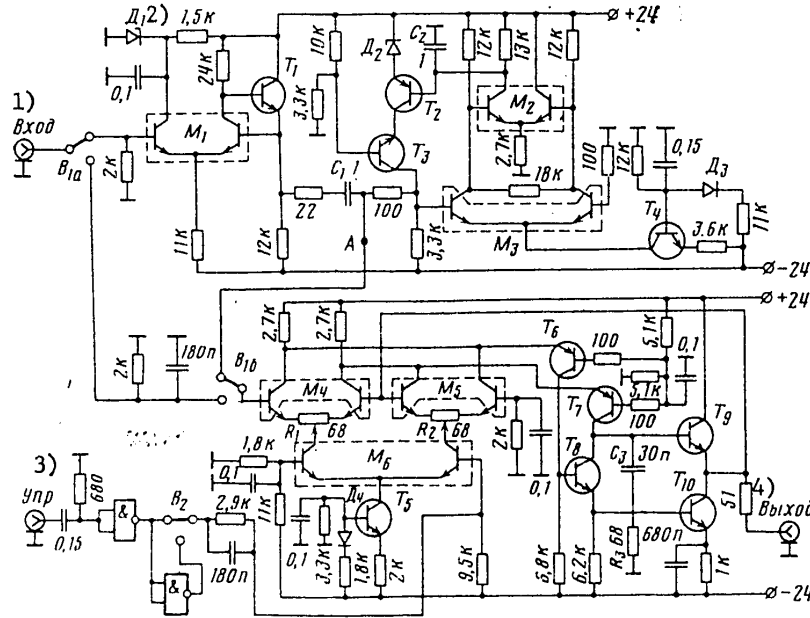
Figure 2. Circuit Diagram of LPU unit: M_1 to M_6--K1NT591B, remainder-- K1LB553; T_1, T_4, T_5, T_8 to T_{10}--KT315V, T_2, T_3, T_6, T_7-- GT308V; D_1, D_2--D818D, D_3, D_4--KD503A

Key:
1. Input   3. Control
2. Diode   4. Output

All differential stages in the LPU unit are assembled from series 159 integrated transistor assemblies. This made it possible to obtain good results with respect to temperature stability without the preselection of elements. The generator for current I_0 is assembled from transistor T_5. For the purpose of improving the temperature stability of current I_0 diode D_4 is included in the base divider. Switching of current I_0 to differential stages utilizing microcircuits M_4 and M_5 is accomplished by means of switches utilizing microcircuit M_6. The LPU is closed if the left transistor of microcircuit M_6 is closed and the right is open and the entire current enters the differential pair in microcircuit M_5 from the current generator. The zero level in the circuit's output is controlled by variable resistor R_2. After arrival of the control signal the right transistor of microcircuit M_6 closes and the left opens and the entire current I_0 enters the differential pair in microcircuit M_4. The LPU opens and the input signal travels to the circuit's output. The zero of the "pedestal" in the output is controlled by means of variable resistor R_1. Circuit C_3R_3 eliminates generation in the circuit.

49

By means of switch B_1 the direct-current restorer is connected to or disconnected from the LPU's input. In the position in which switch B_2 is shown in fig 2, the LPU is normally closed and a positive control signal opens the LPU for the time of the duration of this signal. If switch B_2 is in the lower position, then the LPU is normally open and the positive control signal arriving closes it.

The technical parameters of the unit are as follows: maximum input signal--7 V; transmission factor--0.98; direct passage of input signal to output in the closed LPU is observed in the form of slight changes (less than 1 mV) in output level; temperature instability of the transmission factor is 0.02 percent per degree Celsius in the 20 to 55 °C range; integral nonlinearity with a pulsed input signal is 0.02 percent; temperature instability of the zero level in the unit's output is 40 μV/°C in the 20 to 55 °C temperature range; base level bias with a change in the frequency of input pulses from 500 Hz to 50 kHz and with an input signal length of 2 μs is less than 5 mV; the switch-on delay is 20 ns; and the length of the leading edge of the output pulse is 100 ns. At the moment the LPU is switched noise is observed in the input in the form of a pulse with a height of 25 mV and a length of 50 ns.

Bibliography

1. Koval'skiy, Ye. "Yadernaya elektronika" [Nuclear Electronics], translated from English, edited by I.V. Shtranikh, Moscow, Atomizdat, 1972, p 138.

2. Elad, E. and Rozen, S. NUCL. INSTR. AND METHODS, Vol 37, No 1, 1965, p 58.

3. Matalin, L.A., Chubarov, S.I. and Timokhin, L.A. "Elektronnyye metody yadernoy fiziki" [Electronic Methods of Nuclear Physics], Moscow, Atomizdat, 1973, p 156.

4. Battista, A. NUCL. INSTRUM. AND METHODS, Vol 80, No 1, 1970, p 172.

5. Shilo, V.L. "Lineynyye integral'nyye skhemy" [Linear Integrated Circuits], Moscow, Sovetskoye Radio, 1974, p 66.

6. Baldin, S.A., Vartanov, N.A. and Yerykhaylov, Yu.V. "Prikladnaya spektro-metriya s poluprovodnikovymi detektorami" [Applied Spectroscopy with Semiconductor Detectors], Moscow, Atomizdat, 1974, p 106.

8831
CSO: 1860/74

FOR OFFICIAL USE ONLY

INFRALOW-FREQUENCY TRIANGULAR CURRENT PULSE GENERATORS

[Article by V.I. Danilov, A.A. Popov and V.S. Khabarov, United Institute of Nuclear Research, Dubna]

[Text] Two current generators are described: a triangular current pulse generator for operation on a superconducting load with I_n [load] $= 0$ to 2 A and a linear current buildup (decline) time in the load of $T = 1$ to 20 min , and an economical current generator which is assembled according to a two-stage stabilization circuit and can operate on an $R_n = 0$ to 3 Ω with $I_n = 0$ to 10 A under conditions of direct current in the load with a linear buildup (decline) of it to a prescribed level in $T = 5 \cdot 10^{-2}$ to $1.44 \cdot 10^4$ s , as well as under conditions of triangular current pulses with the same parameters.

For the purpose of studying superconducting materials, as well as in certain biophysics experiments [1, 2], infralow-frequency generators of triangular current pulses with an amplitude of up to 10 A are needed. A specific feature of these devices is that they must make possible a linear buildup (decline) of current in the load to an assigned value over a time measured in minutes and hours. Another problem originating in development is occasioned by the ranges of variation of the load resistance and operating current and is associated with dissipated power in active elements of the device.

In this paper a description is given of two current generators: a triangular current pulse generator (GIT) and a universal current generator (UGT). The GIT is designed for operating on a superconducting load in which it forms triangular current pulses with an amplitude of up to 2 A and a buildup and decline time in the smooth regulation range of 1 to 20 min. The basic elements of the circuit diagram of a GIT are shown in fig 1, from which it is possible to see that it consists of an output power amplifier (UM) and a triangular control voltage former (FNT$_1$). Both circuits are supplied from the electrical main through a transformer and rectifier block (BTV). The power amplifier is constructed according to the circuit of a series-type current stabilizer [3] with 100-percent feedback applied from grounded shunt R_1 and employing a 1UT401A operational amplifier (M$_2$) as the mismatch signal comparison and amplification element. For the purpose of protecting the superconducting load, to the output terminals of the generator via emitter followers, T$_1$, is connected an operational amplifier, M$_3$, in the comparator mode,

51

FOR OFFICIAL USE ONLY

which, when superconduction is impaired, sends through transistor T_8 to FNT_1 a signal which inhibits operation of the generator. The protection triggering threshold is set by means of potentiometer R_2 within the range of 1 to 20 mV.
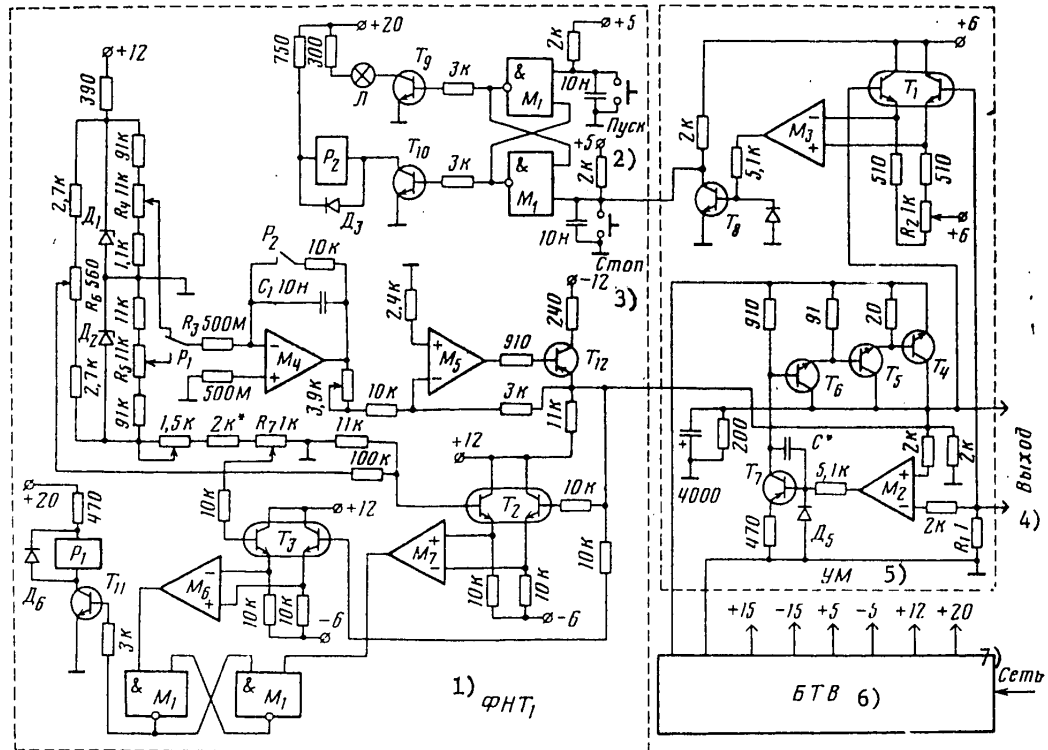
Figure 1. Key Elements of Circuit Diagram of GIT: M_1--1LB553; M_2, M_3, M_5--1UT401; M_4--LN0042; M_6, M_7--K554SA2; T_1 to T_3--K1NT591V; T_4--KT808A; T_5--KT807A; T_6, T_8 to T_{11}--KT315; T_7, T_{12}--KT326B; D_1, D_2--D818Ye, D_3 to D_6--KD522; P_1--REV18A, P_2--RES55A

Key:

1. FNT_1 [triangular control voltage former]
2. Start
3. Stop
4. Output

5. UM [power amplifier]
6. BTV [transformer and rectifier block]
7. Electrical main

FNT_1 determines the time and amplitude parameters of the output current pulses of the generator. Time characteristics are set by integrator M_4 with time setting elements (R_3, C_1). Constant voltages of differing polarity are integrated, which are set by potentiometers R_4 and R_5 and are connected to the integrator's input by means of the contacts of relay P_1. An LN0042 operational amplifier, which can be replaced by a domestic type 140UD8, and a type FT-1 charging capacitor (C_1) are used in the integrator's circuit. The integrator's output voltage, traveling

52

through matching amplifier M_5, via emitter followers T_2 and T_3 enters comparators of the lower (M_7) and upper (M_6) levels of the former's output voltage. The comparators via flip-flop M_1 and switching transistor T_{11} control the operation of relay P_1. The triggering thresholds of the comparators are set by potentiometers R_6 and R_7 and the difference between the threshold voltages of the upper and lower levels sets the peak value of the FNT_1's control voltage pulses and, consequently, of the GIT's output current.

The signal for inhibiting the generator's operation enters from the power amplifier (T_8) into inhibit flip-flop M_1, which controls the operation of relay P_2 and the lamp display. The contacts of P_2 shunt the integrator's time-setting capacitor, C_1, blocking its operation. In addition, it is possible to stop the generator's operation by means of a "Stop" button and to start it by means of a "Start" button. Both states are distinguished from a lamp display (L) on the unit's front panel. Power of $P \sim 10$ W is dissipated in output transistor T_4 (fig 1) and it is placed on a heat sink measuring 400 cm^2 in area. The problem of enabling heat removal arises in the development of a UGT, which must make possible output current in the range of 0 to 10 A over a load resistance range of 0 to 3 Ω. Under the worst conditions for the generator ($R_{load} \sim 0$ and $I_n = 10$ A) power, P , of approximately 400 W is dissipated in the UGT's output power stage (when using a linear current stabilizer in it). Power of this sort is usually removed by means of a fluid [4], which is inconvenient when using the generator as a portable instrument. Therefore, the UGT has been developed according to a two-stage stabilization circuit (fig 2). There is a linear current stabilizer (LST) in the generator's output and an economical series-type pulsed voltage regulator [3, 5] (IRN) automatically maintains a minimum voltage drop, U_{ke} , in its feed-through transistors.

The amplified signal of the output current transducer (R_1, M_3) is compared in operational amplifier M_4 with the control voltage which enters from the switched range divider (KP_3, R_2 to R_7). Amplifier M_4 controls the output power follower utilizing P210A transistors (T_1 to T_4). The voltage in the linear current stabilizer's load is compared with the pulse generator's output voltage in a differential amplifier (T_9, T_{10}) and the amplified error signal switches feed-through transistors T_{13} to T_{17} of the pulsed voltage regulator via a cascode switching stage (T_{11} and T_{12}) and a Schmitt circuit utilizing a 1U401A operational amplifier (M_{10}).

The linear current stabilizer's power transistors, T_1 to T_4, operate in the linear region of their characteristic with $U_{ke} \gtrsim 1.2$ V and the maximum switching frequency of the pulsed voltage regulator's switching elements is approximately 4 kHz. In this circuit power of $P_{max} \sim 40$ W is dissipated in the power transistors of both stabilizers of the UGT. The high-power semiconductor devices of regulators are placed on heat sinks with a total area of 2000 cm^2 and operate reliably without forced cooling.

Protection circuits ensure reliable operation of the UGT. A signal for when the load current exceeds the permissible is picked up from the output of amplifier M_3 and via transistors T_{18} and T_{19} opens thyristor D_{13}, which blocks switching in the pulsed regulator, which is indicated by a lamp indicator (L_1) on the unit's front panel. When the feed-through transistors of the pulsed voltage regulator fail, the voltage of the generator's rectifier enters the output transistors of the linear current stabilizer, which results in their thermal breakdown. In order to avoid this situation, in the collector of transistor T_7 a signal is formed

which inhibits operation of the control unit, thus closing the linear current stabilizer's feed-through transistors.
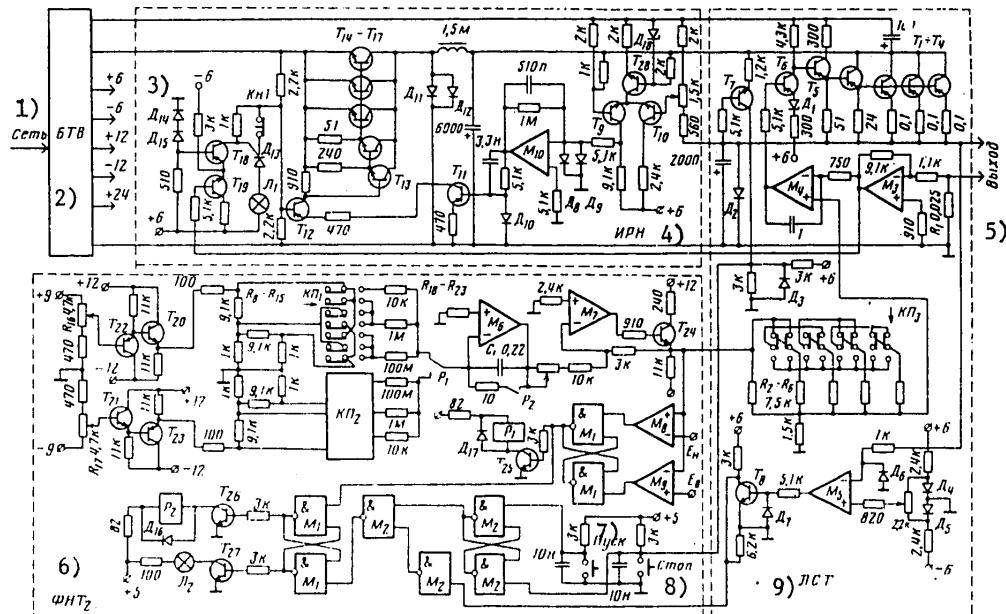
Figure 2. Key Elements of Circuit Diagram of UGT: M_1, M_2--1LB553, M_3--1UT531, M_4, M_5, M_7 M_{10}--1UT401, M_6--LN0042, M_8, M_9--K554SA2; T_1 to T_4--P210A, T_5, T_6, T_{18}--MP26B, T_7 to T_{10}, T_{19} to T_{21}, T_{24} to T_{28}--KT315, T_{11} to T_{13}, T_{22}, T_{23}--KT608B, T_{14} to T_{17}--KT808A; D_1--KS147, D_2--D243, D_3 to D_{10}, D_{14} to D_{17}--KD522, D_{11}, D_{12}--KD213, D_{13}--KU101, D_{18}--KS133; P_1--REV18A, P_2--RES55A

Key:
1. Electrical main
2. Transformer and rectifier block
3. Diodes
4. Pulsed voltage regulator
5. Output
6. FNT$_2$
7. Start
8. Stop
9. Linear current stabilizer

Two units are used in the UGT as control voltage sources: FNT$_2$--a triangular voltage pulse shaper--and a digital-analog integrator developed earlier [5]. The FNT$_2$ block is similar in operating principle to the shaper described above and the necessary elements of its circuit diagram are shown in fig 2. For the purpose of forming a buildup (decline) time in the range of 10^{-3} to 10^4 s, in this circuit are used a set of time setting resistors, R_{18} to R_{23}, connected to dividers R_8 to R_{15} by means of piano-key switches KP_1 and KP_2, and potentiometers for smooth regulation, R_{16} and R_{17}, within each range. FNT$_2$'s output pulses are formed after the current in the UGT's load drops to the zero level, which determines the logic of the shaper's operation. The comparator of the lower level, M_8, of the shaper's output

54

voltage, via transistor T_{26} and flip-flop M_1, blocks the operation of integrator M_6 by means of the contacts of relay P_2 and simultaneously with this switches the polarity of the integrator's input voltage. The next pulse begins to be formed after the arrival of a signal from the linear current stabilizer's zero comparator (M_5, T_8), setting flip-flop M_1 to a state inhibiting the integrator's operation.

The second unit controlling the UGT's operation, the digital-analog integrator [6], is totally interchangeable with FNT_2 and is constructed on the basis of a 12-bit digital-analog converter with a reversible counter and a digital comparison circuit. It serves as a source of precise reference voltage with stepwise linear buildup and decline times in the range of 30 s to 4 h and operates in the constant output voltage mode. Single and periodic triangular pulse modes are also included in it.

Both generators have been developed as individual instruments powered from the electrical main. The GIT has been designed as an insertion unit with a front panel width of 120 X 160 mm^2. The UGT is assembled from four insertion units of the following types: a power supply with front panel dimensions of 100 X 240 mm^2, a 45 X 240 mm^2 linear current stabilizer, a 45 X 240 mm^2 pulsed voltage regulator and a 50 X 240 mm^2 control unit. At the present time the GIT is at work in testing superconducting models and UGT's are being used in studies of the influence of magnetic fields on biological subjects [1, 2].

In conclusion the authors wish to thank A.V. Karpukhin, V.Ye. Zhil'tsov and N.Ya. Kalinkin for assembling and helping to tune the instruments.

Bibliography

1. Danilov, V.I. Collection "Fiziko-matematicheskiye i biologicheskiye prob-lemy deystviya elektromagnitnykh poley i ionizatsii vozdukha. Materialy Vsesoyuznogo nauchno-tekhnicheskogo simpoziuma" [Mathematical Physics and Bio-logical Problems of the Influence of Electromagnetic Fields and Ionization of Air: Materials of the All-Union Science and Engineering Symposium], Moscow, Nauka, 1975, p 175.

2. Gerasimenko, V.N., Govorun, R.A. and Danilov, V.I. Collection "Fiziko-mate-maticheskiye i biologicheskiye problemy deystviya elektromagnitnykh poley i ionizatsii vozdukha. Materialy Vsesoyuznogo nauchno-tekhnicheskogo simpoziuma," Moscow, Nauka, 1975, p 168.

3. Dodik, S.D. and Gal'perin, Ye.I. "Istochniki elektropitaniya na poluprovod-nikovykh priborakh" [Semiconductor Device Power Supplies], Moscow, Sovetskoye Radio, 1969.

4. Bergel'son, I.G., Kamenetskiy, Yu.A. and Nikolayevskiy, I.F. "Tranzistory, parametry, metody izmereniy i ispytaniy" [Transistors, Parameters, Measurement and Testing Methods], Moscow, Sovetskoye Radio, 1968.

5. Nakhratskiy, V.M., Popov, A.A. and Khabarov, V.S. OIYaI [United Institute of Nuclear Research] Preprint No 13-11795, Dubna, 1978.

6. Bychkov, N.S., Lachinov, V.M., Popov, A.A. and Khabarov, V.S. PTE, No 4, 1975, p 146.

8831
CSO: 1860/74

COMMUTATOR CONTROLLED BY SIGNAL FREQUENCY

[Article by A.Ye. Bozhko, Ye.A. Lichkatyy, O.F. Polishchuk and V.I. Savchenko, Ukrainian SSR Academy of Sciences Institute of Problems of Machine Building, Khar'kov]

[Text] A description is given of a commutator controlled by the frequency of a harmonic signal or a signal of the meander type. The circuit's operation is based on comparison of the durations of the half-period of the control signal and a reference pulse determining the switching frequency. The minimum amplitude of the control signal is 0.02 V, the operating frequency range is 1 Hz to 1 MHz, the maximum frequency change rate is 250 Hz/s and the switching error in terms of frequency is less than or equal to 0.1 percent.

The representation of information in frequency form has found extensive application in measuring and data processing systems. Here the need arises of switching information channels, of changing operating modes and of monitoring the required parameters as a function of the frequency of the control signal. One method of designing frequency-dependent commutators is the employment of counting methods of measuring frequency. Circuits implementing this method are complicated and are critical with regard to rapid changes in the frequency of the control signal.

Another method is based on comparing the duration of the half-period of the control signal with the duration of a reference square pulse [1]. However, a commutator of this sort has a limited operating frequency range. For normal operation of the commutator the inequality $f_u < 1/T_0$ must be fulfilled, where f_u is the frequency of the control signal and T_0 is the duration of the reference pulse. If $f_u > 1/T_0$ normal operation of the commutator is upset. The circuit presented in [1] is used as a unit cell in constructing multichannel commutators. Each cell is tuned to a specific commutation frequency. The limitations characteristic of this circuit are thus extended also to a multichannel commutator. The maximum value of the frequency of the control signal for a multichannel commutator equals double the value of the lowest switching frequency.

In this article a description is given of a frequency-dependent commutator whose stable operation is maintained in the range of 1 Hz to 1 MHz with any value of the commutation frequency [2]. A circuit diagram of the commutator is presented in

57

fig 1. The unit contains an amplifier-limiter in M_1, a matching circuit in transistors T_1 and T_2, a shaper in M_{3-1} and M_{3-2}, 10 NAND circuits, and flip-flops M_{5-1}, M_{5-2} and M_{6-1}. The amplifier-limiter is necessary for controlling commutation by means of a harmonic signal.
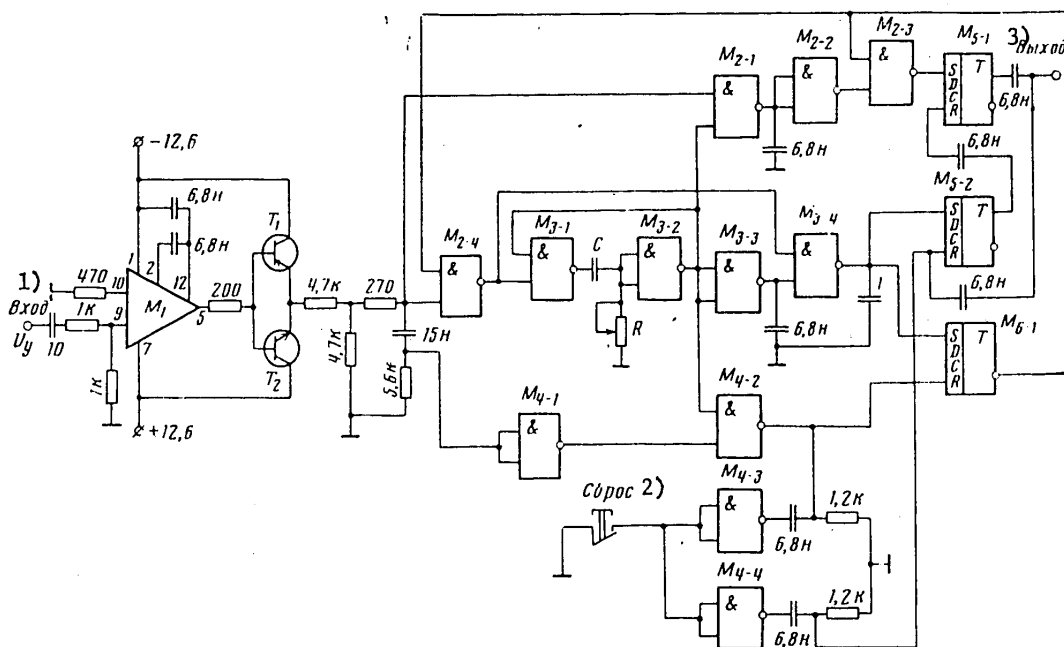
Figure 1. Circuit Diagram of Commutator: M_1--1UT402; M_2 to M_4--1LB553; M_5, M_6--1TK552; T_1--MP42B, T_2--MP38

Key:
1. Input
2. Reset
3. Output

Let us discuss the circuit's operation. By means of the reset signal flip-flops M_{5-1} and M_{6-1} are set to the "1" state and flip-flop M_{5-2} to the "0" state. A square pulse whose duration is equal to half the period of the control signal, U_u, from the output of the limiter through the AND gate, M_{2-4}, to whose second input is supplied the signal of flip-flop M_{6-1}, by means of its trailing edge triggers the shaper consisting of M_{3-1} and M_{3-2}. The shaper generates a pulse whose duration determines the switching frequency. The pulses of the control signal and shaper are compared in terms of duration and the result of the comparison determines the state of flip-flops M_{5-1} and M_{5-2}. If $f_u < 1/2T_0$, the resulting pulses are present in the output of M_{2-1} and if $f_u > 1/2T_0$ in the output of M_{3-4}. With the equality $f_u = 1/2T_0$ a change of state takes place in flip-flops M_{5-1} and M_{5-2}.

58

FOR OFFICIAL USE ONLY

For $f > 1/T_0$ the operation of the circuit is illustrated by the voltage diagram in Fig. 2. Since $f > 1/2T_0$, the first resulting pulse beginning at moments of time t_0 and t_1 will appear in the output of M_{3-4} and flip-flops M_{5-1} and M_{6-1} are set to the "0" state and flip-flop M_{5-2} to the "1" state. In spite of the presence of pulses in the output of M_{2-1} the state of flip-flops M_{5-1} and M_{5-2} remains stable since the signal from flip-flop M_{6-1} closes circuit M_{2-3}. After termination of the shaper's pulse (output of M_{3-2}) the first pulse from the output of M_{4-2}, corresponding to the leading edge of the output pulse of the limiter, sets flip-flop M_{6-1} to the initial state, circuits M_{2-3} and M_{2-4} are opened and the process of the comparison of durations is repeated. Circuit M_{2-4} eliminates triggering of the shaper before flip-flop M_{5-1} is set to the initial state and M_{4-2} eliminates resetting of flip-flop M_{6-1} before termination of the process of comparison of the durations of the pulses of the shaper and limiter.
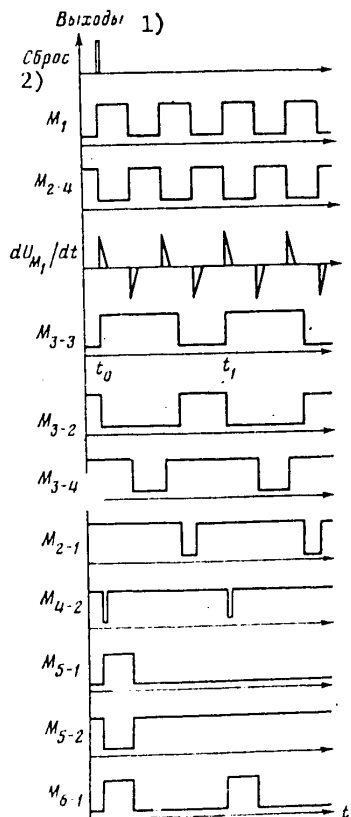
Figure 2. Time Diagram of Voltages Existing in the Circuit

Key:
1. Output   2. Reset

59

FOR OFFICIAL USE ONLY

If the frequency of the control signal becomes lower than the switching frequency, the resulting pulses appear only in the output of M_{2-1}. Flip-flop M_{5-1} is set to the "1" state, changing the state of flip-flop M_{5-2} to the "0" state. Flip-flop M_{6-1} remains in the "0" state permitting the passage of pulses through M_{2-3} and M_{2-4}. A discrete change in the commutation frequency is accomplished by changing the capacitance of capacitor C and smooth change by changing R .

Thus, normal functioning of the circuit is maintained regardless of the value of the commutation frequency. A multichannel commutator can be constructed by means of a set of several of the circuits described, each of which is tuned to its switching frequency. The commutator's specifications are as follows: The control signal is harmonic or of square shape; the minimum peak value of the control signal is 0.02 V; the operating frequency range is 1 Hz to 1 MHz; the maximum commutation error in terms of frequency is 0.1 percent; and the maximum rate of change of the frequency of the control signal is 250 Hz/s.

Bibliography

1. Yelisov, L.N. and Sergeyev, N.P. PRIBORY I SISTEMY UPRAVLENIYA, No 10, 1976, p 43.

2. Bozhko, A.Ye., Lichkatyy, Ye.A., Polishchuk, O.F. and Savchenko, V.I. USSR Patent No 712964, published in BYULLETEN' IZOBRETENIY, No 4, 1980, p 195.

8831
CSO: 1860/74

UDC 621.373

SUBNANOSECOND-RANGE HIGH-POWER SEMICONDUCTOR PEAKERS

[Article by I.V. Grekhov, A.F. Kardo-Sysoyev and S.V. Shenderey, USSR Academy of Sciences Physicotechnical Institute, Leningrad]

[Text] A method is discussed of forming pulses with a height greater than 1 kV with subnanosecond leading edges by means of a semiconductor diode peaker. A description is given of a circuit making it possible to form leading edges with a length less than 0.2 ns.

The basic method of producing pulses with subnanosecond leading edges is peaking the leading edge of the original pulse by means of peakers included in breaks in the transmission line. However, the use of peakers employing tunnel diodes or diodes with charge storage is restricted by the low operating voltages (less than 1 and approximately 10 V, respectively). In this article a description is given of the operation as peakers of semiconductor diodes with a breakdown delay effect, first described in [1, 2], which make it possible to form voltage pulses with subnanosecond leading edges and heights greater than 1 kV.

A study was made of diode peakers (DO's) in the circuit shown in fig 1. A pulse 30 ns long formed by a thyratron was supplied via a 90-ns delay line to a diode peaker connected in series with a load resistance of $R_n = 50 \, \Omega$, equal to the wave impedance of the RK-50-4-21 cable lines used. The inclusion of $L_f C_f$ networks made it possible to change the rate of voltage buildup in the pulse's leading edge. The signal for recording the current was picked up from a silver contact in the form of a band inserted on type MOU-5 resistor R_n at a distance of 1/8 of its length. The employment of an exponential shield made it possible to obtain with a set of standard dividers a current time resolution better than 0.2 ns. Voltage was tapped from the diode peaker at the end of the transmission line for the purpose of registration through resistor R_d (TVO-0,5). The selection of the position of R_d near the shield, as well as the use of a tubular coaxially positioned capacitor as the blocking capacitor made possible voltage resolution of better than 0.4 nm. The maximum operating frequency of the circuit was determined by the mean power dissipated in the circuit's elements and equaled 1 kHz.
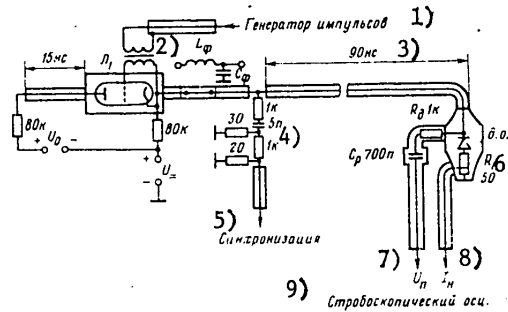
Figure 1. Circuit Diagram of Experimental Unit: L_1--TGI-3/30

Key:
1. Pulse generator
2. L_f
3. 90 ns
4. 5 pF
5. Synchronization

6. Diode peaker
7. U_n
8. I_N [load]
9. Sampling oscilloscope

The diode peakers fabricated in keeping with [1, 2] were in the form of washers 7 mm in diameter and 0.3 mm thick soldered onto a tungsten plate 1.5 mm thick and were connected in the break coaxially in front of R_n. A constant bias voltage, U_{sm}, was applied to the diode peaker in the cutoff direction. Oscillograms of the incident wave, U_n, and of the voltage across the load, U_N, for various U_{sm} are given in fig 2. It is obvious that after reaching the maximum of the voltage, U_m, of the incident wave a rapid increase in current takes place to the peak value, and the minimum current buildup time corresponds to the maximum value of U_{sm}. It has been established that the value of U_{sm} with which the diode peaker switching time is minimal must equal (0.7 to 0.8)U_{st}, where U_{st} is the breakdown voltage of the diode peaker with a slow increase in voltage.
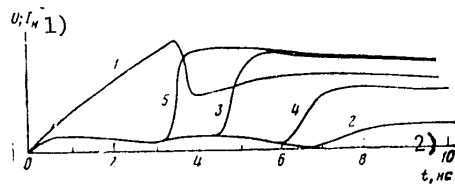
Figure 2. Oscillograms of Transient Processes: 1--incident wave; 2 to 5--voltage across load with various U_{sm} in V: 2--200, 3--400, 4--700, 5--1000

Key: 1. U ; I_N [load]　　　　　　　2. t , ns

62

The rate of the increase in voltage U_n (dU_n/dt) is of great importance in the diode peaker's operation. An increase in dU_n/dt results in an increase in U_m and, consequently, in an increase in the amplitude of the current. It has been established experimentally that U_m and dU_n/dt are related as follows:

$$U_m = U* + \tau * dU_n/dt, \tag{1}$$

where $\tau* = 1$ to 2 ns and $U*$ is close in magnitude to U_{st} .

For the purpose of finding the value of dU_n/dt with which peaking begins, the dependence of $U_N = I_N R_N$ on U_m was plotted. This dependence is at first sharply nonlinear and then it asymptotically approaches a linear one, $U_N = U_m$, which corresponds to short-circuiting conditions of the diode peaker. The nonlinearity is determined by the degree of modulation of the diode peaker's volume during its switching. The nonlinear part of the dependence can be represented by the following empirical formula:

$$U_{\text{н}}, \text{ B} = 110 \left(e^{U_m/\Delta} - 1\right), \tag{2}$$

where $\Delta = 200$ V . Uniting (1) and (2), we get

$$dU_n/dt, \text{ B/c} = \frac{1}{\tau*}\left[\Delta \ln\left(\frac{U_{\text{н}}}{110} + 1\right) - U*\right].$$

Of great practical interest is the question of the stability of the diode peaker's switching delay. As was already demonstrated in [1], the time instability was less than 50 ps and was determined only by the synchronization circuits and the stability of the power supply. It is necessary to mention that during operation the diode peaker must be isolated from the influence of external factors resulting in the generation of excess carriers in the semiconductor (e.g., light). Oscillograms of the current through a diode peaker recorded with different degrees of illumination have demonstrated that illumination seriously worsens the transient process of switching of a diode peaker.

In conclusion it must be said that the diode peakers described open up a unique opportunity to form voltage pulses with a height greater than 1 kV and with current of dozens of amperes during a time of less than 0.2 ns.

Bibliography

1. Grekhov, I.V. and Kardo-Sysoyev, A.F. PIS'MA V ZHTF, Vol 5, No 15, 1979, p 950.

2. Grekhov, I.V., Kardo-Sysoyev, A.F. and Kostina, L.S. PIS'MA V ZHTF, Vol 5, No 16, 1979, p 961.

COPYRIGHT: Izdatel'stvo "Nauka", "Pribory i tekhnika eksperimenta", 1981

8831
CSO: 1860/74

UDC 621.373.43

SYSTEM FOR CONTROLLING CLOSING OF SPARK GAPS BY FIELD DISTORTION METHOD

[Article by A.I. Gerasimov and Ye.G. Dubinov]

[Text] A spark gap - peaker filled with gas to 1 MPa is connected to breaks in 26 segments of cable charged to an identical potential difference of 15 to 30 kV and each connected with its inner conductor to the control electrode of its own spark gap. When all cables (2 Ω impedance) are short-circuited by means of a joint commutator the length of the front, T_1 = 40 to 70 ns , of the current wave of their discharge is shortened by the peaker to 3.8 ns. The spread in moments of breakdown of the peaker is less than or equal to 0.1 T_1. The breakdown is of a multichannel nature with a gap of 1 to 2 mm between the peaker's electrodes and when it is filled with nitrogen.

In spark gaps with distortion of distribution of the electric field it is necessary to change rapidly the polarity of the potential of control electrodes [1]. In the synchronous closing of a great number of spark gaps segments of coaxial cable are used whose inner conductors unite the control electrodes of the spark gaps and a commutator common to all the cables [2-4]. The accuracy of the mutual trig- gering of spark gaps as well as the uniformity of the development of current channels in them and of the distribution of current over these channels depends substantially on the length of the front of the current wave for discharging of the cables [2, 3]. If the number of cables connected in parallel to the short- circuiting commutator equals a few dozen and their charge voltage, U_0 , is equal to or greater than 20 kV, then the length of the front of the current through the commutator usually is equal to or is greater than 10 ns.

In this article a description is given of a system of 26 segments of RK-50-11-13 cable connected in parallel (total impedance of $\rho = 2 \Omega$), which makes it possible to form a current wave for discharging of the cables with a front length of less than or equal to 5 ns with $U_0 \geq 15$ kV .

The circuit of a system for controlling the triggering of 26 spark gaps, P_1 to P_{26} , which switch capacitor tank C or individual tanks to load Z is illustrated in fig 1. To each control electrode, 1, of the spark gap is connected the inner conductor of a segment of RK-50-11-13 cable 10 m long. High-voltage electrodes 2 and tank C are under a potential of U and electrodes 1 and the central con- ductors of the cable under a potential of U_0 of the same polarity; U_0 usually

65

equals (0.3 to 0.5)U. To breaks in the inner conductors of the cables is con-
nected a joint gas-filled spark gap - peaker, RO, similar to that described in
[5]. Leveling of the potentials of sections of the cables of the shaping (FL)
and peaking (OL) lines separated by the peaker's electrodes is accomplish-1 via
induction coil L and resistor R_1; the OL section can be connected to the charge
source in the same manner as the FL section. Switch K serves the purpose of short-
circuiting the cables. The parameters of the discharge current pulses of FL and
OL cable sections are measured through shunt resistors R_2 and R_3 consisting of
20 TVO-0,25 resistors connected in parallel and placed in the breaks of the
outer conductors, and the parameters of voltage pulses in electrode 3 and in con-
trol electrodes 1, by capacitive dividers D_1 (C_1, C_2) and D_2 (C_3, C_4), respective-
ly.
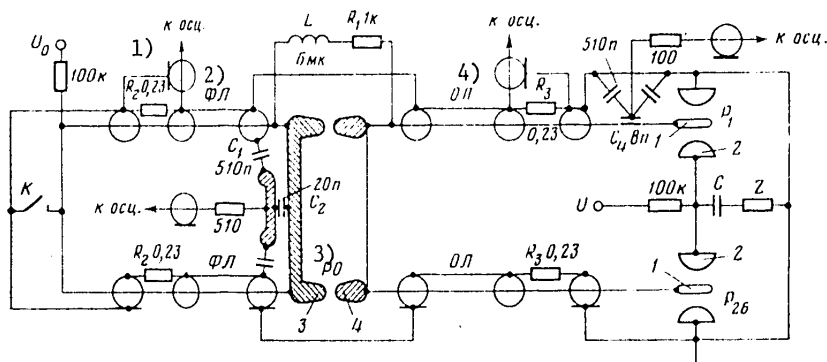
Figure 1.   Circuit of System for Controlling the Triggering of 26 Spark
            Gaps Which Switch Tank C to the Load: C_1 and C_3--10 units of
            51 pF each

Key:
    1. To oscilloscope   3. Spark gap - peaker (RO)
    2. Shaping line (FL)   4. Peaking line (OL)

After switch K operates, a discharge current wave is created in the FL cables;
it is reflected from spark gap RO as from an open end with a change in the polar-
ity of the potential of electrode 3. With $Z_1 \gg \rho$, where Z_1 is the impedance
of series-connected R and R_1, the maximum pulse difference of potentials between
electrodes 3 and 4 equals $2U_0$. By selecting the distance, δ , between elec-
trodes, the pressure, p , and the type of gas in the RO, with high overvoltage
across the gap it is possible to produce in the RO a multichannel discharge which
peaks the leading edge of the discharge current pulse of the cables in the peaking
line. The current wave, reaching electrodes 1, has a front which is shorter than
the front in the shaping line, which stabilizes the operation of spark gaps P_1 to
P_{26}.

FOR OFFICIAL USE ONLY

The system was studied with U_0 = 15 to 30 kV , spark gap – peaker RO was filled with N_2, SF_6 gas and mixtures of them [6], and as the commutator, K, an air-gap discharger or a discharger with film insulation which can be broken down mechanically was used. Studies were conducted in series consisting of one-time switching on of the system followed by polishing of the electrodes before each next start. Inspection of the surfaces of the electrodes of the spark gap – peaker showed that the number of erosion spots on electrodes of a spark gap with a diameter of 135 mm filled with N_2 is greater than when filling with a mixture of SF_6 + N_2 and with pure SF_6 and is equal to or greater than three; one discharge channel, as a rule, forms in SF_6. The registration of current pulses in two diametrically positioned cables of the peaking line confirmed the multichannel nature of a discharge in N_2; the difference in the moments the wave reached resistors R_3 did not exceed the transit time at the speed of light for one sixth of the length of the circumference of the ring electrodes of the RO. Uniformity of the distance between electrodes 3 and 4 over the entire length of the circumference (spread of less than or equal to 0.05 mm) is important for normal operation of the spark gap. The calculated time for propagation of the electromagnetic wave over half the length of the circumference of the electrodes equals approximately 0.7 ns; this time difference was observed to be 0.6 ns in mixtures of gases and in SF_6. The difference in the peaker's breakdown time, ΔT , in N_2 is also less with the same gaps between the electrodes of the RO. Taking these facts into account, the measurement results presented below are given for filling the RO with N_2.

In fig 2 [photograph not reproduced] typical oscillograms are shown for the discharge current pulse in cables of the shaping line (FL) and of the change, corresponding to it, in voltage in electrodes 1 of spark gaps when using in switch K solid insulation consisting of a Lavsan [Therylene] film, when the cables are charged with a voltage of U_0 = 23 kV , the gap measures δ = 2 mm and the pressure is p = 0.85 MPa N_2 . It is obvious that with a length of the switching current front of $T_1 \sim 40$ ns the voltage change time equals $T_2 \sim 5$ ns . When δ is reduced to 1 mm time T_2 is reduced to approximately 3.8 ns. With fixed U_0 and δ an increase in pressure p shifts the moment of breakdown of the RO to the peak of the current pulse, but T_2 is thereby changed but slightly. The spread, T , in moments of breakdown of the RO relative to the start of the current pulse in the shaping line, measured with the application of 10 or more signals (fig 2b), is less than or equal to 4 ns in a series of 100 closings of switch K. Under the same conditions the spread in SF_6 is approximately twofold greater. Shortening of front T_1 of the current pulse in the shaping line reduces the time spread, ΔT ; when an air-gap discharger is used, T_1 increases to 70 ns and accordingly ΔT is increased to 7 ns. The splitting of each cable in the peaking line near spark gaps P_1 to P_{26} into wires up to 2 m long matched with respect to wave impedance (100 Ω) did not worsen at their ends the speed of the reversal of the polarity of potential, which makes it possible to control the operation of 52 spark gaps.

The spark gap – peaker operated reliably over the entire range of variation of U_0 , since a difference in potential is not created between electrodes 3 and 4 of this spark gap with a static and pulsed charge for approximately 100 μs.

A similar system can be executed with a greater number of cables. The further shortening of T_2 can be achieved by the sequential breakdown of several peaking gaps [7].

67

FOR OFFICIAL USE ONLY

Bibliography

1. Barnes, P.M., Gruber, J.E. and James, T.E. J. SCIENT. INSTRUM., Vol 44,
    No 8, 1967, p 599.

2. Bosamykin, V.S., Gerasimov, A.I., Zenkov, D.I. et al. "Gas Discharge Devices"
    in "Trudy konferentsii po elektronnoy tekhnike" [Proceedings of the Conference
    on Electronic Engineering], Moscow, TsNII "Elektronika", No 2 (18), 1970,
    pp 94, 95.

3. Pavlovskiy, A.I., Gerasimov, A.I., Tananakin, V.A. et al. PTE, No 2, 1970,
    p 122.

4. Pavlovskiy, A.I., Gerasimov, A.I., Zenkov, D.I. et al. ATOMNAYA ENERGIYA,
    Vol 28, No 5, 1970, p 432.

5. Pavlovskiy, A.I., Kuleshov, G.D., Gerasimov, A.I. et al. PTE, No 6, 1976,
    p 134.

6. Gerasimov, A.I. and Saltykov, V.B. PTE, No 4, 1979, p 265.

7. Vorob'yev, P.A. and Potalitsyn, Yu.F. Collection "Elektrofizicheskaya
    apparatura i elektricheskaya izolyatsiya" [Electrophysical Apparatus and
    Electrical Insulation], Moscow, Energiya, 1970, p 140.

8831
CSO: 1860/74

HIGH–VOLTAGE PULSE GENERATOR FOR LOW–RESISTANCE LOAD

[Article by A.Yu. Ushakov, Leningrad Polytechnical Institute]

[Text] A description is given of a generator for producing square voltage pulses with an amplitude of 10^2 to $4 \cdot 10^3$ V with an approximately 2 Ω load. The length of the pulses is 0.25 µs and regulation of length is not provided for. The pulse repetition rate is 1 to 100 Hz.

The generation of pulses of microsecond length and kilovolt height with a low–resistance load is complicated by the fact that it is difficult to implement high–current generator circuits in the form of elements whose wave impedance would be on the order of the load resistance. It is possible to solve this problem by maximum reduction of the inductance of the generator's high–current circuit, primarily by reducing its dimensions.

Of the generator circuits and their elements described in the literature most suited to our purpose is a generator with a switch--a gas-filled spark gap--and with a shaping circuit in the form of parallel-connected LC networks whose resonance frequencies and wave impedance are in conformity with the Fourier spectrum of the pulses generated [1]. A shaping circuit of this type differs advantageously from the more widespread artificial long lines by the fact that it can be made considerably more compact and with a smaller number or elements necessary for enabling a specific form of the generated pulse close to square. The spark gap, operating at a gas pressure on the order of atmospheric, can also be made miniature and its speed of response and permissible current values conform to our objective.

The generator's circuit is presented in fig 1. The storage line is formed by four series LC networks whose resonance frequencies, ω_k , and wave impedance, ρ_k , according to [1], are calculated by the following equations:

$$\omega_\kappa = \pi k/\tau, \quad \rho_\kappa = \pi \rho k/4,$$

where $k = 2n - 1$; $n = 1, 2, 3, 4, \ldots$; and τ is the length of the pulse generated.
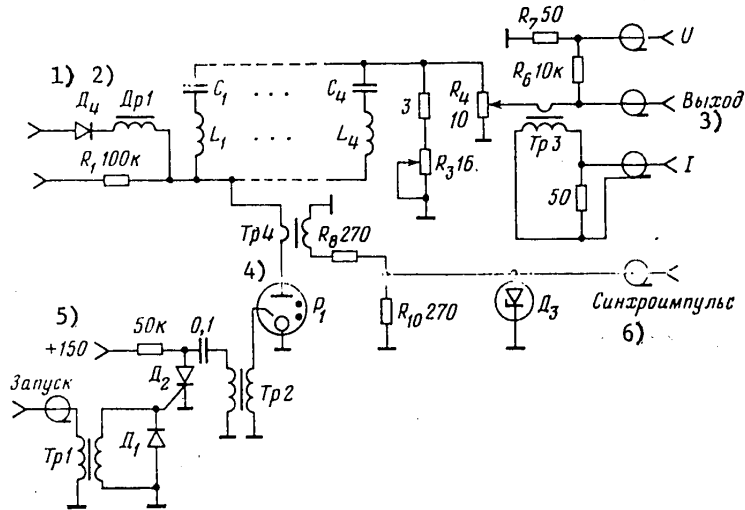
69

Figure 1.   Circuit Diagram of Generator: C_1--K41-1a (0.047 μF, 6.3 kV);
C_2--KVI-3(3300 pF, 10 kV); C_3--KVI-3 (800 pF, 10 kV); C_4--
KVI-2 (100 pF, 10 kV); D_1--D9V, D_2--KU202I, D_3--D814V, D_4--
KD202R (10 each); L_1--two turns, L_2--three turns, L_3--five turns,
L_4--12 turns (diameter of turns 12 mm, PEV-2-0.6 mm wire)

Key:
1. Diode   4. Transformer
2. Choke   5. Start
3. Output   6. Synchronizing pulse

Taking into account the fact that for an oscillatory circuit $\omega_k^2 = 1/L_k C_k$ and
$\rho_k^2 = L_k/C_k$, the values of the inductances, L_k , and capacitances, C_k , of the line
will equal

$$L_\kappa = \frac{\rho_\kappa}{\omega_\kappa}, \quad C_\kappa = \frac{1}{\omega_\kappa \rho_\kappa}.$$

In the circuit two modes are provided for charging the shaping line. With low re-
petition rates of the generated pulses (up to 10 Hz) charging is performed through
resistor R_1 from a source with a voltage of 0.3 to $8 \cdot 10^3$ V. A disadvantage of this
variant is its low efficiency, less than 50 percent, and with high frequencies the
charging resistor is heated intensely. In these cases it is feasible to use a
circuit with a charging choke and diode, which, of course, doubles the voltage in
in the line as compared with the supply voltage. The choke has a winding with 800

70

turns of PEV-2 wire 0.4 mm in diameter and a core of transformer steel with a steel cross-sectional area of 9 cm^2, assembled with a 1-mm air gap.

The spark gap (fig 2) with a regulated discharge gap is cemented together with epoxy resin. Its electrodes are made of Duralumin and its case, with pulse repetition rates of less than or equal to 10 Hz, can be made of acrylic plastic and with repetition rates of 10 to 100 Hz out of ceramic. The spark gap is filled with a gas mixture--air with 30-percent He. The addition of He facilitates firing of the spark gap with low line supply voltages and reduces erosion of the electrodes. The gas is supplied through a capillary tube in one of the screws fastening the spark gap to the generator's case, under low overpressure--from a ball chamber. The rate of flow of the gas is determined by the leakage between the case and anode.
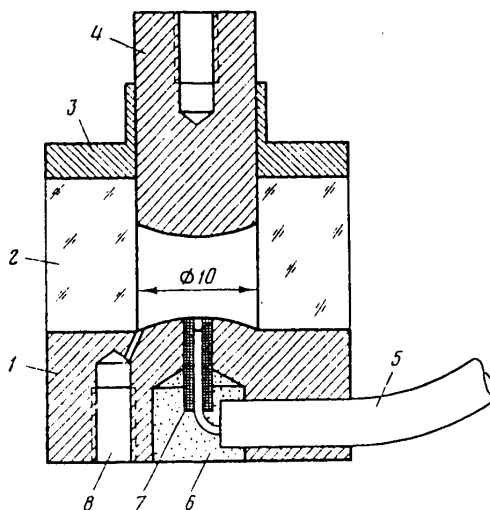

Figure 2. Construction of Spark Gap: 1--lower electrode; 2--case; 3--contact lid; 4--moving electrode; 5--cable with firing electrode; 6--epoxy resin with quartz sand; 7--porcelain tube; 8--gas inlet

The durability of the spark gap is determined mainly by failure of the porcelain insulator of the firing electrode. With a current of 1 kA it withstands $2 \cdot 10^6$ pulses. The interelectrode gap is set, depending on the supply voltage, within a range of 0.5 to 8 mm. The diameter of the anode and cathode is selected to be 8 mm greater than the diameter of the discharge channel, which equals approximately 2 mm. The spark gap is fired by means of a high-voltage pulse supplied from the step-up winding of transformer Tr2 (the line transformer of an "Elektronika VL-100" television is used).

The generator's output voltage is measured by means of divider $R_6 R_7$ and the current by means of a Rogovskiy loop placed on the wire going to the output connector. This loop's winding is made of wire with a diameter of 0.15 mm with a 0.5-mm spacing on a dielectric ring with an outside diameter of 25 mm and a cross section

71

of 5 X 5 mm^2. Simultaneously with the output pulse the circuit containing Tr4, R_8, R_{10} and D_3 forms a synchronizing pulse of fixed amplitude. The load resistance is matched with the line's wave impedance and the output voltage is regulated by means of resistors R_3 and R_4. For the purpose of lowering their inductance these resistors are wound onto flat cores made of glass-cloth-base laminate 0.5 mm thick with 0.4-mm-diameter Nichrome wire.

Shielding of the generator, which is necessary for suppressing noise originating during its operation, is performed by means of an enclosure of copper 0.5 mm thick. For the purpose of preventing infiltration of the noise signal, the contact between the enclosure and the removable front wall to which the entire circuit is fastened has been improved by using spring tabs on the lid. This sort of shielding made it possible to use photodetectors with a sensitive amplifier in the direct vicinity of the generator.

Bibliography

1. Krylov, N.N. "Impul'snaya tekhnika" [Pulse-Driven Equipment], Moscow, Svyaz'izdat, 1950, p 71.

8831
CSO: 1860/74

UDC 621.374.32

CONTROL CIRCUIT FOR SEVEN-SEGMENT ELECTROLUMINESCENT INDICATORS

[Article by Ya.L. Gesin and G.A. Korotkevich]

[Text] A description is given of a control circuit, operating in the dynamic mode, for K514ID2 7-segment indicators. Utilization of switching of the cathodes of indicators as opposed to switching of the grids made it possible to simplify the code converter circuit.

Certain circuits for controlling vacuum tube luminescent 7-segment indicators in the dynamic mode call for supplying an enabling potential to the indicator's grid. However, with this method of switching indicators it is necessary to use a great number of mounted elements and an additional disabling voltage source [1]. Changing from switching the grids of vacuum tube luminescent indicators to switching the cathodes makes it possible to use a considerably simpler circuit for controlling a multidigit digital indicator, as well as to make fuller use of the capabilities of integrated microcircuits with a medium degree of integration as compared with [1].

The advantages of this method of constructing a code converter are obvious in the example of the 4-place digital display unit whose circuit diagram is presented in fig 1.

A 2-bit code with an information replacement frequency of approximately 400 Hz for enabling a dynamic display mode enters the address lines of a K155ID1 binary-decimal decoder and two doubled K155KP2 multiplexers. The individual outputs of counters in direct code are led to the information inputs of the multiplexers. The combination of multiplexers transfers the direct code from one of the counters to the input of a code converter depending on the current address. The code converter consists of a unit for decoding the binary-decimal code into the code of K154ID2 7-segment light-emitting diode indicators and of seven high-voltage switches employing two K1NT661 microcircuits for controlling the anodes of the digital indicators.
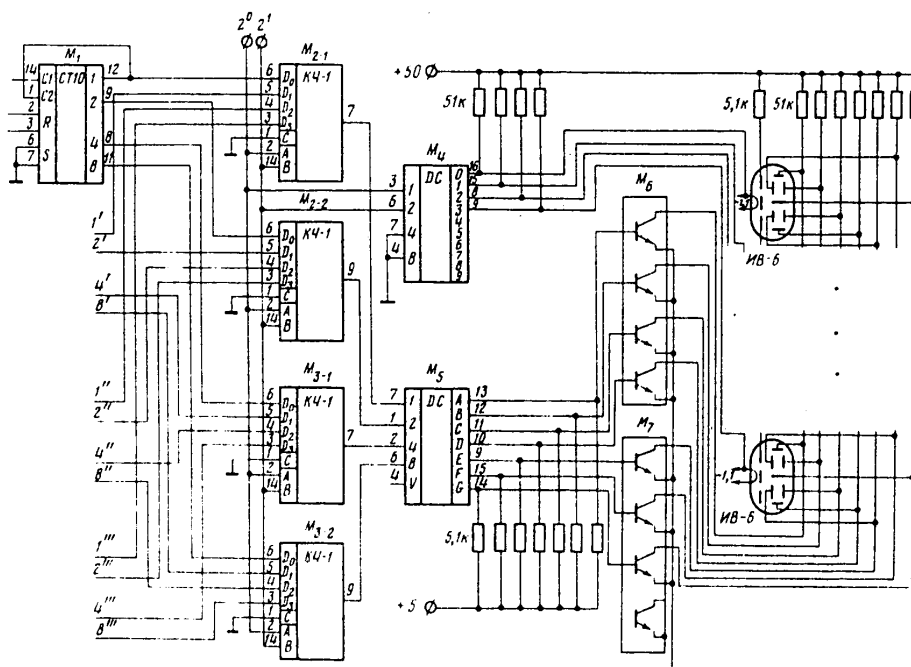
73

Figure 1. M_1--K155IYe2; M_2 and M_3--K155KP2; M_4--K155ID1; M_5--K514ID2; M_6 and M_7--K1NT661

The grids of the indicators are under positive d.c. voltage and of the four cathodes at each moment of time only one is connected to the minus line of the anode supply. The row position of the indicator turned on corresponds to the position of the counter whose information is indicated at a given moment. The frequency for switching indicators from the indicating to the passive state equals 100 Hz, which makes blinking unnoticeable. In view of the fact that the cathodes of the indicators with this method of control must be galvanically decoupled from one another, the power transformer has four separate windings for supplying the incandescent filaments. The slight complication of the power transformer, of course, is compensated by the simplicity of the code converter circuit, which requires six cases of microcircuits for its realization. Only two nominal supply voltages are used: +5 and +50 V . When digital indication with a great number of bits (as many as eight) is required, the K155KP2 multiplexers must be replaced by K155KP7 microcircuits and a 3-bit address code must be drawn from the counter.

74

Three-stage logical isolation of the counters from the high-potential circuits makes possible exceptionally high noise immunity of the circuit.

Bibliography

1. Babanin, V.B., Musonov, V.I. and Chizhikov, V.A. PTE, No 1, 1977, p 103.

COPYRIGHT: Izdatel'stvo "Nauka", "Pribory i tekhnika eksperimenta", 1981

8831
CSO: 1860/74

FREQUENCY DIVIDERS WITH VARIABLE DIVISION FACTOR

[Article by V.V. Krochakevich, Riga Polytechnical Institute]

[Text] A description is given of pulse frequency dividers with a variable division
factor (from 1 to 10 and from 1 to 256) in which the pulse counter is preset by
a certain number with the subsequent continued counting of pulses to complete
filling of the counter. These dividers are constructed with series 164 microcir-
cuits and have a speed of response of 1 MHz.

Frequency dividers with a variable division factor (DPKD's) containing a pulse
counter, decoder and gated setting unit [1] have the disadvantage that they require
the use of a multiposition switch capable of reliably switching current in the nano-
ampere range. Designing a DPKD on the basis of a parallel–series or series circuit
[2] has proven to be disadvantageous from the viewpoint of minimizing the number of
integrated microcircuit cases.

In figs 1a and 2 circuits are given for DPKD's for which the division factor, K ,
can take on values of

$$K = N - n ,$$

<div align="right">(1)</div>

where N is the total capacity of the pulse counter, n is the presetting number
assigned from without by a coding switch, set of switches, analog-digital converter
and the like. Both DPKD's are designed on the basis of the integrated microcircuit
of a 5-bit pulse counter, the K164IYe2, which has terminals for asynchronous pre-
setting of the first four bits and operates in the binary–decimal or binary mode
depending on the potential in the counting control terminal. The overall synchroni-
zation system of the DPKD provides for gated presetting of counters by a number, n ,
assigned from without, upon termination of the cycle for the filling of the counter
(counters) with pulses up to its total capacity, N , in each operating cycle of the
DPKD. Competition phenomena among signals in the synchronization circuit are elimi-
nated, since the counters and synchronization unit are clocked through a single
line, but here the counter is switched by the trailing edge and the synchronization
unit by the leading edge of the clock pulse. In addition, pulses of all operations

FOR OFFICIAL USE ONLY

of the synchronization circuit are strictly separated over time and have flat peaks at the maximum clock rate of 1 MHz.
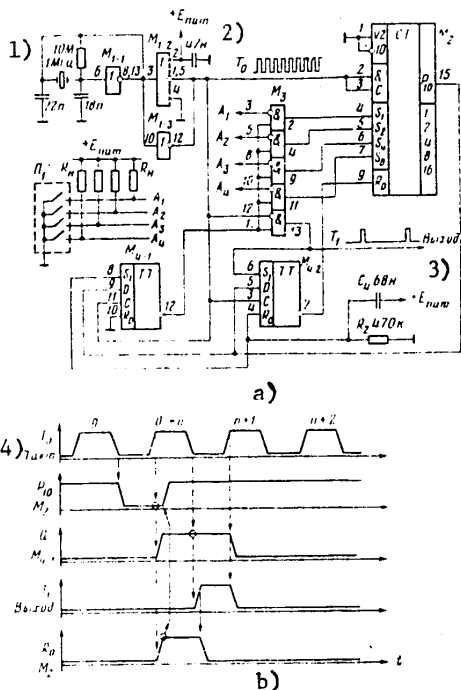

Figure 1.   Clock and Frequency Divider with Variable Division Factor (from 1 to 10) (a) and Time Diagram of Divider's Synchronization Cycle (b): M_1--K164LP1, M_2--K164IYe2; M_3--K164PU1; M_4--K164TM2; P_1--PP10-MV; R_n--1MΩ

Key:

1. MHz
2. Power supply

3. Output
4. Timing

In fig 1a is shown the circuit of a clock and DPKD with a division factor of K = from 1 to 10 . The binary-decimal operating mode of counter M_2 is set by a low potential in counting control terminal 1. The decimal carry signal is picked up from terminal 15, which is the output of a built-in element (2NAND) for bringing together signals from the outputs of the first and fourth bits of the counter. At the leading edge of the next (after the carry signal) clock pulse the synchronization (M_4) and gated presetting (M_2) circuit is included. A time diagram of the synchronization cycle is presented in fig 1b. Counter M_2 is reset to zero by means of a signal from the output of flip-flop M_{4-2} and the signal at the output of flip-flop M_{4-1} is the presetting gate. The divider's output signal, produced from the initial clock pulse put into the presetting gate, is picked up from output 13

77

FOR OFFICIAL USE ONLY

of integrated microcircuit M_3. The diagram in fig 1b reflects the operation of the synchronization unit of a DPKD operating with any division factor, K, not equal to one. With $K = 1$ the signal in the decimal carry output of counter M_2 has a constantly low potential and the signal in the output of flip-flop M_{4-1} a high potential, and inverted clock pulses from its input are present in the output of the divider.
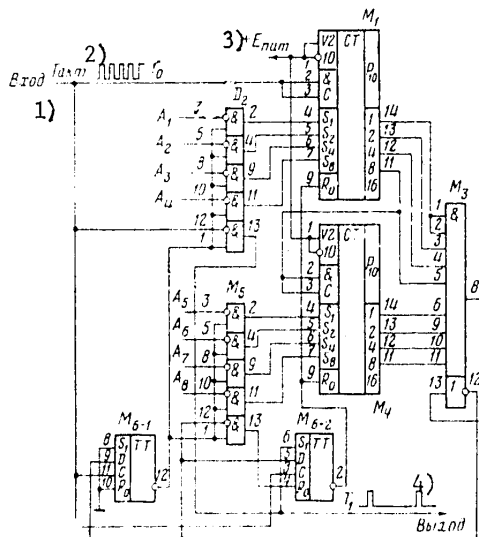

Figure 2. Frequency Divider with Variable Division Factor (from 1 to 256):
M_1, M_4--K164IYe2; M_2, M_5--K164PU1; M_3--K164LI1; M_6--K164TM2

Key:
  1. Input   3. Power supply
  2. Timing   4. Output

The division factor for the clock pulse frequency is set by presetting number n in terminals 4 to 7 of counter M_2 in the form of a binary code. The code for controlling the division factor set from without through lines A_1 to A_4 is inverted by means of element M_3. Therefore, the code supplied to these lines must be represented as the inverted code of binary number n.

If the code for controlling the division factor of the DPKD is set in lines A_1 to A_4 by means of a set of switches or a coding switch (e.g., P_1 in fig 1a) then the common wire for the set of switches or coding switch is connected to one terminal of the power supply and lines A_1 to A_4 are connected via resistors R_n to the other terminal of the power supply. The value of each resistor R_n is determined by the minimum current for reliable switching of the switch chosen (or coding switch).

The circuit of the gated presetting unit and for forming the output signal (M_3 in fig 1a) is organized on the basis of a K164PU1 level converter integrated

78

microcircuit containing five inverters with two-way current switches in the output of each inverter. Internal coupling of the output current switches with the common conversion level line makes it possible to use this line (terminal 1 of M_3) for gating for the output of all five inverters.

Circuit R_2C_4 in fig 1a is intended to exclude a possible combination of switching of the flip-flops of the synchronization unit and pulse counter to a random state during the supplying of power from which the DPKD circuit cannot automatically leave. Setting inputs of flip-flops M_{4-1} and M_{4-2} of the synchronization unit can be used for controlling the operation of the DPKD. For example, with a high potential in the line connecting terminal 8 of M_{4-1} and terminal 4 of M_{4-2} pulses are absent in the output of the DPKD. On the other hand, with a high potential in terminal 10 of M_{4-1}, the frequency of pulses in the output of the DPKD equals the frequency of clock pulses and the picture of the initial cycle is inverted. When the operating mode of the DPKD is controlled through the setting inputs of the flip-flops of the synchronization unit the initial state of these flip-flops is determined by the control signals and loop R_2C_4 is eliminated from the circuit. For the purpose of interrupting the operation of the DPKD it is convenient to use one of the terminals of the built-in 2AND gate in the clock input of pulse counter M_2.

On the basis of the K164IYe2 integrated microcircuit of the counter it is possible to set up the circuit of a binary-code-controlled DPKD with any division factor. If the circuit of the DPKD in fig 1a is supplemented with a multi-input NAND gate in the circuit for coupling the counter with the synchronization unit, then in formation of the counter's overflow signal, by bringing together through the 4NAND gate the first four bits of the counter the division factor of the DPKD can be set from 1 to 16 (whereby the operation of the counter itself, M_2, in the binary mode is set by the high potential in counting control terminal 1). If the outputs of all five bits of the counter are brought together for synchronization through a 5-input NAND gate, then with the same control of the DPKD division by 2, 4, 6, ..., 32 is carried out. A further increase in the division factor is achieved by increasing the number of bits of the pulse counter and the number of elements of the presetting unit. As an illustration, in fig 2 is given the circuit of a DPKD with a division factor of K - 1, 2, 3, ..., 255, 256. Division factor K is set in keeping with (1) through lines A_1 to A_8 in the form of the inverted code of number n . In the circuit in fig 2 the first four bits of both counters, M_1 and M_4, are brought together through an 8-input NAND gate into the synchronization unit through integrated microcircuit M_3 (a K164LI1) containing a 9-input AND gate and one inverter. The unused ninth input of the AND gate can be connected to the positive terminal of the power supply or, as shown in fig 2, it can be connected to any input used for the circuit. The operation of the synchronization unit (M_{6-1} and M_{6-2}) of the DPKD in fig 2 is similar to the operation of the same unit (M_{4-1} and M_{4-2}) in the circuit in fig 1a with any division factor different from one (cf. the synchronization clock period time diagram in fig 1b). The difference between the circuit diagrams of the synchronization units of these dividers is that to the setting input (terminal 4) of flip-flop M_{6-2} in fig 2 is connected a logic circuit which eliminates self-locking of the DPKD in any possible combination of inclusion of the flip-flop structures of the entire circuit of the divider when supply voltage is supplied. For the purpose of controlling (similarly to the DPKD in fig 1) the operation of the DPKD in fig 2 it is possible to use the setting inputs of flip-flop M_{6-1} and the logic in the clock input of counter M_1.

79

In further development of DPKD's based on the circuit in fig 2 it is necessary to take into account the fact that with an increase in the divider's word length the load capacity of its output decreases. This is explained by the specifics of the use of K164PU1 level converter integrated microcircuits as gates for the presetting unit of a DKPD, namely: The sum of the output currents of all gates is equal at the limit to the current of the common conversion level line (terminal 1 of the K164PU1), connected in these DPKD circuits to the output of the first flip-flop of the synchronization unit. Thus, whereas in the circuit in fig 2 the load capacity of the output of flip-flop M_{6-1} (K164TM2) equals 100, then the load capacity of the output of the DPKD equals 90 with total connection capacitance of approximately less than 100 pF. DPKD's according to the circuits in figs 1a and 2 were tested in the ambient temperature range of -20 to +40 °C with a supply voltage of 6 to 9 V with timing by means of pulses with a frequency of 1 MHz from the clock shown in fig 1a. With a supply voltage of 5 V a frequency of 0.5 MHz has been determined as the maximum speed of response for the circuits tested.

Bibliography

1. Melen, R. and Garland. G. "Integral'nyye mikroskhemy s KMOP strukturami"
    [Integrated Microcircuits with CMOS Structures], translated from English,
    edited by V.M. Bogachev and S.M. Smol'skiy, Moscow, Energiya, 1979, p 115.

2. Kostyukov, V.I. and Reger, P.O. PTE, No 5, 1977, p 89.

8831
CSO: 1860/74

80

UDC 621.375.024

WIDEBAND DIRECT-CURRENT AMPLIFIER

[Article by Dzh.K. Parsamyan and M.G. Tokhmakhyan, Armenian SSR Academy of Sciences Institute of Radio Physics and Electronics, Ashtarak]

[Text] A description is given of a wideband direct-current amplifier with a drift compensation channel constructed according to a modulation-demodulation structure. The amplifier's gain is 60 dB, its transmission band is 0 to 100 kHz and its voltage temperature drift is 0.5 $\mu V/^{\circ}C$.

A major disadvantage of the familiar structures for wideband amplifiers with a parallel amplification channel is the complexity of ensuring uniform amplitude-frequency response (AChKh) in the region of the corner frequency [1]. In the amplifier which has been developed, whose circuit is shown in fig 1, the modulation-demodulation channel, M_1, M_3 and M_5, is designed to compensate the drift of the direct-current amplifier (UPT), M_2, M_4 and M_6. With this structure the amplifier's amplitude-frequency response is determined by the parameters of the d.c. amplifier channel [1].

The direct-current amplifier is assembled from three operational amplifiers (OU's), M_2, M_4 and M_6 (140UD8A [2]) with a gain of 20 dB for each stage. Since with this structure the current component of the drift is not compensated, for the purpose of reducing it, in the first stage of the direct-current amplifier an operational amplifier with field-effect transistors in its input is employed. The MDM [modulation-demodulation] channel with a total gain of 100 dB contains a modulator, demodulator, generator, M_1 (140UD13 [3]), and two amplification stages, M_3 and M_5 (140UD8B). The output voltage of the direct-current amplifier, via divider R_5 to R_8 with an attenuation factor of $K_d = K_{UPT}$, and the input voltage enter the differential input of M_1. In the output of the MDM channel voltage is produced which is proportional to the drift presented to the input of the direct-current amplifier. An integrating RC network (R_9C_3) with a time constant of 10 s is used as the low-frequency filter. The compensation voltage isolated in the filter enters the noninverting input of M_7, which makes it possible to maintain both a high transmission factor and a high time constant.

The balancing outputs of operational amplifiers M_7 and M_2 are used for coupling the MDM channel with the direct-current amplifier. The compensation voltage is

added to the input of the second stage of operational amplifier M_2 (terminal 6) from the output of the first stage of operational amplifier M_7 (terminal 6). Filters R_1, R_2, C_1 and R_3, R_4, C_2 prevent the penetration of commutation noise into the input of M_2 and the output of the amplifier. Diodes D_1 and D_2 prevent M_6 from going out of order from input overloads.
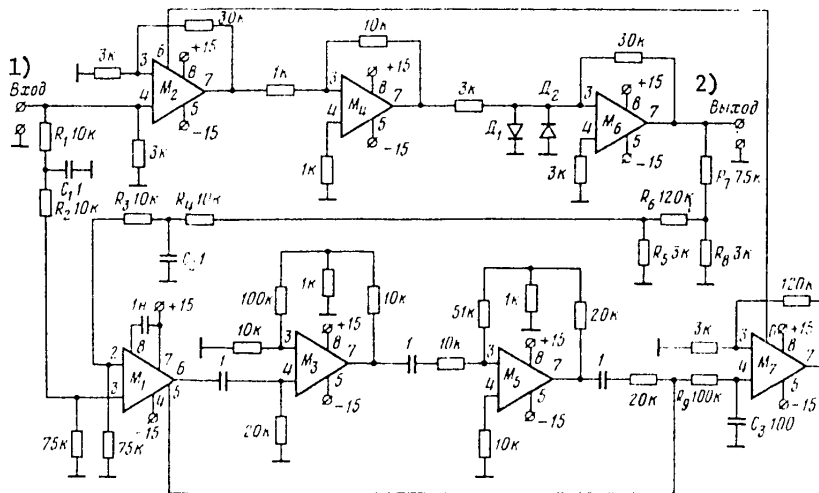

Figure 1. Circuit Diagram of Amplifier: M_1--K140UD13; M_3, M_5, M_7--140UD8B; M_2, M_4, M_6--140UD8A; D_1, D_2--2D503

Key:
1. Input   2. Output

The voltage temperature drift of the direct-current amplifier is determined by the drift of M_1. Uniformity of the amplitude-frequency response is determined by the identity of filters R_1, R_2, C_1 and R_3, R_4, C_2. From the results of labora-tory tests the amplifier possesses the following parameters: gain of 60 dB; transmission band of 0 to 100 kHz; voltage temperature drift of 0.5 μV/°C; noise e.m.f. at a frequency of 1 kHz not greater than 400 nV/Hz$^{1/2}$. The amplifier's operating temperature range is determined by the temperature range of the K140UD13 operational amplifier.

The amplifier is assembled on a printed circuit board measuring 95 X 190 mm^2.

Bibliography

1. Polonnikov, D.Ye. "Reshayushchiye usiliteli" [Operational Amplifiers], Moscow, Energiya, 1973.

82

2. Blumberg, M.R., Meyer, V.V., Nesterov, V.I., Ryutel', A.R. and Strizh, A.A.
    ELEKTRONNAYA PROMYSHLENNOST', No 4, 1978, p 7.

3. Lyakhovich, V.V., Moskalenko, N.I., Ozhogin, M.A. and Stepanenko, I.P.
    ELEKTRONNAYA PROMYSHLENNOST', No 5, 1979, p 26.

8831
CSO: 1860/74

UDC 621.376.55

HIGH-SPEED PULSE PHASE DISCRIMINATOR

[Article by Ye.P. Vetlugin, A.I. Lavrushev and T.P. Yartsun, Kiev Polytechnical Institute Zhitomir Branch]

[Text] A pulse phase discriminator is described which is designed from series 500 microcircuits. The discriminator's operation is based on the formation of a time-base voltage of asymmetric trapezoidal form, which makes it possible to create an intermediate storage, to improve noise immunity and to reduce the aperture error. With a comparison frequency of 2 MHz the discriminator makes it possible to suppress noise 20 dB greater than with time-base voltage of asymmetric triangular form.

Pulse phase discriminators (IFD's) are widely used in crystal frequency band control systems. IFD's of the "accessing-storage" type, executed according to the time-base balancing method, have high speed of response but noise of high amplitude at the comparison frequency is present in their outputs [1]. It is possible to reduce the amplitude of this noise by changing the form of time-base voltage. In [2] it is demonstrated that if asymmetric triangular voltage is employed instead of sawtooth then it is possible to reduce voltage overshoots at the moment scanning is begun.

In the IFD's described, for the purpose of further reducing noise in the discriminator's output sweep voltage of asymmetric trapezoidal form is used.

A structural diagram of the IFD is shown in fig 1a and a time diagram of its operation in fig 1b. The phase difference discrimination unit (UVRF), to whose information inputs are supplied the reference (f_{op}) signal and the signal being studied (f_x), generates pulses (diagram in fig 1b) whose length is proportional to the difference between the phases of f_{op} and f_x. A control unit consisting of flip-flops Tg1, Tg2 and an OR gate at the leading edge of this signal turns on and at its trailing edge cuts off the scanning unit (RU). The integrating capacitor, C, having had in the initial state a charge corresponding to the initial level, U_0, is charged to a level, U_p, proportional to the length of the pulse in the output of the UVRF and remains in this state until the discharging unit (UR) is turned on (b in fig 1b).

Simultaneously with cutting off of the RU, from flip-flop Tg2 a signal is supplied to the switching unit (K1U), which opens for period of time Δt_1 (b in fig 1b), equal to the delay time of delay line LZ_1, and the storage unit (ZU) is connected via input buffer stage BK_1 to integrating capacitor C, and storage of potential U_p takes place in the storage unit. During time Δt_2 , equal to the delay of delay line LZ_2, the switching unit is closed (d in fig 1b) and storage of the signal takes place in the storage unit until the next "accessing" (e in fig 1b).
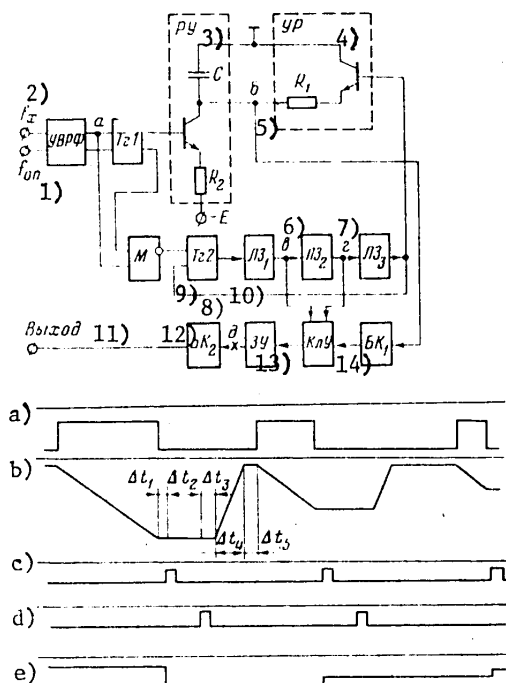
Figure 1. a--Structural Diagram of Unit: UVRF--phase difference discrimination unit, RU--scanning unit, UR--discharging unit, Tg1 and Tg2--flip-flops, M--OR gate, LZ_1 to LZ_3--delay lines, K1U--switching unit, BK_1 and BK_2--source followers, ZU--storage unit; b--Time Diagram of Unit's Operation

Key:

1.	$\bar{t}$ [reference]	8.	e)
2.	UVRF	9.	Flip-flop 2
3.	RU	10.	Delay line 1
4.	UR	11.	Output
5.	b)	12.	Buffer stage 2
6.	c)	13.	Storage unit
7.	d)	14.	Switching unit

85

During time Δt_3 , after K1U is closed, equal to the delay in LZ_3, the discharging unit is cut in and integrating capacitor C is discharged relatively slowly through resistor R_1 (b in fig 1b). Thus, the integrating capacitor of the scanning unit in this circuit emerges in the role of an intermediate storage. Besides, charging of the capacitance of the storage unit (ZU) takes place when transient processes associated with charging of the integrating capacitor, C, of the scanning unit have already been completed and transient processes associated with its charge have not yet begun, since the switching unit (K1U) connecting the storage unit to capacitor C is open after the charge and closes before the beginning of the discharging of capacitor C. In other words, the scanning unit (RU) accomplishes accessing and storage of the sweep voltage for the period of copying into the storage capacitance of the storage unit, which stores the information until new accessing. The storage time in the scanning unit's integrating capacitor does not depend on the value of the phase difference and is constant, since it is determined by the total delay of the three delay lines (LZ's).

The length of the pulse opening the switching unit (K1U) (c and d in fig 1b) is determined by the time constant of the storage unit's charge, i.e., by the product of the capacitance of the ZU and the resistance of an open switch of the K1U. In this circuit this length is also constant, which creates favorable conditions for operation of the K1U switch.

Time Δt_5 is a variable quantity. It varies in inverse proportion to the length of the phase difference, $\Delta\phi$, pulse from 0 to $(1/2)f_{pp}$, but for the purpose of protecting the sweep voltage at the initial moment from overshoots of the transient process associated with discharging of integrating capacitor C, the minimum value of Δt_5 is limited by the condition: $\Delta t_{5\,min} \geq \Delta t_p$, where Δt_p is the time of the transient process of the discharging of capacitor C. Under these conditions the scanning unit will begin to operate after termination of all transient processes of the preceding cycle, i.e., each start of the operation of the scanning unit is pre- ceded by quiescent conditions, when $U_{RU} = U_0$ for period of time Δt_5 .

The entire circuit of the discriminator, with the exception of source followers BK_1 and BK_2 and the switching unit (K1U), is executed with series 500 digital integrated microcircuits. The circuit diagram of the pulse phase discriminator is shown in fig 2. The UVRF is executed with NOR gates (M_1, M_2, M_4 to M_7 and M_9). This unit repre- sents a phase discriminator which generates two pulses for the period of f_{op} , comparing signals f_{op} and f_x . The first time, comparison takes place during the time of the duration of the pulse, and the second time, during the time of the dura- tion of the pause. The operating principle and characteristics of the phase dis- criminator are given in [3]. The scanning unit is executed with two NOR gates, M_{10} and M_{13}, integrating capacitor C_1 and resistors R_1 and R_3, and the discharging unit with one gate of the same kind, M_{14}, and resistor R_5. The control unit is constructed with flip-flops Tg1 and Tg2 and NOR gate M_8. Flip-flop Tg1 controls the scanning unit (RU) and flip-flop Tg2 the switching unit (K1U) and RU.

Delay lines LZ_1 to LZ_3 are constructed with differential receivers from the line, DP_1 to DP_3, which perform the function of comparison circuits [4], and three NOR gates, M_{11}, M_{12} and M_{15}, forming together with capacitor C_2 and resistors R_2 and R_6 (fig 2) a sawtooth voltage generator (GPN). Flip-flop Tg4 and NOR gate M_{16} control

86

the K1U and flip-flop Tg3 together with circuit DP_4 serve the purpose of returning the entire circuit to the initial state.
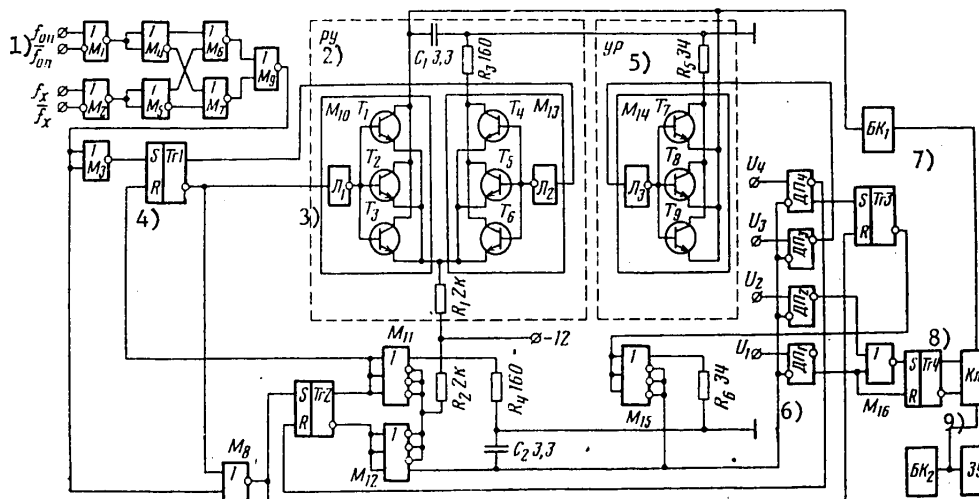

Figure 2. Circuit Diagram of Pulse Phase Discriminator: M_1 to M_9 and M_{16}--1/3 K500LM105M; M_{10} to M_{15}--1/2 K500LYe11M; Tg1 to Tg4--1/2 K500TM131M; DP_1 to DP_4--1/3 K500LP116M

Key:

1. f_{op}
2. Scanning unit
3. Left half (L_1)
4. Tg1 [flip-flop]
5. Discharging unit
6. DP_1 [differential receiver]
7. Buffer stage
8. Switching unit
9. Storage unit

Of definite interest is the execution of scanning unit and sawtooth voltage generator circuits with NOR gates. The circuit diagram of a scanning unit containing two NOR gates is shown in fig 2. Each gate consists of the logic section itself and three output transistors with open emitters and a common collector output. It is obvious from fig 2 that the scanning unit is in the form of a current switch, one arm of which is loaded onto capacitor C_1 and the other onto resistor R_3. In the initial state the left half (L_1) and transistors T_1 to T_3 are closed--capacitor C_1 is charged to potential U_0--and the right half is open. When the scanning unit is cut in the left half of the switch is opened and the right half is closed--capacitor C_1 is charged to potential U_p by means of the current generator (R_1 = 2 kΩ and E_e = -12 V). When the scanning unit is cut off capacitor C_1 remains charged until the discharging unit is cut in, which occurs by means of a signal from the output of element DP_3 a period of time of Δt_3 after closing of switch K1U (cf. fig 1). Upon this signal transistors T_7 to T_9 open, connecting in parallel capacitor C_1 of the scanning unit and resistor R_5 of the discharging unit, thus making possible

87

smooth discharging of the integrating capacitor (cf. diagram b in fig 1b). In the circuit discussed integrating capacitor C_1 is charged according to a law close to linear, and not an exponential one, since charging of the capacitor is produced by the current generator.

The delay line sawtooth voltage generator is constructed similarly, but its output voltages have an asymmetric triangular form since its integrating capacitor is not fixed in the charged state, i.e., after charging discharging ensues at once. The sawtooth voltage generator is controlled by flip-flop Tg2.

The formation of time intervals by delay lines LZ_1 to LZ_3 is accomplished as the result of the operation of DP_1 to DP_3 in comparing the output voltage of the sawtooth voltage generator with reference voltages U_1 to U_3 . Circuit DP_4 operates similarly with respect to reference voltage U_4 .

Buffer stages BK_1 and BK_2 are in the form of source followers with dynamic loading and reduced input capacitance, assembled from KP303V field-effect transistors and KT363B bipolar transistors performing the role of an output stage designed as a balanced circuit. This circuit has a transmission factor of 0.98, input impedance of 1 MΩ, output impedance of 50 to 100 Ω and input capacitance of less than 1 pF.

The switching unit is executed as a series-parallel circuit employing KP305Zh MOS field-effect transistors having low open-channel impedance. The switch consists of three stages and makes possible attenuation of a signal in a pause of 120 dB (at frequencies up to 30 MHz). For the purpose of matching the control input of the switching unit with ECL logic element levels and for producing the required voltages for effectively controlling field-effect transistors, a control circuit is used consisting of two differential stages with direct coupling. The first of these is executed with KT325B silicon transistors with reverse conductance, and the second with KT363B silicon transistors with forward conductance. This circuit for the switching unit control unit has high stability and the use in it of high-frequency transistors makes it possible to produce a short leading edge for the control signal (less than 30 ns) and to reduce the time for turning the switch on and off.

The use of an asymmetric trapezoidal form of sweep voltage makes it possible to reduce considerably the amplitude of voltage overshoots and the time for the establishment of transient processes of the scanning unit, especially when the scanning mode is replaced by the discharging mode. In addition, the use of sweep voltage of this form makes it possible to reduce the unit's aperture error, which is especially important when using the discriminator in measuring equipment systems.

The pulse phase discriminator was studied at a frequency of f_{op} = 2 MHz . Suppression of voltage with the comparison frequency was produced to an extent of 118 dB, which is 20 dB greater than with a pulse phase discriminator with an asymmetric triangular form of sweep voltage. The phase shift measuring range equals $\pm \pi$. Within the range of measuring the phase shift the phase pulse discriminator's characteristic is a straight line passing through the origin [1] and nonlinearity equals $\varepsilon < 0.07$. Structurally the pulse phase discriminator is executed in a sectional shielded case. Power supply voltages equal -2, -5.2 and -12 V.

88

Bibliography

1. Galin, A.S. "Diapazonno-kvartsevaya stabilizatsiya SVCh" [Microwave Crystal Band Stabilization], Moscow, Svyaz', 1976, p 72.

2. Gelozhe, Yu.A. and Kibirev, A.A. USSR Patent No 484636, published in BYULLETEN' IZOBRETENIY, No 34, 1975, p 140.

3. Mashbits, L.M. RADIOTEKHNIKA, Vol 28, No 9, 1973, p 1.

4. Vetlugin, Ye.P., Lavrushev, A.I., Povidayko, P.M. et al. PTE, No 1, 1979, p 82.

COPYRIGHT: Izdatel'stvo "Nauka", "Pribory i tekhnika eksperimenta", 1981

8831
CSO: 1860/74

COMMUNICATIONS

UDC 621.391 (075.8)

LABORATORY PROJECTS ON COMMUNICATION LINE STRUCTURES

Moscow LABORATORNYYE RABOTY PO LINEYNYM SOORUZHENIYAM SVYAZI in Russian 1981
(signed to press 6 Mar 81) pp 2-3, 153

[Annotation, foreword and table of contents from book "Laboratory Projects
on Communication Line Structures", by Aleksandr Vasil'yevich Obukhov, reviewed
by G. N. Azarenkov and M. Ye. Smolyanskiy, Izdatel'stvo "Radio i svyaz'", 12,000
copies, 153 pages]

[Text] This laboratory manual describes laboratory projects based on the curricu-
lum. The necessary theoretical material is presented for each project; instructions
on the methods, work schemes, graphs and tables are given, as well as a short de-
scription of the instruments to be used and the rules for using them. At the end
of each project, a list of questions for programmed testing is given.

This manual is intended for use by students of communication tekhnikums specializing
in the following: "Automatic and Multichannel Electrical Communication" and "Tele-
graph Communication and Data Transmission".

Foreword

Under present conditions, practical training of students of specialized secondary
educational institution is an integral part of the educational process as a result
of which students acquire professional skills, and in technical fields of special-
ization, they also acquire qualifications for a practical profession. Practical
laboratory work is one of the forms of practical training.

The teaching aid on the subject "Line Structures" contains laboratory projects com-
piled in accordance with the program of the course. The engineering of line struc-
tures of communication lines has changed substantially. There appeared new types
of communication cables, cabling technology has been improved, new instruments have
been created for work on communication lines, new instruments and equipment were
created, and normative technical documentation was developed and approved. This is
reflected in this manual. It contains the necessary theoretical material for each
project, instructions on methods, work schemes, graphs and tables, descriptions of
the instruments to be used and rules for using them. At the end of each project,
a list of questions is given for a programmed test covering the material of the pro-
ject. This manual is intended for use by students of tekhnikums in the areas of
specialization "Automatic Electrical Communication", "Multichannel Electrical

90

Communication" and "Telegraph Communication and Data Transmission". The programmed tests for each project will also make it possible for the teacher to use the class time more rationally.

The author is grateful to the reviewers M. Ye. Smolyanskiy and G. N. Azarenkov for their useful comments and advice which contributed to the improvement of the content of this book.

<div align="center">Contents</div>

COMPUTERS

SIGNAL PROCESSING UNIT BASED ON 'ELEKTRONIKA B3-18' MICROCALCULATOR

[Article by S.V. Klevtsov, Ye.A. Putsyato, Yu.P. Firstov and N.P. Chistyakov, Moscow Engineering Physics Institute]

[Text] A description is given of an accessory for the "Elektronika B3-18" microcalculator making it possible to process signals according to an assigned routine, in particular to compute the phase shift angle, ψ , between two signals, U_1 and U_0 , according to the routine $\psi = \arccos U_1/U_0$. Angles are measured in the range of 0 to 90° ($\pm$ 45°) with an accuracy of 0.03 percent with a maximum input voltage of 10 V. It is possible to change the computation routine, as well as the sequence for performing operations.

In conducting a physics experiment it is convenient to use a standard microcalculator for automatic processing of its results. In combination with an accessory which converts analog signals into digital form and inputs this information, a microcalculator processes these signals according to an assigned algorithm and displays the result obtained.

In this article a description is given of an accessory making it possible in combination with a "Elektronika B3-18" microcalculator to measure the phase shift between two signals.

In measuring the phase shift, ψ , between two signals, U_1 and U_0 , it is necessary to perform an operation of the type $\psi = \arccos U_1/U_0$. These operations are performed by means of the computer-processor whose structural diagram is illustrated in fig 1. The unit operates in the following manner. When pulse Gate 1 is supplied signals from the output of voltage-to-frequency converter PNCh 1 begin to enter through commutator K the input of counter line SCh 1 (five decades) and at the trailing edge of pulse Gate 1 the numerical equivalent of quantity U_0 entered in SCh 1 during the time of this pulse's action is copied into register R_0 . Similarly, when pulse Gate 2 is supplied the numerical equivalent of quantity U_1 is entered into register R_1 .

Execution of the computation routine begins with the arrival of pulse Gate 3. Clock pulses enter SCh 2, which controls multiplexer MP, in whose output is formed the code of the operation to be executed at this step. The operation code then enters the

92

decoder, Dsh, which controls the actuating unit, IU, which replaces the microcalculator's keyboard input. Registers R and R_1 are connected to inputs 1 to 5 and 7 to 11 (outputs 4 to 8 and 1, 2, 2Ÿ to 23) of the multiplexer, MP. In this variant of the computer code 1011 (:) is supplied to input 6 (output 3) of the multiplexer by connecting the corresponding output to the common line or to the power line. Codes are assigned similarly for inputs 12 to 15 (outputs 17 to 20), whereby a "wired-in program" is made possible.
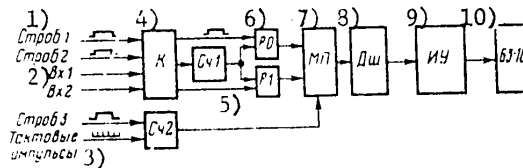
Figure 1. Structural Diagram of Phase Shift Meter

Key:

1. Gate 1
2. Input 1
3. Clock pulses
4. Commutator
5. Counter No 1

6. Registers
7. Multiplexer
8. Decoder
9. Actuating unit
10. B3-18

The circuit diagram of voltage-to-frequency converters PNCh 1 and PNCh 2 is shown in fig 2. The operation of this unit is described in detail in [1]; therefore, let us indicate only that the clock frequency for the voltage-to-frequency converters equals 20 kHz. An output frequency of 10 kHz corresponds to an input voltage of 10 V, conversion nonlinearity is not worse than 0.01 percent and instability is not greater than 0.02 percent in the 0 to 35 °C temperature range.
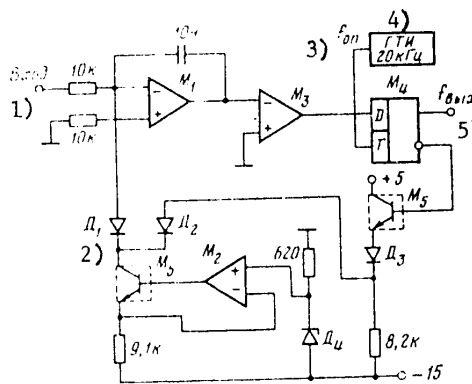
Figure 2. Circuit Diagram of Voltage-to-Frequency Converter: GTI--clock;
M_1 and M_2 --140UD7, M_3 --521SA3, M_4 --155TM2, M_5 --159NT1A;
D_1 to D_3 --D223, D_4 --KS196G
[Key on following page]

93

Key:
1. Input
2. Diode No 1
3. Operating frequency
4. 20 kHz clock
5. Output frequency

The circuit diagram of the phase shift meter processor is presented in fig 3. The processor is constructed with series 134 and 155 microcircuits and consists of an input commutator, M_1 , counters, M_5 to M_9 , an auxiliary counter, M_{10} , register R_0 --M_{11} to M_{15}, register R_1 --M_{16} to M_{20}, a multiplexer, M_{21} to M_{24}, and a decoder, M_{25}. The actuating unit is implemented with RES-64B (RS4.569.745) hermetically sealed reed relays with an operating current of approximately 3 mA connected in parallel with the control keys of the microcalculator.
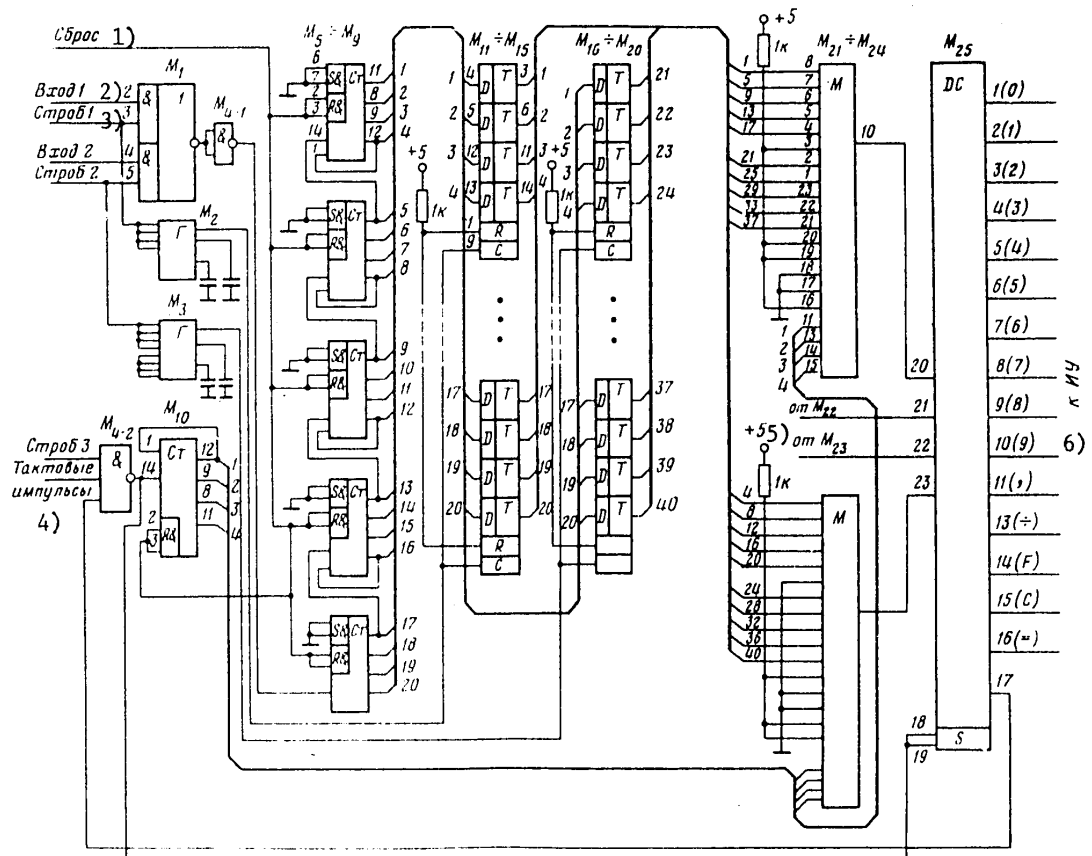
Figure 3. Circuit Diagram of Meter: M_1--155LR1, M_2 and M_3--134KhL1, M_4--155LB4, M_5 to M_9--155IYe2, M_{10}--155IYe5, M_{11} to M_{20}--155TM8, M_{21} to M_{24}--155KP1, M_{25}--155ID3
[Key on following page]

94

FOR OFFICIAL USE ONLY

Key:

1. Reset
2. Input 1
3. Gate 1

4. Clock pulses
5. From M_{22}
6. To actuating unit

The key technical characteristics of the phase shift meter are as follows: range of angles measured--0 to 90° ($\pm$ 45°); maximum relative error--0.03 percent; input signal range--10 V; measuring time--1 s; clock frequency--10 kHz; floating-point result presented on 8-decade display.

This signal processing unit constructed on the basis of a microcalculator, with small overall dimensions and simplicity in debugging. has high precision characteristics and makes it possible to alter flexibly the computation routine and sequence of operations.

Bibliography

1. Sheyngold, D.M., editor. "Spravochnik po nelineynym skhemam" [Nonlinear Circuit Handbook], translated from English, Mir, 1977, p 92.

8831
CSO: 1860/74

FOR OFFICIAL USE ONLY

MULTIFUNCTION GENERATOR

[Article by I.K. Gerasin, Moscow Institute of Electronic Engineering]

[Text] A description is given of an analog converter constructed with series K140, K198 and K159 circuits. The basis of the converter is a K140MA1 balanced modulator. The converter multiplies and measures ratios and can be used for extracting the square root and for amplitude and phase detection in phase-locked loops. The maximum input voltage is $\pm$ 10 V, the dynamic range is 50 dB, nonlinearity is less than or equal to two percent and the input bandwidth is 2 MHz.

Multiplication-division and root extraction devices are necessary for reproducing trigonometric functions, computing vector quantities and a root-mean-square value and other computing and measuring operations. The operating accuracy of these devices depends on the methods and element base employed for their design [1-3]. Here the added problem arises of coordinating various function generators in a single measuring complex. A unified element base partly solves this problem.

Differential stages have received extensive application in the design of function generators. Multiplication devices have been implemented most simply by their means [1]. The integrated circuits of 526PS1. 525PS1 and K140MA1 balanced modulators can serve as an example [4]. The last one of these was used as the basis for constructing a multifunction generator which can be used for extracting the square root, squaring, finding ratios and multiplying voltages.

The generator whose circuit is shown in fig 1 is implemented with series K140, K198 and K159 integrated circuits. When the device is used in the multiplication (squaring) mode the signals to be multiplied are supplied to inputs X and Y of the voltage-current converter, M_4, and a multiplication stage, M_8, respectively. M_4 and the differential transistors, M_2, loading it, with the diodes included, represent a logarithmic amplifier with mutually inverse outputs by means of which multiplication stage M_8 is linearized for input X [5]. The output current of M_8, proportional to the product of the input signals, is supplied to current reflector M_7 and current-to-voltage converter M_9. The generator current in transistor 2, passing through transistor 1 of the current reflector and the current-to-voltage converter makes it possible to shift the level of the multiplication stage.
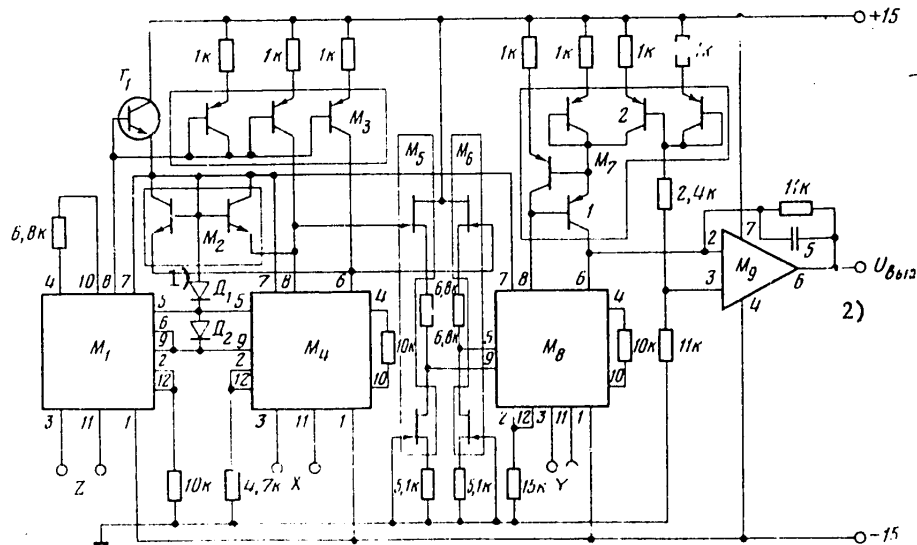
Figure 1. Circuit Diagram of Multifunction Generator: M_1, M_4, M_8--K140MA1; M_2--K1NT591V; M_3, M_7--K1NT986A; M_5, M_6--KPS104D; M_9--K140UD10; T_1--KT342V; D_1, D_2--KD503A

Key:
1. Diodes   2. Output

In the division mode input Y of circuit M_8 is connected to a source of reference voltage whose value determines the function generator's transmission factor in this mode. The voltage of the dividend is supplied to input X and of the divisor to input Z of individual voltage-to-code converters M_1 and M_4. The latter via current reflector M_3 controls the transconductance of diodes M_2. Control can be accomplished by voltage of both polarities supplied to the corresponding input of M_1, whereby the other input is connected to ground.

For the purpose of reducing the influence of the input current of M_8 on the trans- conductance of diodes M_2, its input is connected to the output of M_4 via source followers with dynamic loading of M_5 and M_6. For the purpose of compensating the emitter-base difference voltage of the diodes of M_2, resulting in biasing of the function generator's zero level, to the drains of the field-effect transistors re- sistors are connected, by selecting which it is possible to reduce this voltage, in terms of the input of M_8, to zero.

The voltage drop in the diodes of M_2 is proportional to the logarithm of the dividend and inversely proportional to the transconductance of the diodes and accordingly to the voltage at input Z. Thus, the voltage at the output of M_9

97

will be equal to the ratio of voltages at inputs X and Z . When the output of M_9 (taking into account the polarity of the output voltage) is connected to input Z of circuit M_1 the output voltage of the function generator will be proportional to the square root of the voltage supplied at input X . Matching of integrated circuits M_1, M_4 and M_8 in terms of potential levels is made possible by transistor T_1 and diodes D_1 and D_2.

The function generator has the following characteristics: maximum input voltage-- $\pm$ 10 V, dynamic range--50 dB, nonlinearity less than or equal to two percent, input bandwidth--2 MHz.

Bibliography

1. Greben, A.B. "Proyektirova·iye analogovykh integral'nykh skhem" [Designing Analog Integrated Circuits], translated from English, edited by Ye.Kh. Karayerov, Moscow, Energiya, 1976.

2. Zhilinskas, R.-P.P. "Izmeriteli otnosheniya" [Ratiometers], Moscow, Sovetskoye Radio, 1975.

3. Volodyagin, Yu.S. and Kudryavtsev, V.N. PTE, No 4, 1978, p 152.

4. Yakubovskiy, S.V., Barkanov, N.A. and Kudryashov, B.P. "Analogovyye i tsifro-vyye integral'nyye skhemy" [Analog and Digital Integrated Circuits], Moscow, Sovetskoye Radio, 1979, p 231.

5. Timonteyev, V.N., Kuz'menko, V.N. and Tkachenko, V.A. PTE, No 4, 1978, p 156.

8831
CSO: 1860/74

UDC 681.14:621.396.96(024)

COMPUTER-ASSISTED RADAR OPERATOR TRAINERS

Moscow TRENAZHERY DLYA PODGOTOVKI OPERATOROV RLS S POMOSHCH'YU EVM in Russian
1980 (signed to press 5 Dec 79) pp 2-4, 125-256

[Annotation, introduction and table of contents from book "Computer-Assisted
Radar Operator Trainers" by Anatoliy Nikolayevich Romanov, Voyenizdat, 6000 copies,
127 pages]

[Text]   Annotation

This book examines the basic technical design principles of computer-based trainers,
and presents the requirements for trainers. Methods of modeling targets and noise
on the display screen using computers are explained, as are principles of simulat-
ing signals in trainers.

Some questions of the psychological training of operators are explained, and the
methodology for teaching operators using trainers and methods of evaluating their
level of training are given.

The book is intended for military specialists involved in developing and operating
trainers.

Introduction

Units and subunits of radio technical troops are equipped with the most modern combat
technology, incorporating the latest achievements of Soviet science. This increases
the requirements for the level of training of the personnel which service it.

When operators are working at a high professional level, they are able to master
modern radar technology and automated control systems, and to exploit their combat
capabilities with confidence.

Life has made it necessary to find ways to train radar operators more rapidly.

Reducing the time required to train specialists is only part of the problem.
Another part is to increase operator performance using combat equipment. In
organizing and conducting combat training, commanders, political workers and
staff officers use as their basis the fact that continuously increasing power

99

and complexity of military technology are amplifying the relationship between the degree to which it is mastered by personnel and the effectiveness of its battle application.

The level of training of radio technical subunit crews has a direct influence on the accuracy with which ground-to-air missile troops and fighter aviation execute their tasks. Therefore, one of the most important requirements for crew training should be the detection of targets at maximum ranges, providing radar information with maximum accuracy, and full utilization of the capabilities of battle technology in determining the composition of aerial targets.

The progress in science and technology in recent years has led to the extensive utilization of complex technical systems. The decisive role of the human operator in such systems, the complexity of analyzing the data and implementing control functions have put forth the problem of improving the quality of training and teaching of operators. This problem is particularly urgent in radar, where operator training using real targets involves major expenses and significant consumption of materials.

Regardless of the rather widespread utilization of simulators and trainers as technical devices for teaching the operators proper habits for controlling targets of various types, their application has not been sufficiently effective until recently. Analysis of trainer development has shown that their creators originally tried to simulate aerial situations using simplified models which provided training only in a limited number of modes. The requirements for the quality and methodological capabilities of trainers were increased, and led to the necessary for increasing the completeness and accuracy of utilization of dynamic and information models, which demanded that computers be included as part of trainers.

The advantages of computer-based simulators and trainers include the capability of simulating any aerial situation, to complicate it or simplify it, to change the parameters of the target trajectories in real time, to repeat the information models of the aerial situation and to study them one part at a time, and to automatically obtain an objective evaluation of the level of training of the operator and to monitor the progress of their training.

These advantages of trainers based on computers promote more efficiency training, improve its quality and reduce the amount of time required. The results of operator training can provide the basis for evaluating their suitability for controlling a specific system and for comparing operators in order to make operator selections.

Table of Contents

FOR OFFICIAL USE ONLY

COPYRIGHT: Voyenizdat, 1980

6900
CSO: 1860/126

101

FOR OFFICIAL USE ONLY

UDC 681.586-181.4

TUNABLE FUNCTION GENERATOR UTILIZING MICROCIRCUITS

Moscow PRIBORY I TEKHNIKA EKSPERIMENTA in Russian No 4, Jul-Aug 81 (manuscript received 2 Jul 79) pp 112-113

[Article by Yu.A. Klyuyev, V.Yu. Pavlenko and N.S. Tanyanskaya]

[Text] A description is given of a function generator whose transfer characteristic is tunable over a range bounded by the dependences U_{vykh} [output] $= \sqrt[3]{U}_{vkh}$ [input] and $U_{vykh} = \sqrt{U}_{vkh}$.

K284PU1 microcircuits connected in an "ideal diode" circuit are used in the function generator. The basic percentage error is approximately one percent of a 1 V output signal in the input signal variation range of 10 to 1000 mV. The complementary error is less than or equal to 0.5 percent at 10 °C in the -10 to +50 °C temperature range.

This function generator is designed to linearize the transfer characteristic of a gas analyzer for SO_2. The method of piecewise linear approximation with direct simulation of an assigned function is used for linearization [1]. With this design method the output voltage of the function generator is determined by the equation

$$U_{\text{вых}} = U_0 + K_0 U_{\text{вх}} + K_s \sum_{i=1}^{n} (U_{\text{пх}} - U_{\text{оп } i}),$$

where U_0 is the value of the output voltage with a minimum input signal, $U_0 = 215$ mV with $U_{vkh} = 10$ mV ; U_{on} is the reference voltage of the ideal diode; K_0 is the transmission factor determining the slope of the initial section of the function generator's characteristic; K_s is the transmission factor of an ideal diode; and n is the number of ideal diodes.

The coefficients and reference voltages of the ideal diodes were calculated for a conversion function of $U_{vykh} = \sqrt[3]{U}_{vkh}$ with an approximation error of one percent of the maximum output signal of $U_{vykh} = 1$ V . These calculations are presented in table 1.

102

Table 1.

Transmission factors

K_0	K_1	K_2	K_3	K_4
4.9	–2.4	–1.1	–0.5	–0.25

Reference voltages, mV

$U_{op\ 1}$	$U_{op\ 2}$	$U_{op\ 3}$	$U_{op\ 4}$
18	62	70	160

The circuit diagram of the function converter is presented in fig 1. The circuit consists of four ideal diodes (M_1 to M_4), an inverting analog summer, M_5, and an inverting amplifier, M_6. The voltages determining the enabling levels for the ideal diodes are gotten from resistive dividers R_3 to R_5 and are supplied at the inputs of the ideal diodes. The transmission factor for each ideal diode is

$$K_i = \alpha R_{oc}/R',$$

where R_{oc} is the feedback resistance of an individual ideal diode (R_6, ...); $R' = 10$ kΩ for this type of microcircuit; α is the part of the total output voltage of the ideal diode supplied at the summer's input and determined by the output resistive dividers of the ideal diode. Retuning of the conversion function is accomplished by means of the output resistive dividers of the ideal diodes.

Inverting analog summer M_5 adds signals: the input voltage, U_{vkh}, and the output voltages of all ideal diodes and the voltage gotten from the resistive divider, R_{34} to R_{36}, which compensates the internal bias voltage of M_5. The transmission factor of the summer for signal U_{vkh} equals

$$K_0 = R_{37}/(R_1 + R_2).$$

The transmission factors of the summer for signals arriving from the ideal diodes are chosen to be constant and equal one. Thereby their mutual influence on one another in the tuning process is eliminated. Inverting amplifier M_6 is designed to reduce the output signal to unified form, $U_{vykh} = 1$ V . The transfer characteristic of the function generator consists of five linear sections each having its own slope (transmission factor).

The function generator is tuned to the conversion function:

$$U_{вых} = \sqrt[3]{U_{вх}}.$$
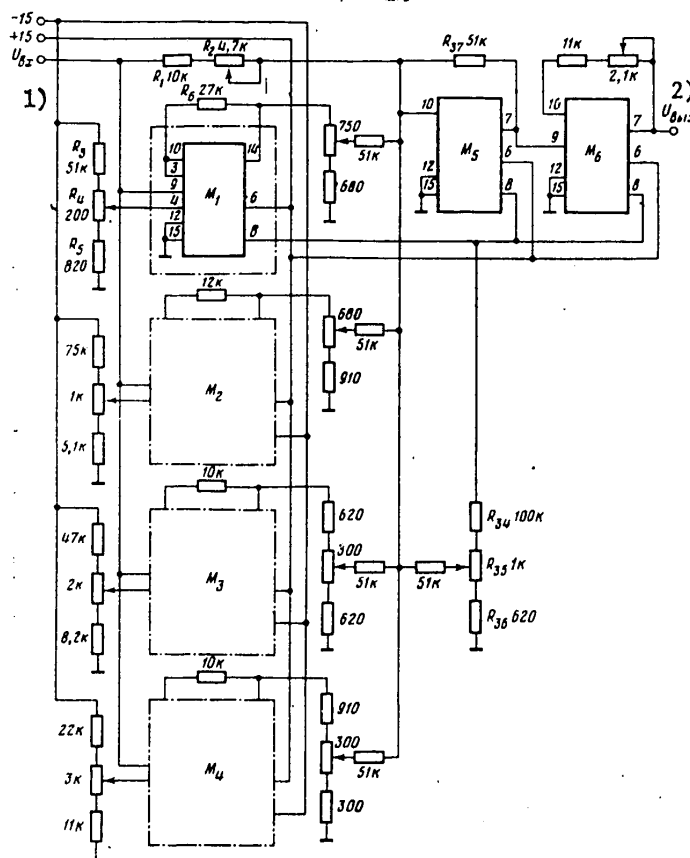
Figure 1. Circuit Diagram of Function Generator: M_1 to M_6--K284PU1

Key:

1. U_{vkh}

2. U_{vykh}

Thereby the individual values of the reference voltages of the ideal diodes are
set. When it is necessary to retune the function generator it is possible to use
only adjustments of the transmission factors of the ideal diodes, K_s , and of the
transmission factor of the summer, K_0 .

104

FOR OFFICIAL USE ONLY

Bibliography

1. Smolov, V.B. "Diodnyye funktsional'nyye preobrazovateli" [Diode Function Generators], Leningrad, Energiya, 1967, p 5.

8831
CSO: 1860/74

FOR OFFICIAL USE ONLY

ELECTRON DEVICES

UDC 621.385.832.84

ANALCG MULTIPLEXER IN THE CAMAC STANDARD

Moscow PRIBORY I TEKHNIKA EKSPERIMENTA in Russian No 4, Jul-Aug 81 (manuscript received 3 Jan 80) pp 258-259

[Article by A.G. Kuchinskiy, V.M. Savchenko and A.K. Yakushev]

[Text] This module is designed for the parallel connection of four out of 120 inputs to four individual outputs in keeping with instructions arising from a crate line. The module can be used in designing multichannel measuring systems and other electronic apparatus making possible the multichannel processing of analog information. The circuit of the common section and of the analog signal commutator for one of the four outputs of the multiplexer is given in fig 1; an external view of the module is shown in fig 2 [photograph not reproduced].

The module contains the following functional units: an analog signal commutator executed with 20 K590KN1 microcircuits (16 microcircuits are commutation switches and 4 microcircuits are level restoration switches (KVU's)) and one K155LA8 microcircuit; a 3-bit binary address register; a 4-bit binary control register; a crate line instruction decoder and an interrogation processing circuit, L. The contents of the address and control registers, as well as the state of interrogation, L , are indicated on the module's face panel.

Analog signals enter via connectors located on the module's face panel into individual inputs (1 to 30) X 4 of the analog commutator. Upon an instruction arriving from the crate line into the instruction decoder, D_{sh}, the simultaneous switching of four analog signals takes place to the individual outputs of the multiplexer (outputs 1 to 4) by means of the address register, RgA, and the control register, RgU. The codes of the switched channels are written in the address register and the codes of the individual groups of channels in the control register. Interrogation L is formed in the interrogation processing circuit, SOZ(L), 1.5 μs after the arrival of an instruction from the crate line and informs the control unit of the completion of the switching of input signals.

The multiplexer has the following specifications: open-channel impedance less than or equal to 200 Ω; leakage current in input less than or equal to 500 nA; switching time--1 μs; switched current--10 mA; switched voltage--± 5 V; duration of overshoots less than or equal to 1 μs; amplitude of switching overshoots--100 to 250 mV.

The protection of inputs from voltage overloads is provided for maintenance convenience.

106

FOR OFFICIAL USE ONLY
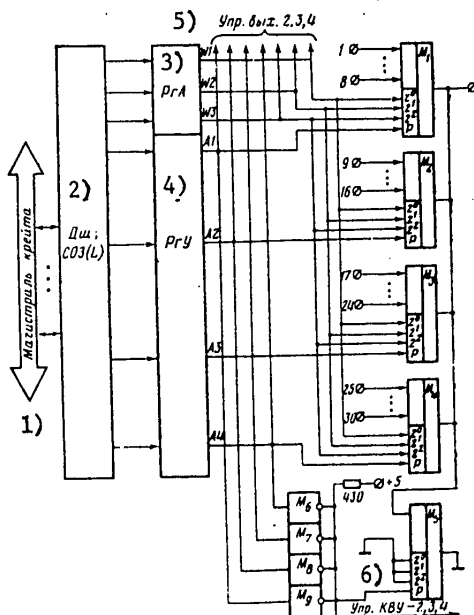
Figure 1. Circuit of Common Section and of Analog Signal Commutator for One
of Four Outputs of the Multiplexer

Key:

1. Crate line
2. Decoder, SOZ(L)
3. Address register

4. Control register
5. Control of outputs 2, 3, 4
6. Control of level restoration
   switches 2, 3, 4

The following instruction operations are used for the purpose of controlling the
multiplexer: NF(26)A(0)S1--enabling signal L ; NF(24)A(0)S1--inhibiting the
signal; NF(8)A(0)--L interrogation check; NF(27)A(0)--analysis of state of in-
terrogation flip-flop; NF(1)A(0)--reading module state word (R1 to R11);
NF(17)[A(1) to A(4)]--writing address of switched channels into switching register
(W1 to W3); NF(11)A(0)S2--clearing address and control registers; NF(25)A(0)S1--
switching channels selected; (Z + C)S2--preparation for operation.

Signal X is generated and used according to standard. The unit is designed as a
CAMAC module of double width. The power requirement is + 6 V, 0.8 A; - 15 V, 0.3 A.

COPYRIGHT: Izdatel'stvo "Nauka", "Pribory i tekhnika eksperimenta", 1981

8831
CSO: 1860/74

107

INSTRUMENTATION & MEASUREMENTS

UDC 535.853; 621.3.029.65

MILLIMETER AND SUBMILLIMETER BAND PULSED SPECTROMETER

[Article by V.M. Naumenko, V.V. Yeremenko and A.V. Klochko, Ukrainian SSR Academy of Sciences Physicotechnical Institute of Low Temperatures, Khar'kov]

[Text] A description is given of a resonatorless spectrometer of the transmission type with a direct amplification receiver for making studies in the 0.3 to 6 mm wavelength region in a pulsed magnetic field of up to 300 kOe with the temperature of the specimen determined by the liquid coolant (He, H_2, N_2). A quasi-optical system for irradiating the specimen is used in the spectrometer. A description is given of a method of fastening the specimen with fine adjustment of its position in the solenoid channel with an accuracy of 0.5'. Automatic recording of the zero and 100-percent resonance absorption levels and of the zero level of the magnetic field is employed in the instrument, which makes it possible to determine the parameters of resonance lines with high precision.

Modern physical studies of the magnetic properties of materials are carried out over a wide range of frequencies and magnetic fields. Oscillators of the backward wave tube type [1] and high-sensitivity receivers [2] are often used in wideband spectrometers.

In [3] a description is given of a spectrometer operating in the 0.2 to 2 mm wavelength band, in which the retunable Fabry-Perot resonator with the specimen lies in the channel of a superconducting solenoid with a maximum magnetic field strength of 40 kOe. However, when operating at longer wavelengths it is necessary to increase the inside diameter of the solenoid, which considerably complicates the production of high-strength magnetic fields. Besides, magnetic fields with strength of up to 300 kOe are usually produced by the pulse method and furthermore it is not permissible to place the massive metal parts of the resonator inside the solenoid channel.

In this article a description is given of a pulsed resonatorless spectrometer of the transmission type for a wide range of wavelengths and magnetic fields and for low temperature of the specimen. In the spectrometer there is a circuit for producing a signal proportional to the differential magnetic susceptibility of the specimen studied, as well as a unit for precisely adjusting its position in the solenoid channel during an experiment. The spectrum is turned by means of the magnetic field with a fixed frequency of the microwave oscillator.

108

A block diagram of the spectrometer is presented in fig 1 and the measuring cell with the cryostat (downward cross-sectional view) in fig 2. The microwave radiation source, 1 (fig 1), is connected to a transmission line which consists of a horn antenna, a system of matching lenses, 2, and a 20-mm-diameter hollow dielectric light guide with a number of additional devices, such as polarization plane rotators (VPP's), 3 and 4, a beam splitter (DL), 5, and an absorption wave meter, 6. The transmission line based on a hollow dielectric light guide and the quasi-optical devices were fabricated at the Ukrainian SSR Academy of Sciences Institute of Radio Physics and Electronics and operate in the 0.3 to 2 mm band. An optoacoustic receiver, 7, is connected to one of the arms of the beam splitter for the purpose of registering the signal reflected from the absorption wave meter. Standard wave meters of the transmission type, e.g., V1184-A and Ch2-26, are connected between the microwave source and horn antenna when operating in the 2 to 6 mm band.
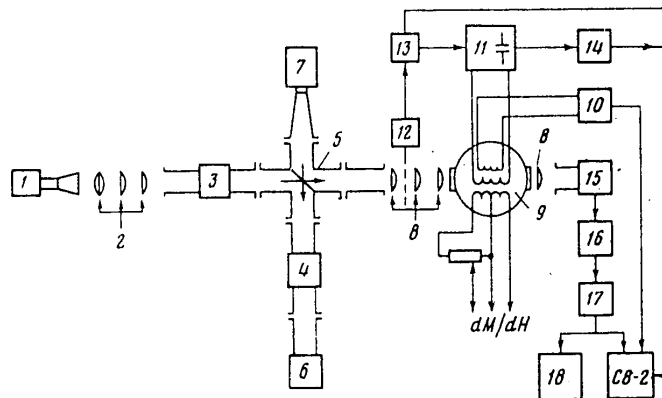
Figure 1. Block Diagram of Spectrometer: 1--microwave oscillator with horn; 2, 8--confocal lens light guides; 3, 4--polarization plane rotator; 5--beam splitter; 6--absorption wave meter; 7--optoacoustic receiver; 9--cryostat with solenoid and specimen; 10--integrator; 11--solenoid power supply; 12--mechanical modulator; 13--automatic calibration unit; 14--delay unit; 15--n-InSb detector; 16, 17--preamplifier and final amplifier; 18--monitoring oscillograph

Then the radiation is channeled by means of a confocal lens light guide, 8, with a distance between lenses of 120 mm. Microwave power losses in the lens light guide with $\lambda \geq 2$ mm are caused basically by diffraction [4]. These losses are minimal for a TEM_{00} wave and the TEM_{00} wave is practically established in the tranmission line after five to seven lenses. In a hollow dielectric light guide in the 0.3 to 2 mm band a wave of the EH_{11} type is propagated, which is rather close in structure to a TEM_{00} wave, which makes it possible easily to match the dielectric light guide with a confocal lens light guide. Losses of microwave power in a 20-mm-diameter hollow dielectric light guide in the 0.5 to 2 mm wavelength range are within the range of 1 to 7 dB/m.
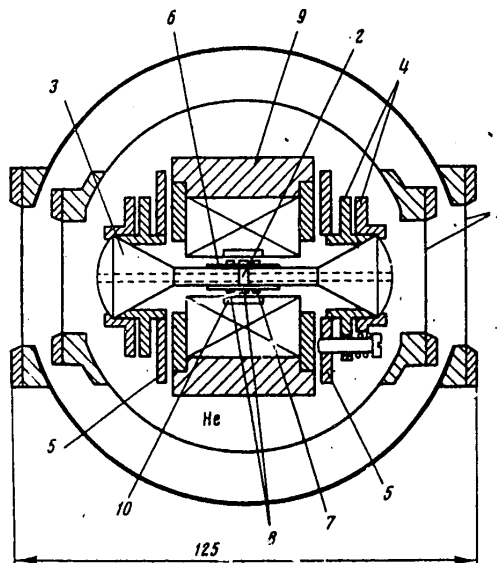
Figure 2. Cross Section of Specimen Cryostat: 1--windows made of Therylene
(Lavsan) film; 2--specimen; 3--Teflon cones; 4--holders; 5--
moving frame; 6--Therylene bushing; 7, 8--coils for measuring
dH/dt and dM/dH , respectively; 9--steel band of solenoid; 10--
fabric-base laminate insert

Between the last two lenses of the light guide, 8 (fig 1), is installed a cryostat,
9, with film windows, 1 (fig 2), inside of which a measuring cell with the specimen
to be studied is placed. Special attention has been paid to the method of irradia-
ting the specimen. After testing several variants a quasi-optical system consisting
of two conical lenses, 3 (fig 2), converting into waveguides proved to be optimum.
The lenses are made of fluoroplastic and have a 16-mm aperture. The use of these
lenses makes it possible to irradiate a specimen with an area of 3.5 X 3.5 mm^2 and
less with a minimum radius of the Gaussian beam in the lens light guide, R =
= $\sqrt{\lambda d/2\pi}$, equal to 2.4 to 10 mm for a distance between lenses of d = 120 mm (in
the 0.3 to 6 mm wavelength band). The transmission of the cryostat with the sole-
noid and two conical lenses (in the circuit in fig 1) in this wavelength band is
30 to 70 percent (with a cross section of the waveguide part of the cones of 3.5 X
X 3.5 mm^2), whereas without conical lenses it equals a total of only 3 percent
(with a solenoid aperture diameter of 6 mm). In order to eliminate stray passing
of the wave past the specimen, the side surface of the cones is coated with con-
ducting paint. There are 2.5-mm-diameter axial openings in the conical lenses for
the purpose of improving transmission in the 0.3 to 0.5 mm region.

The specimen to be studied, 2 (fig 2), 0.1 to 3 mm thick, is placed at the center
of the solenoid between the conical lenses, which are fastened to holders, 4.
The holders are installed on a frame, 5, which can be turned around two mutually
perpendicular axes (perpendicular also to the axis of the solenoid) at angles of

110

$\pm$ 3° with an accuracy of 0.5'. The turning knobs are on top of the cryostat. One of the holders with a conical lens is installed fixed to the frame and the other can be moved in the axial direction and is spring mounted, which makes it possible to choose the optimum pressure on the specimen with which it does not crack in strong magnetic fields, resonance lines are not distorted and the shortening of the conical lenses when they are cooled to 4.2 °K is compensated. Bushing 6 (made of Lavsan), onto which the measuring coils are wound, prevents the waveguide sections of the conical lenses from shifting to the sides.

A signal proportional to the rate of change of the strength of the magnetic field, dH/dt, is picked up from coil 7 (fig 2) and is supplied to the input of integrator 10 (fig 1) and then to the oscillograph. From the other two coils, 8 (fig 2), a signal is supplied to the two inputs of the differential amplifier of an S8-2 double-beam storage-type oscillograph on whose screen is recorded the amplified difference signal proportional to the differential magnetic susceptibility, dM/dH.

The solenoid with the quasi-optics and turning unit together (65 X 65 mm^2, height of 105 mm) is fastened to a rod and is inserted into the cryostat from above, which makes it possible easily to change specimens without disturbing the vacuum in the cryostat. The pulsed solenoid coils are wound onto a tube made of German silver 25 mm long with an opening 6 mm in diameter. For the purpose of increasing their mechanical strength the windings are impregnated with an epoxy compound and are put into a band of stainless steel, 9. Two solenoids were used in the study: The first contains 80 turns of a copper line with a cross section of 1.08 X 2.44 mm^2 and the other 350 turns of PELShO-0,72 wire. The field pulse rise time for the first solenoid during the dischargirg of a 7-mF capacitor bank equals 0.9 ms, and for the second 2.5 ms (with a 3.5-mF capacitor bank). A cylindrical fabric-base laminate insert, 10 (fig 2), was used in the last solenoid for the purpose of improving homogeneity of the magnetic field. An ignitron is used as the discharger. In the solenoid's power supply there is a capacitor bank charge level stabilizer which charges the bank after a few seconds to the assigned voltage and maintains it with an accuracy of one percent. The solenoid's magnetic field is calibrated to the EPR [electron paramagnetic resonance] line of α-diphenyl-β-picryl hydrazyl (DFPG) contained in a preform of molded polyethylene placed alongside the specimen. A signal proportional to dM/dH is also used for calibration if the fields of magnetic phase transitions in the specimens being studied are known.

In recent times much attention has been paid to the precise measurement of the intensity and width of resonance lines in radio spectroscopy. We used a method making it possible to increase the accuracy of these measurements and to a certain extent to automate them. The microwave radiation is modulated by means of a mechanical interrupter, 12 (fig 1), with a frequency somewhat lower than $(1/2)\tau$, where τ is the duration of the magnetic field. During startup, the automatic calibration unit, 13, (operating in the one-time startup mode) in phase with modulation of the radiation generates successively three control pulses. The first two pulses correspond to the moments of opening and shutoff of the microwave beam by the interrupter's segment and produce a successive two-time startup of the storage-type oscillograph's sweep action. The zero and 100-percent absorption levels and the zero level of the field (or dM/dH), respectively, are entered on its screen. At the moment of the next opening of the microwave beam by the interrupter's segment the automatic calibration unit forms a third pulse which enters the power supply of the solenoid, 11, and the capacitor bank is discharged onto the solenoid. At the

111

same time this pulse is fed to the delay unit, 14, and after this to the storage-type oscillograph for starting its sweep action a third time. The absorption spectrum and the field magnitude (or dM/dH) signal are recorded on the scale selected.

The presence of zero and 100-percent levels on the oscillograph's screen along with recordings of the spectrum make it possible to improve substantially the accuracy of determining the parameters of resonance lines. Since the duration of the entire cycle is less than 10 ms, during this period the amplitude of the micro-wave oscillator, the position of the oscillograph's zero lines and the gain of the receiving and recording system practically do not change during this time. This technique is especially helpful when working with a backward wave tube, which as a rule has a strongly divided amplitude characteristic. The use of calibration marks, taking into account the nonlinearity of the S8-2 oscillograph's measuring channels, the presence of a beam biasing circuit (as in [5]) as well as the auto-matic recording of the zero level of the magnetic field make it possible to bring the accuracy of measuring the magnetic field up to one percent.

An n-InSb chip placed in a separate cryostat and cooled to 4.2 °K is used as the microwave radiation receiver, 15.* The receiver's signal enters preamplifier 16 and then final amplifier 17, each of which has a gain of 100. The transmission band of the receiving and amplifying channel equals 5 MHz at a level of 0.7. In-duction into the receiving and amplifying channel during operation of the pulsed solenoid is at the noise level because of galvanic decoupling between the cryostat of the receiver and specimen. Taking into account the fact that the transmission band of the receiving and amplifying section equals 5 MHz and the short-term in-stability of the backward wave tube's frequency is approximately 10^{-4}, the reso-lution of the spectrometer is determined by the homogeneity of the magnetic field in the bulk of the specimen and equals approximately 500 for a specimen 1 mm thick with an area of 3.5 X 3.5 mm^2, which is completely adequate for the majority of resonance investigations of solids. The homogeneity of the magnetic field in the solenoid was determined from the width of the EPR line of DF1'G contained in pre-forms of molded polyethylene of different thicknesses.

As an illustration of the operation of the spectrometer, in fig 3 [photograph not reproduced] a photograph is presented, of the oscillograph's screen in studying the interaction of antiferromagnetic resonance with impurity resonance in CoF_2 + + Mn^{2+} .

In conclusion we wish to thank V.V. Pishko and V.V. Tsapenko for assistance in tests and in making individual units.

Bibliography

1. Golant, M.B., Vilenskaya, R.L., Zyumina, Ye.A. et al. PTE, No 4, 1965, p 136;

*Let us use this opportunity to express our heartfelt thanks to F.F. Kharakhorin for offering high-quality low-noise chips.

Golant, M.B., Alekseyenko, Z.T., Korotkova, Z.S. et al. PTE, No 3, 1969,
p 231.

2. Aganbekyan, K.A., Vystavkin, A.N., Listvin, V.N. and Shtykov, V.D. RADIO-
TEKHNIKA I ELEKTRONIKA, Vol 11, 1966, p 1252.

3. Petutin, A.I., Zvyagin, A.I., Dyubko, S.F. et al. PTE, No 4, 1970, p 163.

4. Valitov, R.A., Dyubko, S.F., Katyshan, V.V. et al. "Tekhnika submillimetrovykh
voln" [Submillimeter Wave Equipment], Moscow, Sovetskoye Radio, 1969.

5. Gurevich, A.G., Golovenchits, Ye.I., Voronkov, V.D. and Gromzin, D.Ye.
PTE, No 4, 1967, p 121.

COPYRIGHT: Izdatel'stvo "Nauka", "Pribory i tekhnika eksperimenta", 1981

8831
CSO: 1860/74

UDC 621.317.761

HIGH-SPEED TRACKING FREQUENCY METER

[Article by G.G. Vorob'yev]

[Text] A description is given of a tracking frequency meter constructed from a reversible counter, a reference frequency generator, a direct-counting counter and a multiplication logic circuit installed in a feedback loop between counters. The number entered into the reversible counter directly expresses the value of the measured frequency, f_{izm} . With a generator frequency of 1 MHz the upper value of f_{izm} = 100 kHz and the lower value is not limited, whereby the measuring accuracy is identical over the entire range and is determined by the stability of the generator. An "acceleration" circuit assembled from logic elements is used for the purpose of reducing the time of the transient process.

Digital frequency meters of two types [1] have gained extensive application in frequency measuring practice. The first type is based on measuring the period of the input frequency while employing the operation of finding the inverse value of the period measured. These frequency meters are used for measuring relatively low frequencies. To the other type belong frequency meters whose operation is based on counting the number of periods of the measured frequency over a reference time interval. These frequency meters make it possible to obtain a direct digital reading of the measuring result and they are convenient to use for measuring high frequencies.

One more type of frequency meter is known--a tracking frequency meter [2] having a reference frequency block, frequency analyzers, frequency mixers, shift registers and a set of electronic switches. However, in view of the high complexity of these frequency meters they have not found a practical application.

The frequency meter described below [3], whose block diagram is shown in fig 1, is without this disadvantage and the use in it of an added "acceleration" circuit has made it possible to increase considerably its speed of response. The frequency meter consists of a reference generator (EG), decade frequency dividers (by a factor of 10), a measurement range selector switch (P), a direct-counting counter (PS), a multiplication circuit (X), a reversible counter (RS), an anticoincidence circuit (SAS), digital indicators (TsI's) and an acceleration element. The latter has a

114

shaper (F), one-shot multivibrators OV_1 and OV_2, flip-flops Tg1 and Tg2, AND gates I_1 and I_2 and an OR gate.
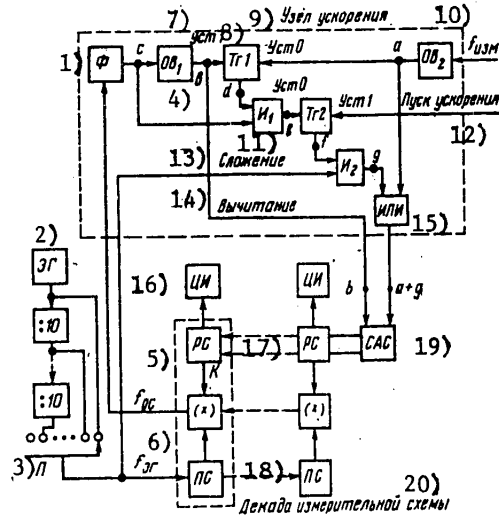
Figure 1. Block Diagram of Tracking Frequency Meter

Key:

1. Shaper	11. AND gate
2. Reference generator	12. Start acceleration
3. Measurement range selector switch	13. Addition
4. One-shot multivibrator No 1	14. Subtraction
5. Feedback frequency	15. OR gate
6. Reference generator frequency	16. Digital indicator
7. "1" setting	17. Reversible counter
8. Flip-flop No 1	18. Direct-counting counter
9. Acceleration unit	19. Anticoincidence circuit
10. Measuring frequency	20. Measuring circuit decade

The operation of the frequency meter in the tracking mode is described by the equations

$$f_{oc} = K f_{эт}, \quad K = \int (f_{изм} - f_{oc}) dt,$$

where f_{os} is the feedback frequency and K is the number obtained in the reversible counter. With the advent of the equality of frequencies in the input of the reversible counter, $f_{os} = f_{izm}$, we get $f_{izm} = K f_{EG}$. If it is assumed that $f_{EG} = 10^n$, where n is a natural number, then it is not difficult to see that K directly reflects the value of the measured frequency.

An added acceleration circuit was used for the purpose of reducing the time of the transient process originating at the beginning of measuring. Its operating principle consists in the fact that with the start of measurement an acceleration frequency (in this case f_{EG}) is supplied to the addition input of the reversible

115

counter simultaneously with f_{izm} . When the necessary readings are reached (K), when f_{izm} becomes equal to f_{os} , the acceleration frequency is cut off and then the frequency meter operates in the ordinary tracking mode. Diagrams of the voltages of the acceleration unit at points a to g are presented in fig 2. The acceleration frequency cutoff moment is determined from the appearance of the first "superfluous" pulse of frequency f_{os} (the right half of the diagrams in fig 2) by means of a trigger circuit executed with elements OV_1, OV_2, Tg1, Tg2, I_1 and I_2. In this case the time for the initial setting of readings is reduced.
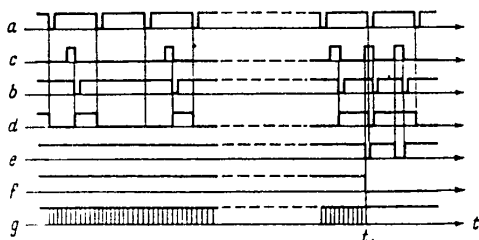
Figure 2. Diagrams of Acceleration Unit Voltages

The circuit diagram of the frequency meter is presented in fig 3. The digital display unit is not shown; for the purpose of implementing it it is necessary to connect to the outputs of microcircuits M_4 via decoders (a K155ID1 microcircuit) IN-12B digital gas-discharge indicators.

Let us discuss the operation of the frequency meter's measuring decade. Changes in voltages in specific outputs of microcircuits M_6 to M_9 of counter PS (diagrams Q_1 to $\overline{Q}_4$ in fig 4) are differentiated by means of the RC networks of microcircuit M_5. From the negative pulses obtained after differentiation a frequency spectrum is created ($dQ_2^{(-)}$ to $d\overline{Q}_4^{(-)}$) with a dynamic code of 4-4-2-1. In the zeroed state of the decade of the reversible counter (microcircuit M_4), in the output of the inverters installed in the bit output of microcircuit M_4 a "1" potential is present (+4.5 V), which cuts off the diodes of microcircuit M_5. Pulses do not enter the common line of the diodes (the input of shaper F). When a "1" is entered in microcircuit M_4 the diode of microcircuit M_5 is rendered conducting, admitting $d\overline{Q}_4^{(-)}$ pulses to the output (cf. diagram 1 in fig 4). Operation of the reversible counter takes place in 1-2-4-8 code, which is convenient for controlling the digital display. For eliminating failures in the operation of the reversible counter an anticoincidence circuit is used which eliminates the entry of pulses coinciding in time into its input. The operation of this circuit is explained by diagrams of the voltages (fig 5) in various points of it. With a sufficient distance of addition and subtraction pulses from one another (time t_1 and t_2 in fig 5) they pass to the input of the reversible counter. And if the addition and subtraction pulses lie in "dangerous" proximity to one another then coincidence of the pulses of the input stretchers (the right half of diagrams a' and b' in fig 5) will take place. The inhibit pulse multivibrator operates (diagram h in fig 5). The input of the reversible counter will be closed.

116
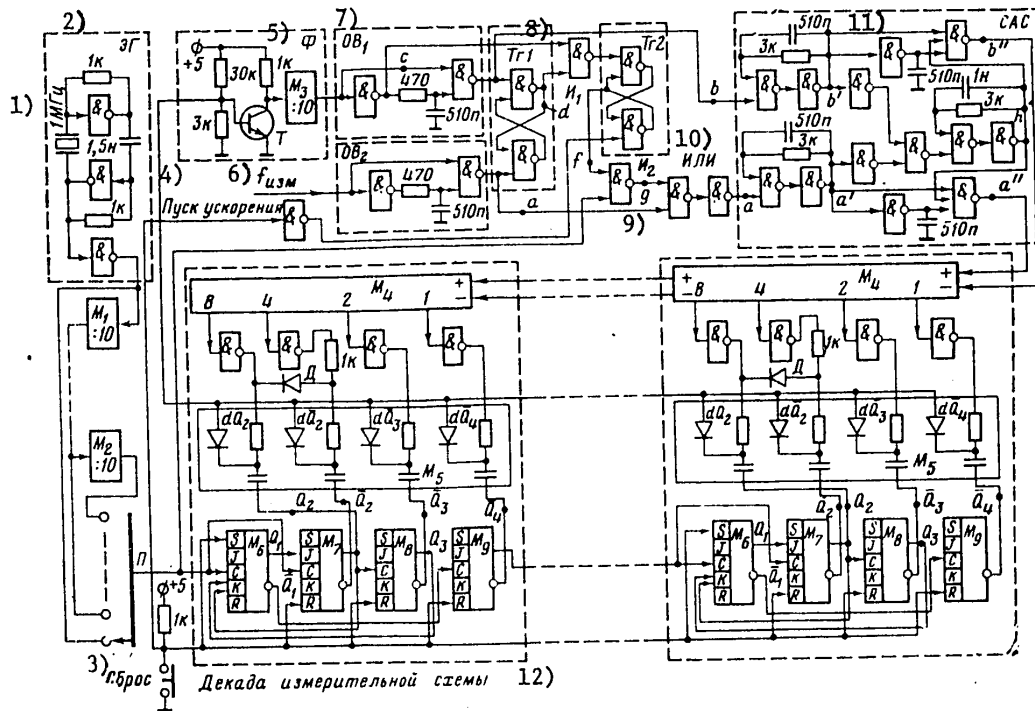
Figure 3. Circuit Diagram of Tracking Frequency Meter: M_1 to M_3--K155IYe1, M_4--K155IYe6, M_5--K2NK041, M_6 to M_9--K155TK1; all inverters-- K155LB3; T--KT315A; D--GD507A

Key:

1. 1 MHz
2. Reference generator
3. Reset
4. Start acceleration
5. Shaper
6. f_{izm} [measuring]

7. One-shot multivibrator No 1
8. Flip-flop No 1
9. AND gate
10. OR gate
11. 510 pF
12. Measuring circuit decade
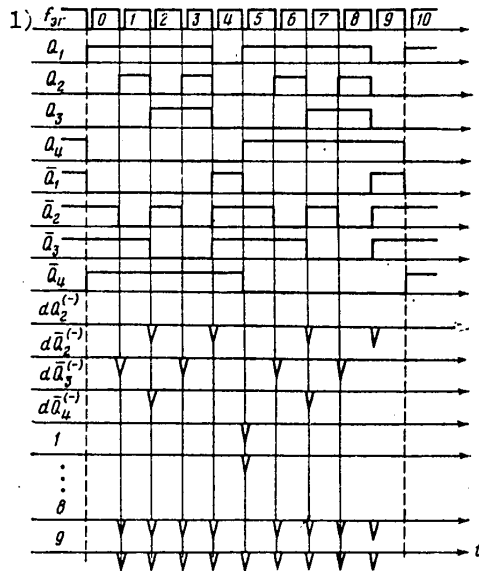
Figure 4. Diagrams of Measuring Decade Voltages

Key:

1. f_{EG} [reference generator]
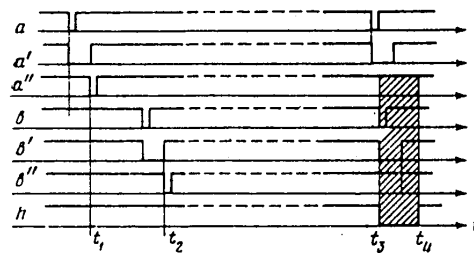
Figure 5. Diagrams of Anticoincidence Circuit Voltages

If an oscillator with quartz stabilization at 1 MHz is used as a reference frequency generator (fig 3), then the upper value of the measured frequency equals 100 kHz. This value is determined by the maximum value of the feedback frequency. In this case it equals $f_{os} = f_{EG}/10$, where 10 is the division factor of the smoothing divider (microcircuit M_3) installed in the feedback loop. The smoothing divider reduces nonuniformity of the feedback frequency and at the same time eliminates

118

the drift in readings of the digital indicator's lower-order bit. The lower value of the measured frequency is theoretically not limited but it must be remembered that then the time of the transient process increases.

The number of measuring circuit decades and the number of scale dividers in the output of the reference generator is determined by the required measurement accuracy, which is identical both for high and for low frequencies and is determined by the stability of the reference generator. A multichannel tracking frequency meter can be designed on the basis of this frequency meter [4].

Bibliography

1. Yermolov, R.S. "Tsifrovyye chastotomery" [Digital Frequency Meters], Leningrad, Energiya, 1973.

2. Shlyandin, V.M. and Lomtev, Ye.A. USSR Patent No 250308, published in B.I. [BYULLETEN' IZOBRETENIY], No 26, 1969, p 64.

3. Vorob'yev, G.G. USSR Patent No 565259, published in B.I., No 26, 1977, p 94.

4. Vorob'yev, G.G. USSR Patent No 393693, published in B.I., No 33, 1973, p 182.

8831
CSO: 1860/74

UDC 621.384

AUGER ELECTRON SPECTROMETER

Moscow PRIBORY I TEKHNIKA EKSPERIMENTA in Russian No 4, Jul-Aug 81 (manuscript received 30 Apr 80) p 257

[Article by A.V. Kozhevnikov, A.M.-S. Li and V.A. Pirogov]

[Text] This instrument makes it possible to make an elemental analysis of the surface of solids in studying processes of adsorption, desorption and diffusion on a surface under conditions of an ultrahigh vacuum. Atomization of the surface by means of an ion beam makes it possible to study the distribution of elements over the specimen's depth.

A beam of primary electrons from an electron gun induces the exiting of secondary electrons from the studied section of the surface of the specimen. The energy distribution of secondary electrons is registered by means of an analyzer of the cylindrical mirror type. The spectrum of secondary electrons is recorded on an N306 XY-recorder. It is possible to observe spectra on an oscillograph, which makes possible on-line monitoring of the state of the specimen's surface. The mode of electronic differentiation of the spectrum of secondary electrons is provided for increasing the sensitivity of the instrument.

The surfaces of specimens are cleaned by bombarding them with an Ar^+ ion beam and by heating them under a superhigh vacuum. The holder with the specimens is in a cryostat cooled by liquid nitrogen. The specimens are heated to a temperature of 1800 °C by means of an electronic heater. The holder with the specimens is replaced through a lock chamber, which makes it possible to maintain steadily a high vacuum in the spectrometer's working chamber. The specimen holder is equipped with a precision manipulator. Visual monitoring of the replacement and placement of specimens in the analyzer is possible. The evacuation system is oilless.

Key Specifications of Instrument

Energy range of Auger peaks which can be registered--0 to 2500 eV; energy resolution of analyzer less than or equal to 1 percent; energy of primary electrons-- 0 to 4 keV; diameter of beam of primary electrons less than or equal to 200 microns; working vacuum not worse than 10^{-7} Pa; time for replacement of holder with specimens--less than or equal to 50 min; dimensions--1350 X 650 X 500 mm ; weight--180 kg.

COPYRIGHT: Izdatel'stvo "Nauka", "Pribory i tekhnika eksperimenta", 1981

8831
CSO: 1860/74

120

MICROWAVE THEORY & TECHNIQUES

UDC 621:386.6(076,5)

MICROWAVE ELECTRONIC DEVICES

Saratov ELEKTRONNYYE PRIBORY SVERKHVYSOKIKH CHASTOT in Russian 1980
(signed to press 5 May 80) pp 2-5, 411-416

[Annotation, foreword and table of contents from textbook "Microwave
Electronic Devices", second edition, revised and supplemented, edited by
by V. N. Shevchik (deceased) and M. A. Grigor'yev, Izdatel'stvo Saratovskogo univer-
siteta, 4500 copies, 416 pages]

[Text] This book deals with studies in electronics and characteristics of modern
devices intended for the amplification and generation of electromagnetic microwave
oscillations (reflex klystron; traveling-wave tube; backward-wave tube; multireson-
ator magnetron; voltage-tunable magnetron; avalanche-and-transit-time diode oscil-
lator; Gunn diode oscillator) and combines a textbook in a theoretical course with
a laboratory manual. The book is divided into parts treating various types of in-
teraction of electrons with electromagnetic fields in a vacuum or in a solid body.
Each part contains theoretical chapters and the related experimental problems for
practical laboratory work on microwave electronics. Primary emphasis is placed on
systematic presentation of the fundamental theoretical information on the electronics
of the devices being studied. Typical circuits of laboratory devices and the neces-
sary methods of microwave measurements are also described. For each concrete pro-
blem, recommendations are given for the order of studies and instructions for practi-
cal studying standard microwave devices, and test question are formulated. This
textbook was written on the basis of many years of experience in teaching microwave
electronics at the Saratov University.

Foreword

This book is based on a laboratory manual on microwave electronics published in 1964*.
That first edition was an attempt to give the students a sufficiently complete guide
for practical laboratory work which, on the one hand, would free them from the neces-
sity of working through a large amount of special and often scattered literature,
and, on the other, would be a basis for a more profound study of physical phenomena
in microwave electronic devices with the use of highly specialized literature. It
was also intended for coordinating the preparation of students for practical work
with the methodology and program of the course of lectures on the fundamentals of

---

*"Elektronnyye pribory sverkhvysokikh chastot" [Microwave Electronic Devices],
edited by V. N. Shevchik, Izdatel'stvo Saratovskogo universiteta, 1964.

microwave electronics offered at SGU [Saratov State University]. The first part of these considerations remained the same in the preparation of this, second, edition.

During the fifteen years since the first edition, the theory and practice of electro-vacuum microwave devices have developed further and, which is most important, solid-state devices are rapidly penetrating microwave electronics. In the final analysis, all this determined the considerations by which the authors were guided in preparing the second revised and supplemented edition of this book. The absence of such teaching aids made it expedient to prepare a textbook which would be useful not only for the students of the Saratov State University, but also for other vuzes of the country which have radio physics and radio engineering departments and fields of specialization.

When revising this book, the authors removed the sections treating oscillators with decelerating fields and electron wave oscillators, since these devices did not find extensive applications in practice. Sections on the reflex klystron, multiresonator magnetron and noise in LBV [traveling-wave tubes] were rewritten and expanded. The remaining parts of the book were also changed substantially and supplemented. For example, in presenting the theory of LBV, considerably more attention was given to the mechanism of the interaction of electrons with traveling waves, electrodynamics of decelerating system and the treatment of the concept of coupling resistance. In the section on the theory of LOV [backward-wave tubes], more attention was given to the operation of the tube, decelerating systems and space harmonics, as well as the results of the nonlinear theory. The following are among the microwave electronic devices which are included in the new book but were not treated in the first edition: the voltage-tunable magnetron as well as the most important solid-state devices -- avalanche-and-transit-time diode oscillator and Gunn diode.

The entire material of the book was systematized by the criteria of the types of interaction of electrons with high-frequency fields (O or M) and types of oscillating systems (resonators or decelerating systems). A separate part of the book treats solid-state microwave devices. Theoretical introductions to various experimental problems (projects) pertaining to the same or related devices were combined into independent chapters. This made it necessary to combine problems which are similar with respect to the basic characteristics of interaction into appropriate experimental chapters which serve as a practical supplement to theoretical chapters. Although this does not change substantially the form of the book, the unified numbering of the problems was retained, which is convenient under laboratory conditions. The contents of the experimental sections (problems) is given in the new book in a a generalized form, which makes it possible to use it in university laboratories having different microwave devices and measuring instruments. For this purpose, only basic block diagrams of experimental devices are given without reference to concrete types of devices, and the recommended measuring methods are described in general terms. The assignments for each problem are formulated as recommendations for conducting studies whose concrete list may vary at the discretion of the instructor. The numerical values of the usually specified parameters and ranges of changes of the physical values used are to be determined by the student on the basis of the manufacturer's certificate and the geometric data of the device being studied, as well as from preliminary theoretical calculations. For each experimental problem, instructions are given on the use of standard microwave electronic devices as the objects of study.

Although the initial purpose of the book as a laboratory manual on microwave electronics was preserved, but, with respect to the volume of theoretical information, which occupies its major part, it is far beyond the scope of the ordinary teaching aids for laboratory studies. In essence, the book became a textbook for a theoretical course in the fundamentals of microwave electronics accompanied by an aid to practical work coordinated with it. On the basis of many years of experience of the operation of the teaching laboratory for microwave electronics at the Saratov University, we believe that this is a necessary quality of the book which expands the possibilities for the instructor who, depending on concrete conditions, can establish one or another theoretical minimum sufficient for admitting the student to performing practical exercises. Of course, this book can also be used as a teaching aid for a theoretical course, because it presents in detail the material corresponding to modern programs in the fundamentals of microwave electronics.

The authors of this book are: V. S. Andrushkevich (Chapters I, II), N. P. Budnikova (Chapter II), Ye. P. Bocharov (Chapter VIII), M. A. Grigor'yev (Chapters II, IV-XIII), Yu. D. Zharkov (Chapters I, II), N. I. Sinitsyn (Chapters IV, V, VII), G. L. Sobolev (Chapters VI, VII), D. I. Trubetskov (Chapters VIII, X), V. L. Fisher (Chapter VI), and B. G. Tsikin (Chapters III, V).

V. V. Kolosov participated in writing section XIII.2 (Problem No 10). Overall processing of the material was done by A. V. Tolstikov. In the process of the preparation of this book for publication, its contents were discussed in detail at the methods seminar of the electronics department of SGU.

The following participated in preparing the manuscript for the press: L. I. Ivanova, V. G. Kravtsova, V. A. Nazarov, V. V. Kolosov, N. V. Belousov, and S. P. Gudkov.

The authors are sincerely grateful to all members of the microwave radio physics department of MGU [Moscow State University] and its chairman, Professor V. M. Lopukhin, for their thorough review of the preliminary wording of the book and useful comments and suggestions, as well as to Professor A. M. Kats of SPI [Saratov Polytechnical Institute] for reading the manuscript and a number of valuable comments in reviewing it.

<div align="center">V. N. Shevchik (deceased), M. A. Grigor'yev</div>

<div align="center">Contents   Page</div>

POWER ENGINEERING

UDC 621.311:519.24

STATISTICAL PROCESSING OF OPERATIONAL INFORMATION IN ELECTRIC POWER SYSTEMS

Irkutsk STATISTICHESKAYA OBRABOTKA OPERATIVNOY INFORMATSII V ELEKTROENERGETICHESKIKH SISTEMAKH in Russian 1979 (signed to press 12 Dec 78) pp 2-4, 254-260

[Annotation, table of contents and 25 abstracts from book "Statistical Processing of Operational Information in Electric Power Systems", edited by A.Z. Gamm, candidate of technical sciences, Sibirskiy energeticheskiy institut SO AN SSSR (SEI), 500 copies, 260 pages]

[Text]   Annotation

Theoretical problems of rough error detection, filtering, and prediction in statistical data processing in automated electric power system dispatcher control systems are considered. Adaptive models of random processes are proposed for solving filtering and prediction problems. Data are presented on corresponding groups of programs and individual programs, and the practical testing and implementation of developments of power systems are discussed.

This collection has been published using materials from a conference conducted at the Siberian Power Institute of the Siberian Department of the USSR Academy of Sciences for workers at a number of scientific-research institutes, institutions of higher learning, and planning and operating organizations involved with problems of improving the quality and reliability of source information for dispatcher control.

Table of Contents

130

ABSTRACTS

UDC 621.311:681.142

WORK ON DEVELOPING A THEORY AND METHODS FOR CONTROLLING THE FUNCTIONING OF
LARGE POWER SYSTEMS

[Abstract of article by Krumm, L.A.]

[Text] The basic methodological conception of integrated optimization and control
of large power systems is examined using the example of electric power systems;
research of the Siberian Power Institute which is being conducted in cooperation
with various organizations is also considered.

UDC 621.31:519.24

CALCULATED TRAJECTORY METHOD FOR DETERMINING QUALITY OF MEASUREMENTS AND ACCURACY
OF ESTIMATES OF STEADY-STATE POWER SYSTEM MODE

[Abstract of article by Bogdanov, V.A.]

[Text] An approach is proposed based on combined utilization of direct and

132

FOR OFFICIAL USE ONLY

interactive calculation methods which allows the mode of a power system to be determined for an arbitrary composition and arrangement of measurements at nodes and branches. When the number, composition and arrangement of measurements cannot be used to determine the mode of the system as a whole, it is still possible to calculate all of those fragments where the necessary measurements are available. In doing this, the problem of estimating the sufficiency of measurements is solved, with each redundant measurement isolated and topologically connected.

UDC 621.311

ALLOWANCE FOR NONLINEAR ELECTRIC POWER SYSTEM PROPERTIES IN ANALYZING OBSERVABILITY

[Abstract of article by Gamm, A.Z.]

[Text] It is shown that nonlinear properties of objects lead to modification of observability conditions. The concept of observability regions is introduced, and it is proved that the introduction of measurement redundancy ensures nonlinear observability. Nonlinear properties of an electric power system are analyzed, and it is proved that there exists a system of nonredundant measurements which ensures full nonlinear observability. It is also asserted that with this system of measurements there is a unique solution to the state estimation problem. Consideration of nonlinear properties when incomplete information is available, especially when telemetry is insufficient, is examined.

UDC 621.311:519.311

STATISTICAL METHOD OF FACTOR ANALYSIS IN PROBLEMS OF ESTIMATING STATUS, OPTIMIZATION AND PLANNING OF ELECTRIC POWER SYSTEM MODES

[Abstract of article by Gurskiy, S.K., Shirma, R.G., Shchur, Ye.V.]

[Text] A modified dynamic approach to state estimation is proposed which is based on avoiding a multidimensional random process describing the mode of electric power systems with correlated components and uncorrelated variables, which makes it possible to reduce the problem to several independent problems of analyzing unidimensional random processes. The mathematical apparatus is based on using factor analysis methods, exponential smoothing and the technique of analyzing cycles in time series.

UDC 658.57.519

OPERATIONAL MATHEMATICAL-STATISTICAL TESTING OF RANDOM PROCESSES

[Abstract of article by Borozdin, O.P., Danilenko, Ye.L.]

[Text] A class of so-called robust (noise tolerant) methods for statistical testing of random processes is described. These methods are less sensitive to changes in conditions than are a priori, which makes it possible to obtain more reliable statistical estimates of the parameters tested.

133

FOR OFFICIAL USE ONLY

UDC 621.311

INVESTIGATION OF DECOMPOSITION OF RANDOM PROCESSES IN ELECTRIC POWER SYSTEMS INTO CHARACTERISTIC COMPONENTS (USING EXAMPLE OF BRATSK-UST'-ILIMSKIY CENTER)

[Abstract of article by Gamm, A.Z., Kurbatskiy, V.G.]

[Text] Application of the Karhunen-Lowe method for obtaining models of random processes in a power system is described, and the possibility of using this approach in processing information in emergency automation systems is analyzed. Experimental findings from analyzing random processes are presented.

UDC 621.311

UTILIZATION OF DATA ON FLUCTUATIONS IN POWER SYSTEM MODE FOR MATHEMATICAL DESCRIPTION OF ITS BASIC OBJECTS

[Abstract of article by Guseynov, F.G., Rakhmanov, N.R.]

[Text] Fluctuations of mode parameters in the region of the frequency spectrum of electromechanical oscillations are examined at the input of typical objects -- load centers and synchronous generators; a device is described for recording these oscillations and ways are indicated for using the data obtained to identify dynamic characteristics of the object. Experimental findings are presented, which show that the characteristics obtained have the same trends as the theoretical characteristics.

UDC 621.311:519.24

ESTIMATION OF STATE AND MODE PARAMETERS OF COMBINED POWER SYSTEMS AS OBJECTS OF CONTROL BY FREQUENCY AND ACTIVE POWER

[Abstract of article by Bushuyev, V.V., Novikov, N.L., Korostyshevskiy, Ye.A.]

[Text] Results of analyzing irregular oscillations of mode parameters of a unified power system using full-scale experiments conducted at various power associations in the country are presented. The statistical characteristics of irregular oscillations obtained made it possible to solve a number of problems of filtering, extrapolation and prediction for frequency and active power regulation systems. The mathematical apparatus is based on the use of a Kalman-Busey filter.

UDC 621.311:519.24

REAL-TIME ESTIMATION OF NONSTATIONARY PROCESS WITH UNKNOWN CHARACTERISTICS

[Abstract of article by Gerasimov, L.N.]

[Text] The requirements imposed on estimation algorithms operating in automatic control systems are analyzed. Based on the analysis, a linear model is proposed

134

which approximates a nonstationary process, for the identification of which adaptation apparatus which "forgets" past data is used. Experimental findings are presented which confirm the methodological assumptions. The high speed of the programs allows them to be used in real time.

UDC 621.311:519.24

LINEAR FILTERING ALGORITHM WITH MINIMUM NUMBER OF MEASURED ELECTRIC POWER SYSTEM PARAMETERS

[Abstract of article by Rakhimov, G.G.]

[Text] It is shown that the observability of a linear model of electric power system elements can be ensured using a minimum number of measurements. Ways are proposed for improving the convergence of the estimation process with minimum measurements.

UDC 621.398

UTILIZATION OF PULSED ELECTRONIC COUNTERS FOR REMOTE MEASUREMENT OF ELECTRICAL ENERGY AND IMPROVING ACCURACY OF POWER ESTIMATION

[Abstract of article by Bogdanov, V.A., Chernya, G.A.]

[Text] It is proposed that the readings of pulsed electronic electric energy counters be used to obtain information about power, which makes it possible to increase telemetry accuracy. Estimates are given of the technical requirements for remote power and energy measurements, and ways are indicated to achieve the required accuracy.

UDC 621.311:681.326.3

EVALUATION OF APPLICATION OF ANALOG DATA INPUT SYSTEMS FOR INFORMATION-CONTROL COMPLEXES IN AUTOMATIC POWER SYSTEM DISPATCHER CONTROL SYSTEM

[Abstract of article by Dorofeyev, V.V., Popov, V.V.]

[Text] Computer data input using existing analog data transmission channels and analog-digital converters is analyzed. Results of experimental investigation of channel noise are presented.

UDC 53.089.68

PROCESSING TELEMETRY DATA USING ADAPTIVE MODEL OF CHANNEL OF TELEMETRY SYSTEM INTERFACED WITH M-6000 ASVT-M UVK

[Abstract of article by Abdullayev, D.A., Makarov, G.N., Arifdzhanov, A.I., Umarov, N.N., Begmatova, M.T.]

[Text] A list of the methodological materials making up the set of metrological support programs for telemetry in power engineering is given. Justification is given for the requirement of processing telemetry data by an adaptive model of the telemetry system channel.

UDC 621.3.05

ERRORS IN ASSIGNING PARAMETERS OF EQUIVALENT CIRCUITS IN ANALYZING POWER SYSTEM MODES

[Abstract of article by Idel'chik, V.I., Novikov, A.S., Palamarchuk, S.I.]

[Text] The influence of weather, mode and construction factors on the accuracy of assigning parameters of equivalent circuits of overhead power transmission lines, transformers and autotransformers is evaluated.

The values of characteristic errors in assigning longitudinal and transverse parameters of the equivalent circuits of these network elements are given. It is shown that most factors can be considered by appropriate functional relationships in creating standard mathematical models of power system modes or by introducing averaged corrections in preparing the source data.

UDC 621.317.3

ERRORS IN MEASURING PARAMETERS OF POWER SYSTEM MODE

[Abstract of article by Idel'chik, V.I., Neyman, V.V., Novikov, A.S., Palamarchuk, S.I.

[Text] The intervals of variation are obtained for errors in measuring voltage, active and reactive load power which characterize the accuracy with which these parameters are assigned in controlling the modes of power systems. A method for determining the resultant error in measuring mode parameters is shown in detail; the values and causes of occurrence of systematic and random components of the resultant error in measuring voltages, active and reactive loads at power system nodes are presented.

UDC 621.311.007.2: 681.3.06

SET OF PROGRAMS FOR OPERATIONAL ANALYSIS AND PLANNING OF POWER SYSTEM MODES FOR M-222 COMPUTER

[Abstract of article by Babeyev, G.S., Plotnikov, I.L., Chelpanov, A.V.]

[Text] The first phase of a group of programs for obtaining and processing source

136

data un the mode of an electric power system is described, and the design principles and initial experience in working with this group are given.

UDC 621.311.007.2:681.3.06

"IRIS" SYSTEM FOR PROCESSING OPERATIONAL INFORMATION REGARDING POWER SYSTEM MODE

[Abstract of article by Babayev, G.S., Gamm, A.Z., Gerasimov, L.N., Grishin, Yu.A., Grunina, R.I., Golub, I.I., Kolosok, I.N., Plotnikov, I.L., Chelpanov, A.V.

[Text] A description is given for the IRIS information system, which is intended to improve the quality and reliability of operational dispatcher data by using mathematical methods. The initial data sources are dispatcher sheets, test measurements, remote measurements and remote signals. The system has been implemented on YeS-1010, YeS-1022 and M-222 computers and is being introduced in the Irkutsk power system.

UDC 621.311:519.24

PROBLEM OF DETECTING BAD DATA AND SOLUTION ALGORITHM

[Abstract of article by Kolosok, I.N.]

[Text] A brief description is given of methods for finding bad data and for calculating the algorithm for a program used to detect bad data using the topological analysis method; the characteristics of this program and analysis of results are given.

UDC 621.311.001.57

YeS-1010 PROGRAM FOR REAL TIME ESTIMATION OF ELECTRIC POWER SYSTEM STATUS

[Abstract of article by Grishin, Yu.A.]

[Text] One possible approach to implementing the evaluation of electric power system status on a small computer is examined. It is shown that the scanning method is most convenient for this purpose, considering interfacing with the equipment in the SOT 4R·0 telemechanical data display system. Numerical results are cited which confirm the possibility of monitoring electric power system mode (for up to 50 nodes) using 30 remote measurements in a five-second cycle, and 150 measurements in a one-minute cycle. Approaches for reducing counting time are indicated.

UDC 621.311.681.3.06

CALCULATION ALGORITHM FOR TEST MEASUREMENT PROCESSING PROGRAM

137

[Abstract of article by Liseyev, M.S., Unger, A.P.]

[Text] A calculation algorithm is described for a program used to process test measurements on the basis of generalized normal estimation and filtering of erroneous data. A characterization is given of the program and its flowchart, and the calculation results are analyzed.

UDC 621.311:681.3.06

EXPERIENCE IN USING COMPUTER PROGRAMS FOR PROCESSING POWER SYSTEM TEST MEASUREMENTS AND PROSPECTS FOR FURTHER DEVELOPMENT

[Abstract of article by Bogdanov, V.A., Liseyev, M.S.]

[Text] A brief characterization is given for two programs for processing test measurements developed at the Central Dispatcher Directorate of the Unified Power System of the USSR and the Moscow Power Institute; the findings are analyzed and prospects for further developments are noted.

UDC 621.311.681.3.06

PROBLEMS OF ESTIMATING ELECTRIC POWER SYSTEM STATUS IN AUTOMATIC DISPATCHER CONTROL SYSTEM OPERATIONAL-INFORMATION SYSTEM AND ARChM [expansion unknown] DIGITAL SYSTEM

[Abstract of article by Shakhanov, V.S., Kamynin, S.M.]

[Text] Ways of constructing information models of electric power systems based on telemetry data are given, as is the possible structure of a group of algorithms for estimating electric power system status. Qualitative estimates of numerical methods are given which must be used to solve the estimation problem.

UDC 621.311:001.57

OPERATIONAL ESTIMATION OF POWER SYSTEM MODE

[Abstract of article by Pershikov, S.F., Yurovskiy, A.G.]

[Text] A group of programs is proposed for operational estimation of power system mode which has been developed at the All-Union Scientific-Research Institute of Power Engineering and the Computer Center of the GTU [expansion unknown]. The problem is solved in a two-machine operational-information computer system consisting of a YeS-1010 and YeS-1033.

138

UDC 621.31:519.24

ACCOUNTING FOR ERRORS IN CONTROLLING CURRENT DISTRIBUTION IN NONUNIFORM NETWORK

[Abstract of article by Kizhner, S.I., Sukhov, A.I.]

[Text] It is proposed that a systematic error filter be used to increase measurement accuracy, and an approach is examined which allows power system modes to be controlled with a minimum amount of information. The source information in the algorithm consists of the branch loads, and the independent variables are the equalizing loop currents.

UDC 621.311:519.24

"RASSTANOVKA TM-I" SYSTEM FOR SELECTING COMPLEMENT OF ELECTRIC POWER SYSTEM MEASUREMENTS

[Abstract of article by Golub, I.I.]

[Text] The "Rasstanovka TM-I" set of programs is described, which is intended for selecting the optimal group of measurements in terms of the electric power system observability quality criterion. The programs are written in FORTRAN for YeS-series machines; the set of programs has been sent to the Moscow Department of the Energoset'proyekt automatic control system.

6900
CSO: 1860/72

UDC 621.316.542.064.241

AIR CIRCUIT-BREAKERS FOR POWER TRANSMISSION APPLICATIONS

Leningrad VOZDUSHNYYE VYKLYUCHATELI in Russian 1981 (signed to press 29 Jan 81) pp 2-4, 380-381

[Annotation, foreword and table of contents of book "Air Circuit-Breakers", by Vasiliy Vladimirovich Afanas'yev and Yuriy Iosifovich Vishnevskiy, Energoizdat, Leningradskoye otdeleniye, 10,000 copies, 382 pages]

[Text] Aspects of theory and design are examined in the book, and designs for high-voltage a.c. air circuit-breakers are described.

The book is intended for engineering and technical personnel engaged in the development, research, installation and operation of high-voltage circuit-breaker devices. It may be extremely useful for teachers and students specializing in high-voltage equipment building.

Reviewer: O. B. Bron

FOREWORD

The practical use of compressed air to suppress the electric arc in high-voltage circuit-breakers was begun in the 1920s. The first examples of air circuit-breakers rated at 10-20 kW, in which suppression of the electric arc was provided by compressed air at a pressure of 10×10^5 Pa (10 kgs/cm²), appeared in experimental operation in 1929. The primary insulation in the circuit-breakers was made from ceramic materials. The design of the first air circuit-breakers was imperfect in many ways. This came about because the pecularities of electric arc suppression in compressed air were still inadequately studied. A certain time was required for designers to overcome these shortcomings and to make air circuit-breakers which could compete with oil breakers.

Particularly intensive developments in air circuit-breakers began in the Soviet Union in 1945, when research and design work was initiated in order to create a series of substation circuit-breakers rated at 35-220 kW. F. F. Baburskiy and Ye. M. Tseyrov, VEI (All-Union Order of Lenin and Order of the October Revolution Electrical Engineering Institute imeni V. I. Lenin) and L. K. Greyner (plant "Elektroapparat") were the initiators and leaders of this work.

140

A new trend in the design of air circuit-breakers was set in 1947 by the proposal of F. F. Baburskiy to place the arc suppressing apparatus in a metallic container filled with compressed air (cf. [3, p. 82]). This permitted the efficiency of the compressed air effect on the electrical arc to be improved significantly. This idea was used somewhat later by a number of foreign equipment building companies in their elaborations of air circuit-breakers.

Air circuit-breakers currently enjoy an extremely wide application, and have replaced oil breakers in many instances. Air circuit-breakers permitted the jump to voltage classes of 750 and 1150 kW; the shift to higher voltage classes is possible, as well as to cut-off currents of 63-80 kAmp at voltages of 110-750 kW and 160-240 kAmp at voltages of 20-30 kW.

The development of air circuit-breakers was to a great extent the basis for creation of other types of gas circuit-breakers, e.g. with sulfur hexafuloride (elegaz) as the insulation medium, although, in perspective, as will be demonstrated in more detail in the first chapter, each of these types will retain a fully determined area of application.

Materials on the design and engineering of air circuit-breakers are assembled and systematized in this book. Moreover, many sections of the book may also concern switches filled with sulfur hexafluoride.

The book being offered consists of 9 chapters. Examples of designs are presented in the appropriate chapters for better mastery of the design methodology for one or another component of pneumatic switches.

The second, seventh and eighth chapters were written by V. V. Afanas'yev, the first, third, fourth, sixth and ninth by Yu. I. Vishnevskiy and the fifth by S. M. Krizhanskiy.

The authors express their deep gratitude to Dr. of Technical Sciences O. B. Bron who reviewed the manuscript and made a number of valuable suggestions.

The authors are grateful to N. M. Adon'yev and R. B. Dobrokhotov, who rendered great assistance in preparation of the present work.

Comments on the book, notes and desires should be directed to the following address: 191041, Leningrad, Marsovo Pole, 1, Leningrad Branch of Energoizdat.

CONTENTS

141

COPYRIGHT: Energoizdat, 1981

9194
CSO: 1860/121

143

QUANTUM ELECTRONICS, ELECTRO-OPTICS

GAS LASER DISCHARGE CURRENT STABILIZER

[Article by V.G. Gudelev, V.M. Kuznetsov and V.M. Yasinskiy, Belorussian SSR Academy of Sciences Institute of Physics, Minsk]

[Text] A description is given of a gas discharge current stabilizer making possible the effective suppression of current fluctuations in the frequency band of approximately 200 kHz with an operating current of 2 to 15 mA. The dynamic output impedance of the circuit is approximately 400 MΩ and the temperature coefficient of current variation is less than or equal to 10^{-4} $^\circ K^{-1}$.

For the reliable operation of measuring systems based on gas lasers--gyroscopes and interferometers stabilized at the frequency of lasers--it is necessary to ensure instability of the discharge current of the laser's active element of less than 10^{-3}, i.e., the power supply must have high dynamic output impedance in a frequency band of maximum width beginning with direct current. Most often used in these systems are He + Ne and Co_2 lasers whose operating currents usually equal 2 to 15 mA with a voltage of 0.5 to 8 kV.

In [1] for the purpose of producing high dynamic impedance of the laser's power supply a current stabilizer is used which utilizes a high-voltage electronic triode with a transistor stage as the cathode load. This circuit solution makes possible the suppression of high-frequency current fluctuations, but because of thermal changes in the current of the transistor's base the instability of output current reaches 10^{-2}. The influence of temperature on the discharge current can be reduced considerably by eliminating current coupling between the control and discharge circuits and by using the compensation principle of stabilization. In fig 1 is shown the circuit diagram of a current stabilizer consisting of a low-voltage precision current generator of the compensation type utilizing operational amplifier M_1 with a regulating element in transistors T_1 and T_2 [2] and of a high-voltage voltage amplifier in electronic tube L_1. GI-7B, GI-11B, 6S50D and GI-30 tubes and K140UD8A and K1UT401B operational amplifiers were tested in the stabilizer. The maximum frequency band for the effective suppression of fluctuations in discharge current (approximately 200 kHz) was obtained when using a K1UT401B microcircuit, and the maximum dynamic output impedance (approximately 400 MΩ) when using a 6S50D triode and GI-30 double tetrode in a triode connection with parallel connection of the anodes and unification of the control and screen grids. The corresponding anode-grid characteristic of a GI-30 tube is shown in fig 2. The gain

144

for the tube's voltage with this connection is approximately 350. A 6S50D
tube has a considerably higher cutoff voltage than a GI-30 tube, which places
strict requirements on the parameters of the regulating unit. The use of a
6S50D tube is preferable in miniature laser systems for supplying active elements
with a combustion voltage of less than 1.5 kV.
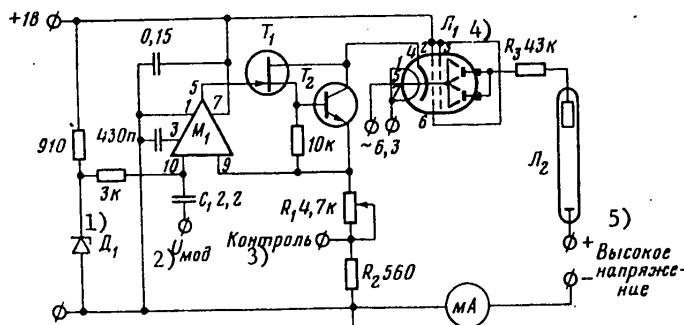
Figure 1. Circuit Diagram of Stabilizer: M_1--K1UT401B; T_1--KP303B, T_2--
KT608B; D_1--D818Ye; L_1--GI-30, L_2--laser gas discharge tube

Key:
1. Diode
2. Modulation voltage
3. Test
4. L_1
5. High voltage

The use of field-effect transistor T_1 made it possible to eliminate the influence
of the thermal drift of the current of the base of transistor T_2 on the discharge
current on account of the equality of the input and output current of the regulat-
ing unit utilizing transistors T_1 and T_2. The stabilizer's output current is de-
termined by the reference voltage, U_{op}, of stabilitron D_1 and by the total resist-
ance of resistors R_1 and R_2:

$$I \approx U_{on}/(R_1 + R_2).$$

Resistor R_2 serves the purpose of limiting the maximum current of the stabilizer.

Thermal changes in current are caused by drift of the reference voltage of stabili-
tron D_1, by the change in resistance of current-setting resistors R_1 and R_2 and by
the drift of the bias voltage, U_{sm}, and input current, I_{vkh}, of the operational
amplifier:

$$\frac{1}{I}\frac{dI}{dT} \approx \alpha + \beta + \frac{1}{U_{on}}\frac{dU_{cm}}{dT} + \frac{1}{I}\frac{dI_{вx}}{dT}.$$

145
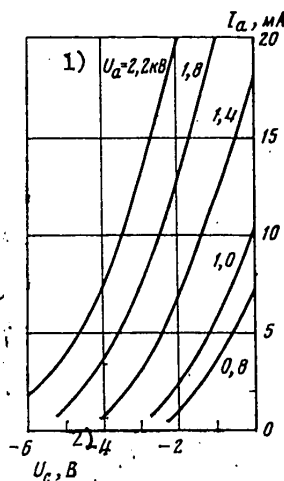
Figure 2. Anode-Grid Characteristic of GI-30 Tube in a Triode Connection

Key:
1. Anode voltage, 2.2 kV   2. Grid voltage, V

Here $|\alpha| \leq 10^{-5}$ K^{-1} is the temperature coefficient of voltage of stabilitron D_1 and β is the temperature coefficient of resistance of the current-setting resistor; the value of the third and fourth terms of the right half is approximately 10^{-5} K^{-1}. If an operational amplifier with field-effect transistors in its input is used in the stabilizer, then the discharge current circuit will be practically totally decoupled with respect to current from the control circuits and the influence of the last term will be eliminated. Consequently, the temperature stability of the discharge current is caused primarily by the temperature coefficient of resistance of the current-setting resistor ($|\beta| \leq 10^{-3}$ K^{-1} for SP-1 variable resistors and $|\beta| \leq 10^{-4}$ K^{-1} for PTMN-1 fixed wirewound resistors). For the purpose of producing current instability of less than 10^{-4} K^{-1} it is necessary to control the temperature of current-setting elements (D_1, R_1, R_2) and the operational amplifier.

In the current stabilizer the ability is provided of modulating the discharge current by supplying a control voltage to the noninverting input of M_1 through capacitor C_1.

The optimum supply voltage for the stabilizer is chosen from the measured combustion voltage for discharging of the active element taking into account the anode-grid characteristic of tube L_1 and the voltage drop in ballast resistor R_3. For stable operation in the region of low current the active element must be connected to the stabilizer by means of wires of minimum length and capacitance. For the same reason it is undesirable to connect the high-voltage source between the anode of the tube and the cathode of the active element. Resistor R_3 must be connected

146

directly to the cathode of the active element or between its anode and the positive terminal of the high-voltage power supply.

The current stabilizer was used to supply the active elements of an He + Ne laser with a discharge combustion voltage of up to 2.5 kV and of an LG-23 CO_2 laser and made possible stable operation in the current range of 2 to 15 mA.

Bibliography

1. Posakoni, M.Dzh. PRIBORY DLYA NAUCHNYKH ISSLEDOVANIY, No 2, 1972, p 90.

2. Rutkovski, Dzh. "Integral'nyye operatsionnyye usiliteli" [Integrated Operational Amplifiers], translated from English, edited by M.V. Gal'perin, Moscow, Mir, 1978, p 301.

COPYRIGHT: Izdatel'stvo "Nauka", "Pribory i tekhnika eksperimenta", 1981

8831
CSO: 1860/74

UDC 621.378.325

POWERFUL POWER SUPPLY FOR PULSED LASERS EMPLOYING VAPORS OF METALS

[Article by A.Ye. Kirilov, A.N. Soldatov and V.F. Fedorov, USSR Academy of Sciences Siberian Division "Optics" Special Design Bureau for Scientific Instrument Making, Tomsk]

[Text] A description is given of an apparatus for studying the energy characteristics of lasers utilizing vapors of metals. The power supply makes it possible to form current pulses with a height of up to 1 kA, a voltage up to 15 kV and a length of 100 to 500 ns with a pulse repetition rate of up to 30 kHz.

One method of increasing the mean power of gas-discharge recurrent-pulse lasers utilizing vapors of metals is increasing the volume of the active medium and the power of pumping sources [1-3]. In this paper a description is given of a unit for forming pulses with a current amplitude of up to 1 kA and a voltage of up to 15 kV with a pulse length of 100 to 500 ns and a repetition rate of up to 30 kHz.

Twelve TGI1-1000/25 hydrogen thyratrons are used as switching elements in the power supply, which make it possible with simultaneous operation to switch power of up to 25 to 30 kW. The circuit diagram of the unit is shown in fig 1.

A ferroresonance voltage regulator (RN) and rectifier, V, executed with TR1-6,5/20 thyratrons, make possible smooth regulation of voltage to 15 kV with a current of 5 A. The resonance charging of working capacitors is accomplished via inductance L_1 (0.5 H) and a block of charging kenotrons, L_1 to L_{36} (V1-0,15/55's). Low-induction capacitors (KVI-3's), C_{T1} to C_{T12}, are used as working capacitors. The capacitors are installed directly at the anode terminals of the TGI1-1000/25 thyratrons and are cooled by fans. The charging inductance in the high-voltage version is composed of sections, each of which is wound on a core with 0.7- to 0.8-mm-diameter wire with an air gap between turns. For stable functioning of the thyratrons when they are connected in parallel, the working capacitors are charged through individual kenotrons (three kenotrons for each thyratron), which makes possible reliable anode decoupling. Each three kenotrons have their own winding in a filament transformer designed with an air gap. The primary winding of the filament transformer is shielded.
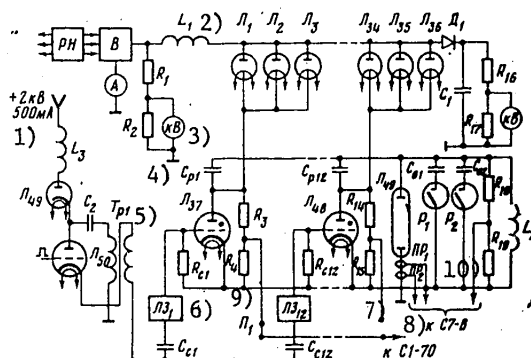
148

Figure 1. Circuit Diagram of 12-Channel Power Supply: L_1 to L_{36}--V1-0,15/55; L_{37} to L_{48}, L_{50}--TGI1-1000/25, L_{49}--gas discharge tube; D_1--KTs106G; R_1--KEV-5-10 MΩ; R_2, R_{17}--MLT-2--selected as a function of type of instrument; R_3, R_{14}, R_{16}--KEV-5-100 MΩ; R_4, R_{15}--MLT-2-100 kΩ; R_{18}, R_{19}--conventional representation of induction-free compensated voltage divider; R_{s1}, R_{s12}--TVO-5-10 kΩ; C_1--KVI-2-20 pF-30 kV, C_2--KVI-3-3300 pF-10kV, C_{r1}, C_{r12}, C_{01}, C_{02}--KVI-3-220 to 4700 pF, C_{s1}, C_{s12}--0.01 μF-3 kV

Key:

1. + 2 kV, 500 mA
2. Kenotrons
3. kV
4. Working capacitor
5. Transformer
6. Delay line
7. Rogovskiy loop
8. To S7-8 oscillograph

The thyratrons are triggered by a 12-channel modulator whose output stage is executed with thyratron L_{50} (TGI1-1000/25). The trigger pulses are formed during discharging of capacitor C_2 through the primary winding of air-core transformer Tr1. Capacitors C_{s1} to C_{s12} and resistors R_{s1} to R_{s12} are included for the purpose of producing automatic bias voltage in the grids of the thyratrons. The thyratrons are triggered by means of a signal from a pulse transformer through cable delay lines LZ_1 to LZ_{12}. Automatic biasing makes possible continuous operation of the thyratrons with a pulse repetition rate of greater than 5 kHz. With a lower rate negative voltage regulated from 0 to 500 V is supplied to the grids of the thyratrons via decoupling induction coils (0.05 H) of the bias source.

With the parallel operation of several thyratrons it is necessary to control their triggering. This is accomplished by means of dividers, R_3, R_4 to R_{14}, R_{15}, the signal from which is supplied via switch P_1 to a pointer instrument or to an oscillograph. The filament supply of the hydrogen thyratrons is stabilized.

For the purpose of optimizing the operating conditions of a self-heated laser it is necessary to select-to-fit the working capacitors, C_{r1} to C_{r12}, the peaking capacitors, C_{o1} to C_{o3}, shunting inductor L_2 and other elements. These elements are usually replaced with the laser shut off; however, during the shutoff period

149

uncontrollable changes take place in the gas discharge tube. Low-induction high-voltage vacuum relays, VV-20's (R_1, R_2 [in Cyrillic]), are used for the on-line switching and fitting of elements with the laser operating. With the simultaneous use of three to six relays it is possible to compare with one turn-on operation the laser's operating conditions with various peaking and working capacitors and shunting inductors. Curves for generation pulses, 1, 1', 2, 2', and voltage pulses, 3, 3', of a laser employing copper vapors are presented in fig 2. Curves 1 to 3 were plotted with the peaking capacitor disconnected and 1' to 3' with a "peaker" connected, when C_r/C_o = 2 : 1 .
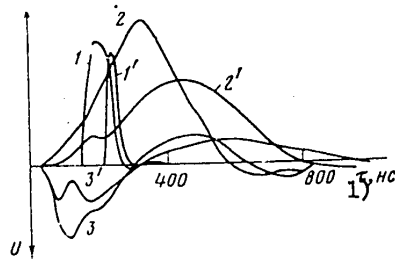
Figure 2.   Experimental Curves for Generation Pulses (1, 1'), Current Pulses
            (2, 2') and Voltage Pulses (3, 3') in a Gas Discharge Tube:
            1 to 3—without peaking capacitor; 1' to 3'—with peaker connected

Key:
     1. τ , ns

The unit described makes it possible to supply two-section gas discharge tubes (fig 3) with slight modification. With this power circuit it is possible to produce higher voltages per unit length and shorter lengths of current pulses, which results in an increase in the pulsed generation power.
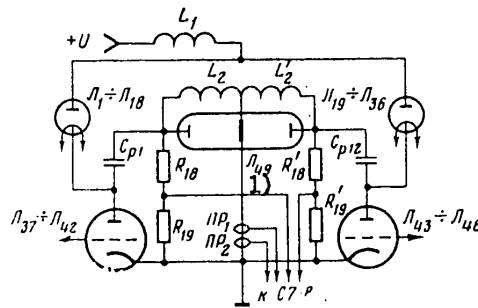
Figure 3.   Circuit Diagram for Connection of a Two-Section Gas Discharge
            Tube, L_{49}

Key: 1. L_{49}

150

FOR OFFICIAL USE ONLY

The measurement of pulses of current through the gas discharge tube and of the voltage across electrodes is performed by means of Rogovskiy loops PR_1 and PR_2 (fig 1) and by means of induction-free compensated voltage divider R_{18}, R_{19}, the signals from which are supplied to an S7-8 two-channel storage-type oscillograph. The oscillograph is triggered by a signal from one of the Rogovskiy loops. Lasing pulses are measured by means of an FEK-02 coaxial photoelectric cell.

An automatic coaxial switch controlled from the oscillograph is used for the simultaneous observation of four signals on the oscillograph's screen.

In conclusion let us mention that this unit made it possible to produce a recurrent-pulse discharge with a frequency of 15 kHz in a mixture of neon and copper vapors in an active volume of 3.5 liters. The amplitude of the current and voltage through the 55-mm-diameter gas discharge tube equaled 1 kA and 15 kV, respectively. The maximum lasing power in a laser employing copper vapors equaled 40 W and was produced in an active volume of 1.25 liters with a power supply power of 8 kW.

Bibliography

1. Isayev, A.A. and Limmerman, G.Yu. KVANTOVAYA ELEKTRONIKA, Vol 4, No 7, 1977, p 1413.

2. Kirilov, A.Ye., Polunin, Yu.P., Soldatov, A.N. and Fedorov, V.F. Collection "Izmeritel'nyye pribory dlya issledovaniya parametrov prizemnykh sloyev atmosfery" [Measuring Instruments for Studying the Parameters of Layers of the Atmosphere Near the Earth], edited by I.V. Samokhvalov, Tomsk, USSR Academy of Sciences Siberian Division Institute of Atmospheric Optics, 1977, p 60.

3. Smilanski, I., Erez, G., Kerman, A. and Levin, L.A. OPT. COMMUN., Vol 30, No 1, 1979, p 70.

8831
CSO: 1860/74

151

SOLID STATE CIRCUITS

UDC 621.382.2/3.001.24

CALCULATION OF SEMICONDUCTOR POWER DEVICES

Moscow RASCHET SILOVYKH POLUPROVODNIKOVYKH PRIBOROV in Russian 1980 (signed to press 16 Oct 79) pp 2-4, 184-185

[Annotation, foreword and table of contents from book "Calculation of Semiconductor Power Devices", by Panteley Georgiyevich Dermenzhi, Vadim Arkad'yevich Kuz'min, Nadezhda Nikolayevna Kryukova, Valentin Ivanovich Mamonov and Valentin Yakovlevich Pavlik, edited by V. A. Kuz'min, Izdatel'stvo "Energiya", 11,500 copies, 185 pages]

[Text] The authors examine the connection between the electrical characteristics and parameters of semiconductor power devices -- diodes and thyristors -- and the physical structure of the device and analyze the interconnection of the basic parameters. They give the methods and formulas which make it possible to calculate power devices and give examples of calculations.

This book is intended for engineers and technicians specializing in the calculation and development of semiconductor devices, and also can be used in designing systems with semiconductor power devices.

Foreword

At the present time, semiconductor power devices, among which silicon diodes and thytistors of various purposes are very important, are used widely in a great variety of areas of electrical engineering and electronics.

Properties and characteristics of thyristors are described in periodicals, as well as in the books by F. Dzhentri et al "Silicon Controlled Rectifiers", V. A. Kuz'min "Low and Medium Power Thyristors", and V. Ye. Chelnokov and Yu. A. Yevseyev "Physical Principles of the Operation of Semiconductor Power Devices". These books discuss in detail principal theoretical propositions and physical processes in thyristors. However, these books are partially outdated. Moreover, in recent years, theoretical and experimental studies have been carried out, making it possible in a number of cases to have a new approach to the calculation of thyristors and to establish more accurate quantitative relations between the electrical characteristics of modern power thyristors and physical and geometrical parameters of multilayer structures. The use of quantitative methods of calculation, including those with the use of electronic computers, makes it possible to reduce the volume of experimental studies in developing new devices, to shorten the time of designing, and to improve the quality of the power devices being developed.

152

In spite of the fact that this book treats the calculation of power thyristors, it can be used also for designing power diodes.

Calculations of breakdown voltage of the p-n junction (Chapter 2) and direct voltage drop (Chapter 4) can be used directly for determining the breakdown voltage and direct voltage drop in power diodes.

For this reason, as well as in connection with the fact that the diode is a considerably simpler device in comparison with the thyristor, the book does not contain a special section treating power diodes.

Much attention in the book is given to presentation of problems connected with the calculation of the effect of the density of shunting the cathode junction to the static characteristic and transient processes. The authors analyzed the special characteristics of thyristors with current regeneration which are used very widely at the present time.

Transient connection processes are examined in application to powerful high-voltage thyristors, whose connection has substantial peculiarities in comparison to low-power instruments. In calculating transient processes of connecting and disconnecting, as well as processes of heating under the effect of current pulses and shock currents, special characteristics of designs and specifics of the modes of measurements of dynamic parameters of thyristors were taken into consideration.

Chapters 1 and 6 were written by P. G. Dermenzhi, Chapter 2 -- by N. N. Kryukova, Chapters 4 and 8 -- by V. A. Kuz'min, Chapter 5 -- by V. Ya. Pavlik, Chapter 7 -- by V. I. Mamonov, and Chapter 3 -- by P. G. Dermenzhi, N. N. Kryukova and V. Ya. Pavlik.

Contents

154

COPYRIGHT: Izdatel'stvo "Energiya", 1980

10,233
CSO: 1860/108

UDC 621.382.2/3.001.41

TESTS OF SEMICONDUCTOR POWER DEVICES

Moscow ISPYTANIYA SILOVYKH POLUPROVODNIKOVYKH PRIBOROV in Russian 1981 (signed to press 25 Mar 81) pp 2-4, 201

[Annotation, foreword and table of contents from book "Tests of Semiconductor Power Devices", by Oleg Georgiyevich Chebovskiy and Lev Gennad'yevich Moiseyev, reviewed by V. A. Labuntsov, Energiozdat, 10,000 copies, 201 pages]

[Text] The book presents methods of testing semiconductor power devices (diodes, thyristors, symmetrical thyristors, photothyristors, voltage limiters, and others). Requirements for semiconductor power devices established by the State Standards and other normative documents are examined; functional diagrams of systems, requirements for the elements of the circuits of these systems are given, as well as the characteristics of methods of testing for reliability and reliability estimation.

This bo ʌ is intended for use by engineers and technicians engaged in the development, manufacturing and testing semiconductor power devices and conversion units.

Foreword

In connection with the rapid development of conversion devices and their introduction into nearly all sectors of the national economy, designers and operators of conversion devices impose new, often specific, requirements for the volume and quality of information on electrical, thermal, mechanical and other parameters and characteristics of semiconductor power devices (PPS).

The available informational materials do not always meet the needs of the consumers, and manufacturing enterprises are not always able to meet these needs.

Moreover, in order to improve the quality of their products, many enterprises have their own PPS quality control for eliminating the defects which are not controlled at the manufacturing enterprises of PPS, or for the purpose of selecting PPS according to some parameters.

This book describes testing equipment used at the present time at the manufacturing enterprises of PPS, defines the requirements imposed on such equipment ensuring the performance of the necessary measurements and studies of the dependence of the PPS parameters on various conditions.

The book consists of four chapters.

The first chapter examines the system of parameters of semiconductor power devices and dependence of these parameters on the conditions of measurements and operation.

The second chapter gives the description of measurement methods, requirements imposed on measurements, and units used both for studies and for measuring the parameters of devices. The operation of individual assemblies and units is illustrated by figures and time diagrams; structural data and specifications of the elements of circuits of some devices are also given.

The third chapter contains the description of circuits of semiautomatic testing complexes for controlling the main parameters of thyristors and simistors.

The fourth chapter examines requirements for conducting mechanical and climatic tests whose entire complex can be done on series-produced stands (therefore, the authors do not consider it necessary to describe these stands).

The authors do not claim that all problems connected with the testing of semiconductor power devices are presented in full, since other circuit designs can be used for testing equipment.

The authors are deeply grateful to engineer V. N. Yunovich for his help in the preparation of the drawings of electrical circuits.

The authors will be grateful to the readers who will send their comments and suggestions to the following address: 113114, Moscow, M-114, Shlyuzovaya naberezhnaya, Building 10, Energoizdat.

Contents

COPYRIGHT: Energoizdat, 1981

10,233
CSO: 1860/109

FOR OFFICIAL USE ONLY

NEW ACTIVITIES, MISCELLANEOUS

ABSTRACTS FROM COLLECTION 'RADIO ENGINEERING'

[Annotation and 20 abstracts from "Republican Interagency Scientific and
Technical Collection: Radio Engineering" edited by A. I. Tereshchenko et al.,
Izdatcl'skoye ob"yedineniye "Vyshcha shkola", 1000 copies, 136 pages]

[Text] The results of theoretical and experimental studies of electronic and
semiconductor SHF devices are presented in the collection. Questions of
calculation and construction of SHF measuring devices, components and sub-
assemblies of SHF equipment are considered.

For science workers and specialists.

List of references at end of articles.

UDC 621.372.82

CALCULATION OF WAVE RESISTANCE OF SOME TYPES OF STRIP LINES

[Abstract of article by V. M. Sedykh, N. V. Lyapunov and S. A. Pogarskiy]

[Text] A comprehensive approach to the question of calculating waveguide
resistance of some types of strip lines is proposed. Wave resistance is com-
puted for screened symmetry and symmetrical strip lines. The accessibility
of limiting transitions to other types of strip lines is shown. Theoretical
graphs are presented and a comparison is given with results of other authors
known from the literature.

UDC 621.372

THEORY OF COUPLED OSCILLATIONS IN RESONATORS

[Abstract of article by A. V. Gritsunov]

[Text] The link between oscillation types in a volumetric resonator is con-
sidered. An equation is derived for excitation for oscillations coupled by a
nonhomogeneous electronic space charge. The equation is solved for the case
of two oscillations. Coupling coefficients are computed for degenerate oscil-
lations H_{11} in a cylindrical resonator.

159

FOR OFFICIAL USE ONLY

UDC 621.376.332

SHF OSCILLATOR AFC SYSTEM FOR RESONANT FREQUENCY OF A CONTINUOUS RESONATOR WITH SUPPRESSED CARRIER

[Abstract of article by V. D. Bobryshev, V. M. Dmitriyev and N. N. Prentslau]

[Text] The use of a limiting resonator with suppressed carrier developed by the authors in an SHF oscillator AFC circuit increases the parameters of the AFC system. The limiting resonator used in the AFC system is described.

UDC 621.372.413

STUDY OF QUASIOPTICAL OPEN RESONATOR WITH ONE OR MORE CONDUCTIVE PLATES BETWEEN MIRRORS

[Abstract of article by B. M. Bulgakov, V. N. Skresanov, A. I. Fisun and A. M. Fursov]

[Text] Results of an experimental study of an open resonator containing extensive nonuniformities in the form of metal plates are cited. Relatively high resonator Q is maintained for specific selection of geometric plate dimensions and arrangement within the resonance chamber. Perturbation of the field in the resonator is comparatively small. Range properties of a perturbed resonator are explained. Distributions of fields within the resonator chamber near the plate surface and far from it are studied. A considerable field intensity gradient is present in the immediate vicinity of the plate surface.

UDC 621.372.413

EFFECT OF JUXTAPOSITION AND MUTUAL ORIENTATION OF COMMUNICATING SLITS ON THE PROPERTIES OF AN OPEN RESONATOR

[Abstract of article by Yu. I. Leonov and A. M. Fursov]

[Text] An experimental study was conducted on the effect of the spectrum of a hemispherical open resonator in which the inlet and outlet of electromagnetic energy is situated on the surface of a flat mirror, and on the juxtaposition and mutual orientation of communicating slits. Questions pertaining to polarization splitting of azimuthal types of oscillations excited in this resonator are considered. Recommendations are made on the optimum selection of mutual orientation of communicating slits for smooth alternation of the communicating coefficient of the open resonator with SHF channel and production of signals at the resonator output having the necessary frequency and polarization.

160

UDC 621.372

CALCULATION OF AMPLITUDE-FREQUENCY RESPONSE OF ELECTRICAL-LY TUNABLE FILTER BASED ON WAVEGUIDE-DIELECTRIC RESONANCE OF FERRITE INSERT IN TRANSLIMITING WAVEGUIDE

[Abstract of article by V. Ya. Dvadnenko and V. A. Korobkin]

[Text] Calculation of the amplitude-frequency characteristics of an electrically tunable filter based on waveguide-dielectric resonance of a ferrite parallelepiped in a translimiting rectangular waveguide is investigated by the generalized scattering matrix method. Expressions are found for determining the coefficient of transmisison of the primary wave. Permissible approximations are considered for calculation of matrix elements and recommendations are made on the choice of matrix size. Results of calculation and experiment are compared.

UDC 621.372

H-PLANAR CONVOLUTED WAVEGUIDE BRANCHBOX AS DIVIDER AND OUTPUT SELECTOR

[Abstract of article by S. V. Butakova]

[Text] Based on improvement of series convergence, formulas are derived for refined computer computation of scattering matrices of waveguide devices with H-waves. Electrical characteristics of convoluted waveguide branch-boxes are computed and analyzed. Under certain conditions the branchbox may serve as an electrical equivalent of a current device: an H-planar bridge or Y-coupling of waveguides.

UDC 621.372.852.1

REJECTION-TYPE SHF FILTER BASED ON WAVEGUIDE-DIELECTRIC RE-SONATOR

[Abstract of article by L. I. Babarika, V. I. Grutsyak and V. A. Korobkin]

[Text] The properties of a waveguide-dielectric resonator excited by symmetrical and asymmetrical graduated notches made directly on a dielectric insert are considered. Based on this resonator, a waveguide band-eliminating filter is created. Methods of thermal stabilization are indicated.

UDC 538.574.6

STUDY OF STARTUP CHARACTERISTICS OF REFLECTIVE DIFFRACTION EMISSION GENERATOR

[Abstract of article by I. M. Balaklitskiy, G. S. Vorobyev, A. I. Tsvyk and L. I. Tsvyk]

[Text] Analytical relations are derived to study startup characteristics of a reflective diffraction emission generator bsed on linear theory. Numerical analysis of startup currents and frequencies of oscillation based on the angle of electron escape in the reflector field are cited. Fields of reflector voltage change are indicated for minimum values of startup current. Results of theory agree well with experiments conducted in the millimeter wavelengths.

UDC 621.317.029.64

RECORDING THE DISTRIBUTION PROFILE OF INTENSIVE ELECTROMAG-
NETIC FIELDS OF SHF OSCILLATIONS. REPORT 1. STUDY OF ORGANIC
LUMINOPHOR SENSORS

[Abstract of article by A. B. Kononov, A. I. Tereshchenko, L. Ya. Malkes et
al.]

[Text] A method for obtaining visible images of the high intensity electro-
magnetic field distribution within volumetric resonators using lumionophors is
considered; quantitative and qualitative estimates of the degree of hetero-
geneity of the electromagnetic field in the cooking chamber of a home mic-
rowave oven are given.

UDC 621.317.029.64

RECORDING THE DISTRIBUTION PROFILE OF INTENSIVE ELECTROMAG-
NETIC FIELDS OF SHF OSCILLATIONS. REPORT 2. STUDY OF LC THER-
MODISPLAY SENSORS

[Abstract of article by V. L. Mironenko, A. I. Tereshchenko, S. P. Tur et al.]

[Text] A method for obtaining visible images of high intensity electromag-
netic field profile within a volumetric resonator using liquid crystal thermo-
displays is considered; quantitative and qualitative estimates of the degree of
heterogeneity of the electromagnetic field in the cooking chamber of a home
microwave oven are given.

UDC 621.317.784

ALL-PURPOSE TRANSIENT WATTMETER FOR UNBALANCED COAXIAL
TRANSMISSION LINES

[Abstract of article by V. N. Zhendubayev, Ye. K. Bogomolov and A. Yu.
Simovskiy]

[Text] A device for measuring pulsed and mean values of transient power
and on-off time ratio of a pulsed radio signal is described. The device is
composed of integrated circuits. The SHF channel consists of a directional
coaxial coupler and thermoelectric transducers. The electronics includes a
differential amplifier, on-off time ratio meter and divider. The output signal
is indicated by a M285K microammeter.

162

FOR OFFICIAL USE ONLY

UDC 621.317.784

PULSED TRANSIENT OUTPUT WATTMETER FOR UNBALANCED SHF WAVEGUIDE TRANS-
MISSION LINES

[Abstract of article by V. N. Zhendubayev, Ye. K. Bogomolov and A. Yu.
Simovskiy]

[Text] A device is described for measuring pulsed transient SHF output,
base on the principle of multiplication of signals proportional to mean
transient output and on-off time ratio of a pulsed radio signal. Device
error and basic test responses in pulsed operation of a transmitter are
analyzed. The wattmeter can be used to monitor waveguide transmission
lines for pulsed SHF signals.

UDC 621.382.2

OPERATING CONDITIONS OF GANN DIODES IN OSCILLATOR HAVING QUASIOPTICAL
RESONANCE SYSTEM

[Abstract of article by V. V. Smorodin]

[Text] Based on the study of conditions of oscillation, amplification
and synchronization of Gann diodes in a solid-state oscillator having a
quasioptical resonance system, it is shown that the very high SHF fields
required for efficient operation of oscillator diodes can be attained in
an open resonator having a transparent diffraction grid. The results
show that favorable conditions exist in the oscillator for summing up
the outputs of many semiconductor diodes.

UDC 621.385.6

STUDY OF FREQUENCY FLUCTUATIONS OF SHF SIGNAL OF DIFFRACTION EMISSION
GENERATOR

[Abstract of article by I. M. Balaklitskiy, Yu. V. Maystrenko,
A. I. Tsvyk and L. I. Tsvyk]

[Text] Theoretical and experimental studies on the effect of lf noises
of electron flux on frequency fluctuation of SHF signals of a diffrac-
tion emission oscillator are discussed. In quasistatic approximation
are obtained relationships for analysis, in the Doppler range of fre-
quencies (1 to 500 kHz), of the extent of effect of power supply noise,
focusing magnetic field (electromagnet) and flicker effects, shot noise
and other phenomena occurring in electron flux, on the spectrum of the
oscillator signal. The results of theory are compared with tests run in
the millimeter wavelengths on GDI devices and resonant LOVO. Calcula-
tions and measurements are graphically illustrated.

FOR OFFICIAL USE ONLY

UDC 621.375.001.24

IDENTIFICATION OF PARAMETERS OF EQUIVALENT CIRCUITS OF SHF TRANSISTORS

[Abstract of article by V.M. Shokalov, A. I. Luchaninov, V. K. Koval'-chuk et al.]

[Text] Methods are developed for identifying the parameters of equivalent circuits of SHF transistors. A goal function is proposed which can be used to greatly reduce solution time of optimization problems and to define equivalent circuit parameters which guarantee coincidence of theoretical and measured responses within the limits of energy dissipation and impedance variables of transistor production lots. Results of identification of equivalent circuit parameters of KT919B transistors are discussed.

UDC 621.375.001.24

METHOD OF CALCULATING OPTIMUM CONDITIONS AND LOAD RESPONSES OF SHF TRANSISTOR POWER BOOSTERS

[Abstract of article by V. M. Shokalov, V. K. Koval'chuk, A. I. Luchaninov and P. L. Tokarskiy]

[Text] An approximate method for calculating optimum parameters of potentially unstable transistors is proposed for all input and output admittances. Questions of designing load repsonses of power transistors are discussed for complex fields of load impedances, within and at the boundary of which are guaranteed at least nominal energy parameters of the booster.

UDC 621.396.67.012.12

SYNTHESIS OF DISCRETE ANTENNAS. REPORT 1.

[Abstract of article by V. A. Pavlyuk and A. M. Rybalko]

[Text] Optimum current distribution is found in a rms approximation ofthe problem of synthesis of antenna arrays with side lobe suppression in a discrete number of directions, based on the presence of errors in antenna parameters.

UDC 621.396.67.012.12

SYNTHESIS OF DISCRETE ANTENNAS. REPORT 2.

[Abstract of article by V. A. Pavlyuk and A. M. Rybalko]

[Text] For antenna arrays with passive elements, the optimum current distribution in problems of antenna synthesis with side lobe suppression is found. An algorithm is proposed for finding optimum reactive loads to synthesize antennas in terms of reactive loading.

164

UDC 621.396.67

SYNTHESIS OF ARC ANTENNA ARRAYS WITH DEEP BLANK SPOTS IN HIGHLY DIREC-
TIONAL AND DIFFERENTIAL BEAM PATTERNS

[Abstract of article by L. G. Korniyenko and A. A. Bychkov]

[Text] The prpoblem of maximizing the directivity factor of a summary
antenna array, or the transconductance of the differential beam pattern
of another antenna array with simultaneous formation of deep blank spots
and zeroes at specific angular bearings is considered. The effect of
random field fluctuations in the antenna aperture on the depth of blank
spot formation in beam pattern is analyzed; the properties of optimum
amplitude-phase response are studied. Results of computer simulation
for arc arrays having various periods are cited.

8617
CSO: 1860/38

ABSTRACTS OF ARTICLES IN COLLECTION ON RADIO ENGINEERING

Khar'kov RESPUBLIKANSKIY MEZHVEDOMSTVENNYY NAUCHNO-TEKHNICHESKIY SBORNIK: RADIOTEKHNIKA in Russian No 53, 1980 (signed to press 17 Oct 80) pp 2, 119-121

[Annotation and abstracts from collection "Republic Interagency Scientific and Technical Collection: Radio Engineering", edited by A. I. Tereshchenko, V. D. Kukush et al., Izdatel'skoye ob"yedineniye "Vyshcha shkola", 1000 copies, 121 pages]

[Text] The results of theoretical and experimental studies of electronic and semiconductor SHF devices are presented in the collection. Questions of design and construction of SHF measuring devices, components and subassemblies of SHF equipment are examined.

For science workers and specialists in radio engineering.

Bibliography at the end of each article.

UDC 621.372.413

STUDY OF POLARIZATION EFFECTS IN OPEN MILLIMETER WAVELENGTH RESONATORS

[Abstract of article by B. M. Bulgakov, Y. I. Leonov and A. M. Fursov]

[Text] The causes which trigger the splitting of higher oscillation types of an open resonator are investigated. 3 figures; 10 references.

UDC 538.574.6

STUDY OF ENERGY PROPERTIES OF RESONANCE SYSTEMS WITH WAVEGUIDE TERMINAL

[Abstract of article by A. T. Golovin, O. A. Tret'yakov and A. A. Shmat'ko]

[Text] An analytical expression is derived for the field amplitude in a waveguide terminal. 3 figures; 9 references.

UDC 621.382.2:621.396.662

SHF OUTPUT LEVEL DISCRIMINATOR

[Abstract of article by N. N. Prentslau, V. M. Dmitriyev and V. D. Bobryshev]

[Text] The generation of lf oscillations by Si mulitiplier diodes in response to SHF output is described. 3 figures; 3 references.

UDC 621.372.413

CALCULATION OF THE FREQUENCY SPECTRUM OF N-OSCILLATIONS OF A COAXIAL RESONATOR WITH DISKS

[Abstract of article by G. G. Kanarik]

[Text] A characteristics equation is written to study N-types of oscillation in a coaxial resonator with capacitive disks. 3 figures; 3 references.

UDC 621.376.332:621.385.6

REFLECTIVE KLYSTRON FREQUENCY STABILIZING SYSTEM

[Abstract of article by N. N. Prentslau and V. D. Bobryshev]

[Text] A system is described in which an active thermostabilized resonator is used as a frequency standard in an automatic frequency conversion system. 1 figure; 4 references.

UDC 621.372.413

STUDY OF CONICAL RESONATORS

[Abstract of article by V. L. Mironenko]

[Text] A conical resonator with one short-circuiting baffle is investigated. 2 tables; 2 figures; 4 rerferences.

UDC 621.318.0

ROUND MAGNETODIELECTRIC WITH STEPWISE CHANGE OF EXCITING FIELD

[Abstract of article by V. I. Antyufcyev, V. N. Krasnikov and V. V. Ovcharenko]

[Text] The process of changing the electromagnetic field in internal and external regions of an infinite cylindrical round magnetodielectric with stepwise change of the exciting field is considered. 2 figures; 3 references.

167

UDC 621.372.822

APPLICATION OF THE METHOD OF DIFFERENTIAL EQUATIONS TO
THE PROBLEM OF WAVE DIFFRACTION IN A TRANSMISSION LINE WITH
LONGITUDINALLY NONHOMOGENEOUS DIELECTRIC MEDIUM

[Abstract of article by V. I. Grutsyak and V. A. Korobkin]

[Text] The method of differential equations is considered as it applies
to the problem of scattering of electromagnetic waves by a nonhomogeneous
dielectric inclusion in a rectangular waveguide. 3 figures; 6 references.

UDC 621.372.854

ELECTRICALLY ADJUSTABLE FILTER BASED ON WAVEGUIDE DIELECTRIC
RESONANCE OF A FERRITE PARALLELEPIPED IN A SUPERLIMITING
WAVEGUIDE

[Abstract of article by V. A. Korobkin and V. Ya. Dvadnenko]

[Text] The design, operating principles and calculation of an electrically-adjustable
filter based on waveguide dielectric resonance of a ferrite parallelepiped
in a superlimiting rectangular waveguide is considered. 2 figures; 4 references.

UDC 621.496.677.4

OPTIMIZATION OF THE INTEGRAL CHARACTERISTICS OF ANTENNA
ARRAYS

[Abstract of article by V. A. Pavlyuk and A. M. Rybalko]

[Text] An effective method is proposed for finding the amplitude and phase
distribution of antenna arrays based on the presence of amplitude and phase
error. 2 figures; 10 references.

UDC 621.396.667.3

CALCULATING THE RADIO ENGINEERING CHARACTERISTICS OF WIRE
ANTENNAS

[Abstract of article by V. I. Tkachenko, A. B. Tarasov and V. A. Pavlyuk]

[Text] The possibility of eliminating problems in calculation utilizing the
method of integral equations is indicated. 2 figures; 8 references.

UDC 621.396.67

THE EFFECT OF A DIELECTRIC DIAPHRAGM ON ELECTRODYNAMIC INTERACTION
OF METAL COMPONENTS OF A METAL FRAME ANTENNA SHIELD

[Abstract of article by O. I. Sukharevskiy]

[Text] Several systems of integral equations of the 2nd order are constructed
and applied with respect to the density of surface current on metal cylinders
and the field in a diaphragm. 2 figures; 2 references.

168

UDC 621.396.677.494

PHASE SYNTHESIS OF SECTORAL ANTENNA ARRAY BEAM PATTERNS

[Abstract of article by L. G. Korniyenko and V. I. Loktin]

[Text] Problems of phase optimization for the conventional maximum beam pattern coefficient and maximum concentration coefficient of emission output of antenna arrays are considered. 1 table; 3 figures; 5 references.

UDC 621.396.67

APPROXIMATE METHOD OF CALCULATING THE EFFECT OF ELLIPTICAL RODS ON THE EMISSION FIELD OF AN ANTENNA

[Abstract of article by A. Ye. Kushch]

[Text] Methods are presented for approximate solution of the problem of scattering of an antenna emission field on elliptical rods situated in front of its aperture. 2 figures; 3 references.

UDC 621.396.67

CALCULATING THE EFFECT OF A SYSTEM OF ROUND METAL RODS SITUATED IN FRONT OF AN ANTENNA APERTURE ON ITS EMISSION PERFORMANCE

[Abstract of article by A. Ye. Kushch and O. I. Sukharevskiy]

[Text] The method of integral equations is used to solve the problem of calculating the effect of a system of round metal rods on the performance of emission for the case where their transverse dimensions are commensurate with the wave length. 2 figures; 6 references.

UDC 621.385.001.6

INITIAL STAGE OF DEVELOPMENT OF OSCILLATIONS IN DIFFRACTION EMISSION GENERATORS

[Abstract of article by D. M. Vavriv, O. A. Tret'yakov and A. A. Shmat'ko]

[Text] The initial stage of interaction of an electron beam with the field of a high-Q resonator with delaying structure is investigated. 1 table; 3 figures; 3 references.

UDC 621.385.642.3

CALCULATION OF NONSYNCHRONOUS INTERACTIONS DURING EMISSION OF A CYLINDRICAL MAGNETRON

[Abstract of article by I. V. Ruzhentsev]

[Text] Results of numerical computer calculation of the effect of nonsynchronous three-dimensional harmonics of the hf field of a delaying system on the formation of an electron cloud in a cylindrical magnetron are cited. 2 figures; 8 references.

169

UDC 621.385

EFFECT OF COMPUTER ERROR ON RESULTS OF ANALYSIS OF PROCESSES IN AN M-TYPE AMPLIFIER WITH DISTRIBUTED EMISSION

[Abstract of article by G. I. Churyumov]

[Text] The effect of computer error is examined based on analysis of trajectories of electron travel in an M-type amplifier with distributed emission. 1 table; 3 figures; 3 references.

UDC 621.385.6

INVESTIGATION OF OSCILLATION SPECTRUM OF MAGNETRON OSCILLATOR

[Abstract of article by S. A. Volin]

[Text] A device for studying the oscillation spectrum of a magnetron oscillator is described. 1 table; 3 figures; 5 references.

UDC 621.385.64

PROBLEM OF MAGNETRON ELECTROSTATICS

[Abstract of article by A. S. Tertyshnyy, A. G. Shein and L. I. Shklyarov]

[Text] The application of the structural method is presented in solving the problem of calculating the electrostatic field in a magnetron. 2 figures; 5 references.

UDC 621.372.852.4

SUBMILLIMETER RADIOWAVE SEMICONDUCTOR GATE

[Abstract of article by V. K. Kononenko and Ye. M. Kuleshov]

[Text] Possible use of the minimum magnetoplasma reflection effect in a semiconductor is considered for creation of a submillimeter wave gate. 1 table; 1 figure; 4 references.

UDC 621.3.029

SYNTHESIS AND APPLICATION OF A DYNAMIC MODEL OF A p-i-n DIODE TYPE SHF ATTENUATOR

[Abstract of article by V. T. Tsarenko]

[Text] The problem of creating a linear mathematical model of a quasi-distributed type is solved in which the variable lag time is considered. 1 figure; 5 references.

UDC 621.373.029

CALCULATION OF PARAMETERS OF A TRANSISTORIZED PHASE INVERTER

[Abstract of article by V. M. Kichak]

[Text] Methods are proposed for analyzing the parameters of a transistorized phase inverter using scattering parameters. 2 figures; 3 references.

UDC 621.382.2

IMPEDANCE CHARACTERISTICS OF CATHODE STATIC DOMAIN TYPE OSCILLATORS

[Abstract of article by E. D. Prokhorov and S. N. Skorobogatova]

[Text] It is shown that short (10-20 micron) Gann diodes with cathode static domain have negative impedance at many superhigh frequencies (25-100 gHz) in evolved impact ionization conditions and can be used as active components for oscillators in this range. 2 figures; 3 references.

COPYRIGHT: Izdatel'skoye ob"yedineniye "Vyshcha shkola", 1980

8617
CSO: 1860/39   - END -